Hitting "Undruggable" Targets: Determining the Properties of Cell Penetrant Stabilized Peptide Therapeutics for Intracellular Targets

by

Lydia Simulu Atangcho

A dissertation submitted in partial fulfillment
of the requirements for the degree of
Doctor of Philosophy
(Chemical Engineering)
in the University of Michigan
2020

Doctoral Committee:

Associate Professor Greg M. Thurber, Chair
Professor Omolola Eniola-Adefeso
Associate Professor Sunitha Nagrath
Professor Brian D. Ross

Lydia Simulu Atangcho

atangcho@umich.edu

ORCID iD: 0000-0003-3120-1545

Dedication

This dissertation is dedicated to my parents whose sacrifices led me to this great achievement, my brother Merius who supported me in many ways throughout my academic journey to get to this point, my partner John who lifted me up in the darkest of times, and my dog Bella who comforted me the way no human could.

I also dedicate this to all the black girls on their journey to a PhD—the journey can feel lonely at times, but I hope seeing another black girl that has crossed the finish line helps motivate you to keep going.

Acknowledgements

This work could not have been possible without the guidance and support of many people and organizations. First, I thank my advisor, Professor Greg Thurber, for giving me the opportunity to join the Thurber Lab and for guidance and mentorship throughout my research project. I also thank my committee members, Prof. Lola Eniola, Prof. Sunitha Nagrath and Prof. Brian Ross, for their useful insights and recommendations. My time in the Thurber lab was filled with many ups and downs, stressful times and joyous times, laughs and even cries. I thank my lab mates, former and present, for pushing me intellectually, engaging in useful discussions, and providing many laughs that I will look back on fondly. I especially thank my fellow Peptide Subgroup members, Tejas Navaratna and Marshall Case, for being not only great colleagues, but for their friendship. I have had the privilege of mentoring many talented undergraduates throughout my PhD—Daniel Tresnak, Hannah Levy, Greg Gueorguiev and Rahul Gopinath. I am thankful to them for all their hard work and am incredibly proud of all they have accomplished and will accomplish in the coming years.

My research could not have been possible without the use of many instruments. I thank James Windak, director of the UMich Chemistry Core, Professor Tim Scott and Scott Polymer Dojo members, James DelProposto, Professor Jeanne Stuckey, the BioInterfaces Institute, and Professor James Bardwell for generously allowing me to use their instruments and for providing assistance when needed. I also thank Dr. Henriette Remmer, director of the UMich Proteomics and Peptide Synthesis Core, for synthesizing many tricky peptides for me and giving me advice on my own syntheses. The final chapter of this dissertation would not have been possible without

the collaborative work contributed by Professor Joshua Kritzer and PhD student Kirsten Deprey from Tufts University. I am so grateful to them for joining us in this work. I also thank my funding sources for sustaining me throughout graduate school—the National Science Foundation Graduate Research Fellowship and the Rackham Merit Fellowship. Throughout my PhD, I benefitted from many resources provided by the university. I would like to thank the office of Counseling and Psychological Services as well as the Engineering Career Resources Center (ECRC). I especially would like to thank Catherine Lund of the ECRC for helping me navigate my job interviews which was extremely instrumental in me securing a job.

My journey to a PhD started as a freshman in undergrad when I was offered my first summer research opportunity by Professor Julie Champion (Georgia Tech). She first introduced me to basic lab practices, from teaching me how to hold a pipette to teaching me cell culture techniques. That experience was what planted the seed in my mind that I perhaps one day could pursue a PhD and I am so very thankful to Professor Champion for taking a chance on me and encouraging me to keep doing research and embark on my journey. I am also very thankful to Professor David Tirrell (Caltech) who offered me my second and third summer research opportunities in his lab. Those experiences cemented my decision to apply to PhD programs and his belief in me (even when others had none) encouraged me immensely. I will never forget the kindness and reassurance that Prof. Champion and Prof. Tirrell bestowed upon me as a budding scientist and I am forever thankful to them for the impact that they had on my trajectory.

Finally, I would like to thank all my close friends and family who supported and cheered me on along the way. First, I thank my mother whose strength inspired me, whose friendship warmed me, and whose love carried me through some of the most difficult moments, both in life in general and in my PhD. I also thank my siblings who I always looked forward to seeing during

visits back home and who cared for my dog during the semester that I couldn't. I am blessed with close friends who supported me in many ways throughout my PhD. I thank my best friend Koushy, who I've only seen sparsely since leaving for College, for being a constant in my life all these years. No matter how far away we are, catching up after long stretches always felt like a warm hug which I often needed in graduate school. Thank you for being someone I can confide in and for inspiring me with your strength and compassion. I also thank my best friend Fan for showing me what it means to chase your passions and thrive. From the time we left high school to now, seeing you cast aside fears and expectations and making your own amazing path helped me decide to do the same. I can't wait to see you finish your PhD soon! To my College girlfriends (#HotThangz)—Samantha Jones, Rae Clark, Chantel Walton and Tonjanika Smith—thank you all for your words of encouragement and for being so thoughtful in my hardest season in graduate school. I will never forget our first Homecoming after graduating when I desperately needed an escape in the middle of my first semester of graduate school. I needed you all then more than you know and I am so grateful to have had such a supportive and fun tribe, then, throughout grad school, and now. To my graduate school ride-or-dies—Dr. Yasmine Doleyres and soon to be Dr. Steven Chavez—I can never look back at my graduate school experience without thinking of you. Your friendship was invaluable in both the good times and bad and my fondest memories of graduate school will always include you two. I also want to thank other graduate school friends who hyped me up, kept me grounded and gave me some of the most fun years of my life—Dominic Bednar, Tejas Navaratna, and Scott Johnson.

Significant others of PhD students don't get the credit they deserve. I would like to say both thank you and sorry to my partner, John Dannenhoffer, for seeing me through the worst of times and sharing my joy through the best of times. I cannot express the gratitude I have for you

coming into my life and being by my side, even when it was unbearable. This PhD could not have happened without you. Most of all, I thank my dog Bella. She will never know how much I leaned on her throughout my PhD journey. When I decided to adopt her at the end of my first year of graduate school, I didn't know how much she would change my life. In a nutshell, she gave me something to look forward to every morning and evening, and that made all the difference.

Table of Contents

List of Tables

List of Figures

Abstract

Nearly two-thirds of all disease-associated proteins are 'undruggable' by modern therapeutics, meaning they are inside cells, out of the reach of biologics, but lack small molecule binding pockets. Stabilized peptides have the potential to hit these targets, which would open a vast array of potential new therapies. One such target is the p53/MDM2 interaction—a protein-protein interaction central to many cancers. Several inhibitors have been developed against the MDM2 protein because this target degrades the "the guardian of the genome" protein, p53. However, few of these peptides demonstrate the serum-independent, on-target efficacy required for clinical translation. In addition to having a strong target binding affinity, these peptides must efficiently penetrate the cell and evade proteolytic degradation. The design criteria for developing agents that can meet all of these requirements are still poorly understood. This work focuses on identifying the most important physicochemical properties that promote overall *in vitro* efficacy, taking into account the relevant molecular and cellular parameters in order to aid in future design of stabilized peptide therapeutics.

The research presented here begins with measuring the effects that lipophilicity and charge have on have on cellular uptake as these are two commonly tuned parameters for promoting stabilized peptide efficacy. Furthermore, cellular membrane penetration is largely thought to be a major limiting factor for this class of drugs. Results showed that incremental increases in charge caused significant increases in uptake and that although lipophilic peptides are more efficient at entering cells than hydrophilic peptides, there is a point at which increased lipophilicity begins to instead decrease uptake (logD>~3.5). After obtaining these results, I

moved on to selecting peptides discovered via bacterial surface display and measuring their binding affinities and *in vitro* efficacies as a precursor to a full physicochemical property profile in order to identify what the biggest contributors to efficacy are. After selecting those peptides, I measured their lipophilicities, cellular penetration rates, membrane interactions, and proteolytic stability. Ultimately, results showed that the cellular potency of this series of compounds appears to be driven by intracellular stability, which correlated with efficacy, rather than permeability, which did not at all correlate with efficacy. This was demonstrated by ATSP-7041, a promising MDM2/p53 inhibiting peptide and the only p53-based peptide that has led to a clinical lead compound, as well as pepC, a novel peptide with efficacy close to that of ATSP-7041. These two peptides showed the highest resistance to proteolytic degradation as well as the highest cellular potency, although ATSP-7041 had the slowest cellular uptake (~3-fold slower than pepC). Characterization of the molecules demonstrated they all had high affinity and modest membrane permeability, leading to stability as the differentiating factor. These results exhibit the need for a wholistic assessment of peptide properties to help inform efficacy outcomes and serve as a basis for future peptide development.

Chapter 1 Introduction

1.1 Dissertation Overview

1.1.1 Objective

The objective of this dissertation work was to elucidate the most important factors for achieving efficacy of stabilized peptide therapeutics. Using literature precedent as a starting point (Chapter 1), we identified the physicochemical properties that drive traditional drug development, including size, lipophilicity and charge, and applied those principles to stabilized peptides that target the p53-MDM2 interaction. Using a series of novel stabilized peptides with high binding affinity to MDM2, we analyzed various physicochemical properties and determined which properties led to *in vitro* efficacy.

1.1.2 Hypothesis

Given that the guidelines set in place for traditional drug development (Lipinski's Rule of Five) are intended to promote efficient cellular uptake, we hypothesized that efficacy would be uptake limited (given high target binding affinity in the single-digit nanomolar range). Much of our focus was therefore centered around the properties that affect uptake, such as lipophilicity and charge, and we hypothesized that those may be the most important determinants of efficacy.

1.1.3 Work Plan

In Chapter 2, we tested the effects that lipophilicity and charge have on cellular uptake and used a double-click stabilized MDM2-inhibiting peptide from literature as a proof-of-concept peptide.

This particular peptide, though not having *in vitro* efficacy, has several carboxylic acid residues that allowed us to make amino acid substitutions with the uncharged analogues in order to create a series of differently charged peptides without making sweeping chemical changes to the sequence. Additionally, using various different fluorescent linkers, we produced a series of peptides with varying lipophilicities and used fluorescence as a means to quantify uptake.

Chapter 3 will focus on characterizing a set of novel MDM2-inhibiting peptides discovered via bacterial surface display and selecting potential peptide drug candidates for further studies. The selection criteria will be based on target binding affinity and *in vitro* efficacy.

In Chapter 4, the peptides chosen for further study are profiled for physicochemical properties including lipophilicity, cellular uptake rate, membrane interactions, and protease stability. Based on the results, we determine that contrary to our hypothesis, the property that correlates best with efficacy for this peptide series is protease stability, not cellular uptake rate. Based on the high affinity and moderate permeability of these peptides, this highlights differences in protease stability, even within stapled peptide sequences, as critical for cell efficacy.

Chapter 5 will summarize all the work presented as well as offer ideas for future work to be done that can further elucidate the most important factors in peptide drug design.

1.2 Publication Information

L. Atangcho, T. Navaratna, G.M. Thurber. Hitting Undruggable Targets: Viewing Stabilized Peptides Through the Lens of Quantitative Systems Pharmacology. *Trends in Biochemical Sciences*. 44(3): 241-257 (2019).

This publication has been modified to adapt to the content of this dissertation.

1.3 Abstract

Stabilized peptide-based therapeutics have the potential to hit currently undruggable targets, dramatically expanding the druggable genome. However, major obstacles to their development include poor intracellular delivery, rapid degradation, low target affinity, and membrane toxicity. With the emergence of multiple stabilization techniques and screening technologies, many groups have demonstrated high efficacy of various bioactive peptides *in vitro.* However, fewer molecules have exhibited success *in vivo*. Here we discuss the chemical and pharmacokinetic barriers to achieving *in vivo* efficacy. Given their small size relative to traditional biologics, the molecular properties of stabilized peptides must be considered in a simultaneous and comprehensive manner in order to achieve the necessary rates for *in vivo* delivery to the target, efficacy, and ultimately, clinical translation.

1.4 Opportunities and Challenges in the Peptide Drug Landscape

The field of peptide therapeutics has come a long way from utilizing unmodified naturally occurring peptides as in the case of insulin therapy discovered in the early 20th century. Today, over 60 peptide-based therapeutic agents have been approved by the FDA and many more are in the drug development pipeline. The majority of these peptide drugs are analogs of previously discovered endogenous peptides, many of which target G-protein coupled receptors or other cell surface receptors with endogenous protein ligands[1]. These receptors, however, make up only a fraction of molecular targets to treat disease. Targeting other protein-protein interactions (PPIs) has proven to be a much larger challenge since most of them occur inside the cell, out of the reach of traditional biologics such as monoclonal antibodies.

Currently, intracellular targeted therapeutics are dominated by lipophilic small molecule drugs that bind ‘druggable’ proteins that contain a small, hydrophobic binding pocket or enzyme

active site. However, the majority of disease-associated proteins lack such features[2]. In contrast, 62% of PPIs have an alpha-helical motif in their binding interfaces[3], and alpha helix-based surrogate peptide structures are able to disrupt the much larger (1000-2000Å^2) binding interfaces between proteins[4]. Therefore, alpha helices are being explored for targeting these PPIs. In principle, alpha helical peptide scaffolds are an attractive drug class for targeting PPIs due to their balanced size: large enough to specifically disrupt PPIs like biologics but compact enough to enter cells like small molecules. However, without modification, they suffer from rapid degradation, fast clearance, low to insufficient membrane permeability, and poor target affinity.

Over the past two decades and continuing with current research, the barriers to intracellular delivery of alpha helix scaffolds are slowly being eroded with the emergence of helix stabilization chemistries, modification of peptide physicochemical properties, and screening technologies to select stand-alone high affinity agents, which is a challenge given the much larger chemical space of macromolecular drugs. Helix stabilization approaches (**Fig. 1.1**)

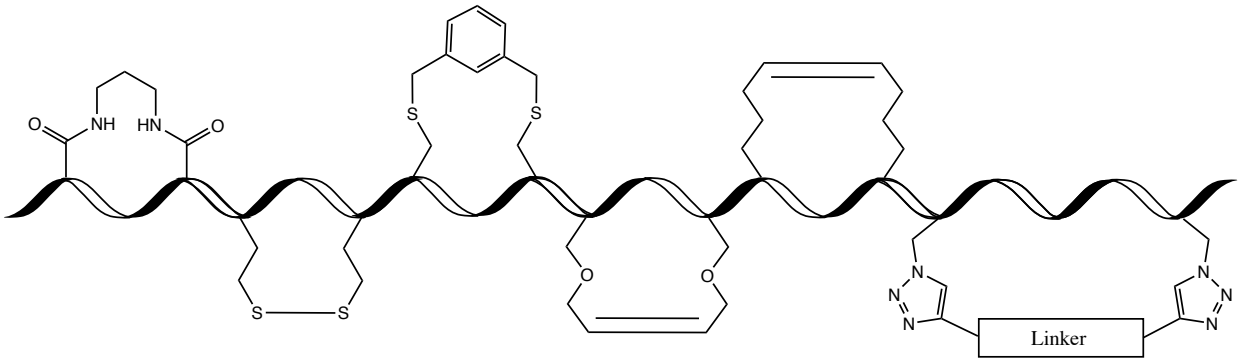

Figure 1.1 Peptide Stabilization Techniques A (non-exhaustive) representation of several reported peptide staples is shown. All examples are drawn as i,i+4 staples except the last which is shown as i,i+7, a more common stapling position for that staple type. From left to right, lactam bridge, disulfide bridge, bis-alkylation of cysteine residues, ring-closing olefin metathesis of O-allylserine residues, all-hydrocarbon staple via ring-closing metathesis of α,α-disubstituted non-natural amino acids with all-hydrocarbon side chains, double-click stabilization of azido non-natural amino acids.

help decrease degradation rates and potentially increase target affinities[5,6]. Several groups have

since adopted these techniques to engineer novel therapeutic and diagnostic constrained alpha helices with targets spanning a variety of human diseases. Combined with the development of various peptide library screening methods (phage, mRNA and bacterial display)[7,8], these advances have propelled the field forward, and some agents have entered clinical trials[9]. Until one or more FDA approved drugs are developed, it remains unclear whether alpha helices are generally suitable for targeting intracellular PPIs. However, multiple approaches have been explored for overcoming the intrinsic challenges in developing these agents, and significant progress is being made[10]. Here, we focus on the quantitative pharmacology aspects of stabilized peptides, where multiple properties must be considered simultaneously for translational development.

This overview will focus on the need for a 'systems' approach to stabilized peptide scaffold development, where changes in one property impact the distribution of the agent across multiple length and time scales within a living organism. In early stages of development, beyond measuring target binging affinities, groups typically establish the efficacy of their peptides via *in vitro* cellular assays such as cell killing and gene reporter assays. Many also perform imaging of fluorophore-conjugated variants to demonstrate cellular uptake (intracellular targets) or cell surface binding (extracellular targets) as well as immunoprecipitation and western blotting to show up or downregulation of native proteins. Much of the development work at this stage is carried out in cell culture, and this makes sense from the standpoint that the most formidable barrier to development of macromolecular agents that bind intracellular targets is accessing the cytosol. However, there are far fewer reports of *in vivo* efficacy studies, the precursor to clinical trials, and some of the strategies and mechanisms employed in cells may have deleterious effects in the context of an animal model or patient. Furthermore, various studies have revealed

uncertainties in how effectively some of these recently developed peptides penetrate cells and bind their targets[11,12]. Efficient cell membrane permeability is just one of many variables to

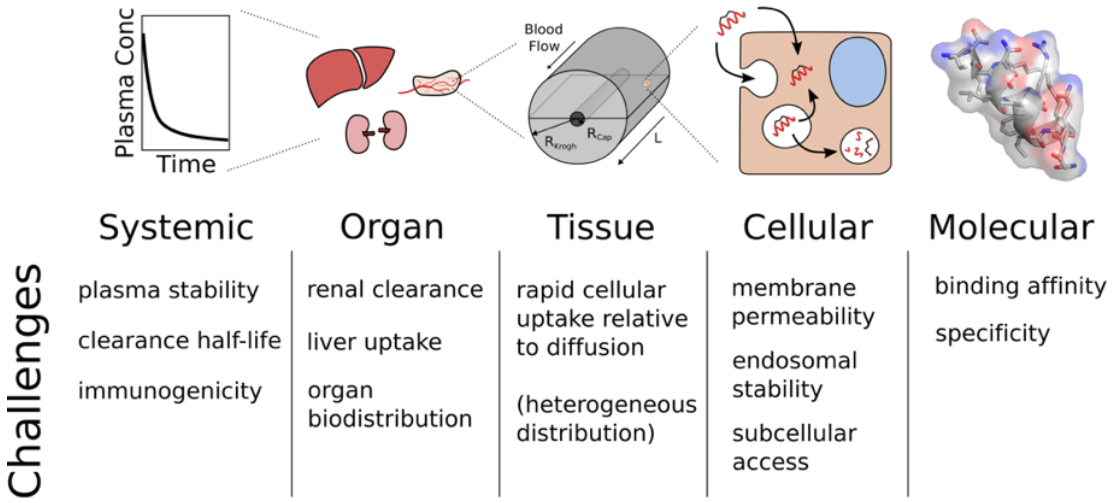

Figure 1.2 Multiscale Pharmacokinetic Challenges of Therapeutic Peptides

consider for successful *in vivo* drug delivery. Ultimately, stabilized peptide design must be focused on reaching systemic circulation (following various routes of administration), remaining in circulation for extended periods of time (delayed renal and/or hepatic clearance), evading protease degradation (systemic and local degradation/'clearance'), reaching target organs and distributing in the tissue, penetrating cell membranes for intracellular targets, reaching the subcellular location (e.g. nuclear targets), and binding tightly to the target (**Fig. 1.2**). In this review, we examine various classes of constrained peptides that have exhibited robust pharmacokinetics for clinical translation from a quantitative systems pharmacology view and examine them in comparison to stabilized peptides specifically.

1.5 Stabilized Alpha Helices as a Peptide Drug Scaffold

It has long been recognized that more rigid/constrained molecules have the potential for higher binding affinity (see **Box 1.1** on helicity), and the alpha helix, one of the most prevalent

secondary structures in proteins, has many attractive properties as a scaffold. The pursuit of structurally locking alpha helices in their conformation began several decades ago. Early techniques included the use of disulfide and lactam bridges (**Fig. 1.1**) as well as metal ion complexes. In 2000, Schafmeister and Verdine published an all-hydrocarbon stapling method adapted from a previously published ring-closing olefin metathesis stapling method by Blackwell and Grubbs[13] (**Fig. 1.1**). These peptides showed increased helicity and proteolytic stability[14] and created significant excitement within the field. By incorporating terminal alkene-functionalized non-natural amino acids with varying chain lengths, R and S stoichiometries to account for stereochemistry effects, and placing the reactive residues in *i*, *i*+4 and *i*, *i*+7 locations of the peptide, they optimized their stapling method to efficiently stabilize the scaffold[15]. This all-hydrocarbon stapling technique was first tested by Walensky and colleagues, who designed peptides after the BH3 domain of a BCL-2-member protein, stabilized these peptides using their all-hydrocarbon stapling technique, and showed that the peptides were able to bind pro-apoptotic proteins and cause apoptosis of cancer cells *in vitro* and *in vivo*[5]. Similarly, Bernal and colleagues, also from the Verdine group, tested their stabilization technique on p53-based peptides. P53 is a transcription factor that regulates cell growth and apoptosis as a response to DNA damage and cellular stress. Its activity is regulated by MDM2, an E3 ubiquitin ligase that marks p53 for degradation when its functions are not necessary. Loss of p53 activity is the most common deficiency in human cancer, whether due to mutation of the gene or due to overexpression of MDM2[16]. Bernal et al. designed several p53-based peptides and showed that one of their variants, p53-SAH-8, had a higher binding affinity for MDM2 (K_d=55nM) than the wild-type p53 (K_d=410nM). They also demonstrated *in vitro* cell permeability, which caused apparent upregulation of native p53—reactivating the apoptotic pathway[17].

The Verdine group took some of the first steps toward the design of stapled peptides with intracellular therapeutic effects that overcome several barriers associated with delivery of peptides. However, particularly in these early days, the slow throughput in synthesizing individual peptide sequences and testing for cell permeability combined with the gap in knowledge around the pharmacokinetic properties of molecules in this size range made progress arduous. Since this time, high throughput screening methods combined with novel chemistry have allowed isolation of high affinity sequences, aiding this step in development[18–20]. Recently, Lau and colleagues designed a p53-based peptide for therapeutic modulation of the p53-MDM2 interaction using two bioorthogonal reactions (an approach first reported by Torres and colleagues[21]). Instead of cross reacting two complementary residues, they placed two azido-functionalized residues in *i, i*+7 locations and stapled the peptide with a di-alkyne linker by copper-catalyzed azide-alkyne cycloaddition—a well characterized click chemistry reaction[22] (**Fig. 1.1**). This strategy, termed "double-click stabilization,"[23] conveniently allows the introduction of additional functionality on the linker (e.g. modification of charge, lipophilicity, imaging tag incorporation, etc.)[6,24]. In addition to modifying the physicochemical properties of peptides, these polyfunctional linkers can contribute to protease stability and binding affinity through reducing the entropic penalty of binding and through direct (enthalpy) contributions (**Box 1.1**).

Stapling techniques allow for added complexity in peptide drug design, giving more nuanced control over the properties one can change to help achieve desired peptide outcomes. Despite these advances in peptide chemistry and molecular engineering, the field of constrained peptides still faces formidable challenges, particularly in the delivery of these agents to the site of action, which will need to be overcome to gain widespread clinical relevance. Now that more

tools are becoming available to generate defined molecular properties, the major question remains: *what properties are needed for clinically translatable drugs?*

Stabilized peptide scaffolds sit at the interface of biologics and small molecule drugs, and guidance for development can be found in both fields. Several of the high throughput approaches have taken advantage of directed evolution from the field of biologics to screen a billion or more (10^9 to 10^{12}) variants. (For comparison, a 12-mer peptide with only natural amino acids has a sequence space of $20^{12} \sim 4x10^{15}$ unique sequences.) To access the cytosol, where many relevant protein-protein interactions occur, inspiration can be found in the world of small molecules.

1.6 Non-Lipinksi Drugs: Cyclic Peptides and Related Macrocycles

Most drugs against intracellular targets are small molecules—a class of compounds containing molecules sharing a specific set of physicochemical properties summed up by Lipinski's Rule of Five (Ro5)[25]. Imaging studies show that this class of agents can enter cells and reach their subcellular target within seconds to minutes[26,27]. Drugs that adhere to these guidelines tend to be well-absorbed making them good candidates for oral delivery. However, due to their small size (<500 Da), they lack large contact surface area for binding, making them prone to low specificity for their intended targets. Conversely, biologic drugs typically have molecular weights above 5000 Dalton (e.g. antibodies). Though they boast high target specificities due to large contact surface areas for binding, they often require intravenous delivery (see **Box 1.2**) and lack intracellular access[28]. Peptides and other non-traditional (non-Ro5) drug molecules falling in between small molecules and biologics have the potential to provide the best of both worlds. Though stapled peptides have yet to be FDA-approved, other non-traditional drug types have been approved or are in clinical development. Among them are cyclic peptides, which compared

to all other peptide drugs have shown the highest abundance of orally bioavailable agents[29]. While oral bioavailability is distinct from intracellular delivery/cytosolic access, many oral drugs are absorbed through transcellular transport across the intestinal epithelium, so they share some stability and permeability characteristics.

1.6.1 Physicochemical Properties

What properties allow cyclic peptides to be well-absorbed? Nielsen and colleagues provide an exhaustive analysis of 125 orally bioavailable cyclic peptides and their properties, including molecular weight, predicted lipophilicity, and polar surface area. They profiled the properties of a variety of cyclic peptides with greater than four residues, including circular cysteine-knotted peptides, termed cyclotides, natural product cyclic peptide Cyclosporin A and its derivatives, and, for comparison sake, the doubly stapled alpha helix SAH-gp41$_{(626\text{-}662)}$—the only stabilized alpha helix with reported oral bioavailability thus far (though percent oral bioavailability was never reported for this peptide). Nielsen examined the correlation between multiple physicochemical properties and oral bioavailability. First, a high molecular weight (>500 Da) did not appear to preclude oral bioavailability as it does in the case of small molecules. They found that even in the higher molecular weight range for the peptides analyzed (960-1350 Da), 23 peptides had oral bioavailability greater than or equal to 10%, and lower molecular weight did not correlate with higher oral bioavailability[29]. This suggests that for peptides, other properties may be of greater importance when considering rates of drug absorption. Furthermore, upon comparing predicted octanol-water partition coefficients (logP, **Box 1.3**) as measured by Molinspiration cheminformatics or QikProp software, Nielsen et al. reports that the lipophilicity of orally bioavailable cyclic peptides tend to fall within Ro5 guidelines, $0 \leq \text{LogP} \leq 5$, but that a slightly higher range of 0-8 (as calculated with Molinspiration) seemed permissible.

Other original Ro5 properties include the number of hydrogen bond donors and acceptors, limited to less than 5 and 10, respectively[25]. Nielsen's study found that cyclic peptides with greater than 6 hydrogen bond donors had oral bioavailability of less than 10%. However, the number of hydrogen bond acceptors, defined as simply the total number of nitrogen and oxygen atoms in the molecule, was greater than 10 for all cyclic peptides in the study, therefore not meeting the Ro5 criteria. A number of studies conclude that few rotatable bonds (no more than 10-13) corresponds to good oral bioavailability, likely due to a decrease in solvent interactions and lower susceptibility to degradation because of structural rigidity[30,31]. Cyclic peptides are advantaged in this area due to the fact that they are inherently constrained[29].

1.6.2 Backbone Modifications

Many peptide macrocycles and other 'Ro5 violators' that have had success in the clinic are derived from natural products[4]. These peptides have been widely studied as models for synthetic derivatives or *de novo* cyclic peptides. Cyclosporin A, for example, is a naturally occurring orally bioavailable (oral bioavailability = 29%) 11-residue peptide macrocycle used as an immunosuppressant drug[32]. Despite definitively falling outside of Lipinksi's standards for drug-likeness, Cyclosporin A and other natural product macrocycles have the uncanny ability to traverse membranes, avoid degradation, and bind efficiently to their targets in their necessary conformations[4,29,32,33]. One of the common characteristics of natural product macrocycles like Cyclosporin A is amide N-methylation[32,34,35]. In a study of 39 peptide macrocycles by Ahlbach and colleagues, all compounds with measurable passive permeability except one had amide N-methylation[32]. N-methylation has been widely shown to improve membrane permeability of natural product peptide macrocycle derivatives, a phenomenon attributed to a decrease in solvent-exposed polar groups (polar surface area), therefore reducing the desolvation energy

required for crossing membranes[33–35]. In addition, designing molecules to enable the formation of intramolecular hydrogen bonds and introducing sterically hindering hydrophobic groups also adds to these permeability enhancing effects[32,36]. This may be particularly important for imparting 'chameleon'-like properties to maintain solubility: solvent hydrogen bonding in aqueous environments and intramolecular hydrogen bonding while crossing membranes[4]. These are all useful insights in the design of stabilized alpha helices since hydrogen bonding via staple choice and sequence optimization could prove useful for achieving enhanced permeability and *in vivo* efficacy.

1.7 Stabilized Alpha Helices: Properties and Challenges

1.7.1 Access to the Cytosol

Membrane permeability of stabilized peptide structures is the most challenging step in delivery to the site of action (the target). After all, membrane partitioning is a basic element of a functioning cell. In recent years, elucidating the nuances of how peptides enter cells has been an increasingly active area of research in the field of stabilized peptides. Early methods of verifying cellular uptake included conjugating peptides to fluorophores, treating cells with the fluorophore-conjugated peptides, and using microscopy or flow cytometry to detect intracellular fluorescence[5,6,17,37,38]. This is a challenging task, since care must be taken to distinguish cellular uptake in endosomes/lysosomes (which do not have access to cytosolic targets) versus localization in the cytosol itself. These methods however, do not directly measure target engagement. Even cell viability assays without the use of proper controls are at risk of false positives. This became clear with the emergence of methods directly assessing whether peptides have off-target toxicity[11]. Adopted from the viral and gene delivery fields, positive charge is one

method of conferring membrane permeability of peptides[6,39,40]. However, methods such as the recombinase enhanced bimolecular luciferase complementation platform (ReBiL) and LDH release quantification highlighted some of the toxicity hurdles inherent in cationic agents and motivated other strategies to achieve membrane permeability[11,12]. Just a few years since the first hydrocarbon stapled peptides were introduced, researchers in the field are developing new membrane permeable peptides with more robust methods of demonstrating on-target efficacy using in vitro assays and giving special attention to physicochemical properties outside of charge that can help improve cytosolic delivery[41–44]. However, careful consideration of drug delivery issues outside of the cellular challenges, including systemic clearance, organ uptake, and tissue distribution, is necessary for *in vivo* efficacy.

1.7.2 Pharmacokinetics Beyond the Cell

Two of the main mechanisms for getting stabilized helices across membranes are charge and lipophilicity. Both are inspired by nature. Many natural compounds like cyclic peptides and cyclotides are highly stable and lipophilic. In contrast, viral approaches, such as the cationic TAT peptide from HIV, use charge to help penetrate membranes. As a cautionary note, cationic charge, particularly in combination with lipophilicity, is also found in a third class of molecules: anti-microbial peptides. These membrane-disrupting agents have the potential for high toxicity and may have narrow concentration windows for efficacy without toxicity. Likewise, viruses (and related gene-delivery payloads) benefit from amplification and integration within the cell, requiring relatively low doses, whereas peptide-scaffold delivery requires target-saturating amounts. Examples of both approaches are prevalent in the literature; how do these strategies, designed to allow access to the cytosol, impact the quantitative systems pharmacology of these agents?

The number of clinical examples of intracellular therapeutics outside Lipinski's Ro5 dwindles dramatically when approaching 1 kDa and above, and so too does the detailed data on tissue, organ, and systemic distribution. However, specific examples (both within and outside the class of stabilized peptides) can highlight some of the challenges and strategies to improve intracellular delivery in a clinically translatable manner. Although these agents do not currently have FDA approval, macromolecules against intracellular targets with significant published clinical results include imetelstat (a non-peptidic 4.6 kDa telomerase inhibitor) and the clinical test compound ALRN-6924[9] (the clinical variant of stapled peptide ATSP-7041). Typically molecules that have made it further in the clinical trial process have improved pharmacokinetic properties[45]. Looking at these molecules in conjunction with the cyclic peptides discussed previously, some trends are clear. Lipophilicity is much more prevalent than cationic charge for cytosolic access. This is also true for BCL-2 inhibitors (e.g. venetoclax and navitoclax), rapamycin, and a host of other 'beyond Lipinski' molecules (500-1500 Da)[46,47]. Even at the other extreme of the 'non-Lipinski' space, close to 5 kDa, molecules with high lipophilicity tend to prevail. Cyclotides, as natural products, are isolated based on their stability and long HPLC retention time (lipophilicity)[48]. By integrating a target-binding helix into a cyclotide's backbone, Ji et al. were able to target MDM2 inside cells with a 5.3 kDa cyclotide. While the doses are high (40 mg/kg in 5% dextrose which can enhance permeability) likely due to slow transport, they have shown remarkable evidence of activity after oral administration against this intracellular target[49]. The use of lipophilicity does not preclude other mechanisms of cytosolic access from being integrated (and may be necessary for the intracellular delivery of larger cargos, such as DNA/RNA). However, it is worth highlighting the strengths of augmenting lipophilicity as an approach from a systems pharmacology perspective.

Focusing first on systemic delivery (plasma concentrations), lipophilicity can help slow down clearance in the blood to enable more efficient uptake in tissue. These peptide scaffolds are well below the roughly 60 kDa molecular weight filtration limit of the kidney, so hydrophilic scaffolds are rapidly excreted by the kidneys[50]. Lipophilic peptides (and small molecule drugs) typically bind albumin and other proteins to avoid renal filtration. Highly charged molecules can also stick to plasma proteins, but these are typically cleared rapidly by the liver. To highlight a clinical example, protamine, a cationic macromolecule that complexes with heparin in the blood, is cleared within minutes in humans (7.4 min half-life)[51]. While protamine may be an extreme, TAT and related peptides tend to exhibit increased clearance and liver/kidney uptake[52,53]. Serum proteins also decrease the cellular uptake of these agents, and care must be used when taking quantitative pharmacology measurements to discern what conditions were used. However, serum proteins tend to have a larger effect on cationic delivery (both peptides and larger cargoes such as PEI-mediated gene delivery) than lipophilic delivery[11]. Even if the serum binding can be avoided, this could potentially result in rapid kidney clearance as described above. High cationic charge can also disrupt membranes at higher concentrations, causing toxicity as previously mentioned. This could cause potential issues with parenteral routes of administration, such as subcutaneous injection or even intravenous delivery (e.g. infusion reactions) due to high local concentrations. Therefore, while exceptions may exist[54], cationic 'cell penetrating peptides' generally have poor *in vivo* pharmacokinetics[52].

Lipophilic agents, though less susceptible to causing membrane toxicity, can suffer from issues of solubility. Here, stabilized peptides may be able to take advantage of the 'chameleon' like behavior of cyclic peptides, where intramolecular hydrogen bonds can form in membranes, but intermolecular bonds can form with water molecules in an aqueous environment[55]. Extreme

lipophilicity may also suffer from slow distribution into different organ systems due to high plasma protein binding (PPB). Although PPB is important to avoid rapid renal filtration, high PPB can slow the extravasation and diffusion rates of the compounds as seen with smaller molecules (e.g. ~1 kDa fluorescent PARP inhibitors)[27].

Tissue heterogeneity is another consideration for stabilized peptides, since the size of these agents may result in transport limitations over the tens to hundreds of microns length scale. Both small molecules and biologics can exhibit heterogeneity in tissue under certain conditions. Small molecules often exhibit heterogeneous distribution if they have rapid cell uptake and immobilization relative to clearance (e.g. Hoechst 33342)[56] or fast metabolism relative to diffusion[57]. Antibodies exhibit heterogeneity when their binding rates exceed their diffusion into the tissue[58]. The large gradients in the drug concentration between the region just outside of the blood vessels and regions more distal to the vasculature arise through a competition between immobilization of the agent (receptor binding, cellular internalization, etc.) versus interstitial transport (typically diffusion dominates over convection in this size range). This ratio of an immobilization reaction to diffusion can be captured by a dimensionless number known as the Damköhler number. Because these agents lack an extracellular target, the relevant "immobilization" reaction rate is uptake into the cell. At first glance, it appears that there will be little heterogeneity in the tissue, since cellular uptake rates relative to diffusion are very slow for this class of agents (e.g. even with macromolecular imaging agents)[59]. However, caution must be exercised, since the strategies for increasing cell permeation (high lipophilicity and/or charge) can also dramatically slow the effective diffusion rate (while increasing the cellular uptake/immobilization rate). Continuous exposure from the blood can eventually overcome any transient gradients, but degradation of the probe could result in a scenario where the drug is

destroyed before it ever reaches distant cells, similar to antibodies[60]. Many tissues have relatively short distances between blood vessels, but tumors are particularly prone to this issue due to their long diffusion distances for efficient delivery[61]. While the stability imparted by cross-linked scaffolds for stabilized peptides and slow cellular uptake of these agents (relative to seconds for small molecules) help mitigate the risk of tissue heterogeneity, this is an important consideration when manipulating the physicochemical properties to optimize cellular uptake.

1.7.3 Clinical Precedent

In the absence of an FDA-approved drug, limited clinical data is available for intracellular targeted macromolecules. The two examples of drugs mentioned earlier that have been administered to patients – the clinical version of ATSP-7041 (a 1.4 kDa all-hydrocarbon stapled p53 mimetic) and imetelstat (a telomerase inhibitor which uses a fatty acid to increase lipophilicity) – illustrate the impacts of lipophilicity on the quantitative pharmacology and development of these agents. ATSP-7041 (Fig. 1.3) was derived from a sequence (pDI) enriched by phage display[62] and outfitted with an *i,i*+7 hydrocarbon staple[51]. This agent had high binding affinity to its target (Kd = 900 pM for MDM2), which is likely required due to low intracellular concentrations. The Verdine group had previously developed a similar p53-based stapled peptide inhibitor of MDM2 called SAH-p53-8[17]; however, this peptide proved not potent enough for therapeutic application beyond very controlled *in vitro* assays[63]. It is therefore useful to look at

the differences between ATSP-7041 and SAH-p53-8 that may provide insight into properties needed for success.

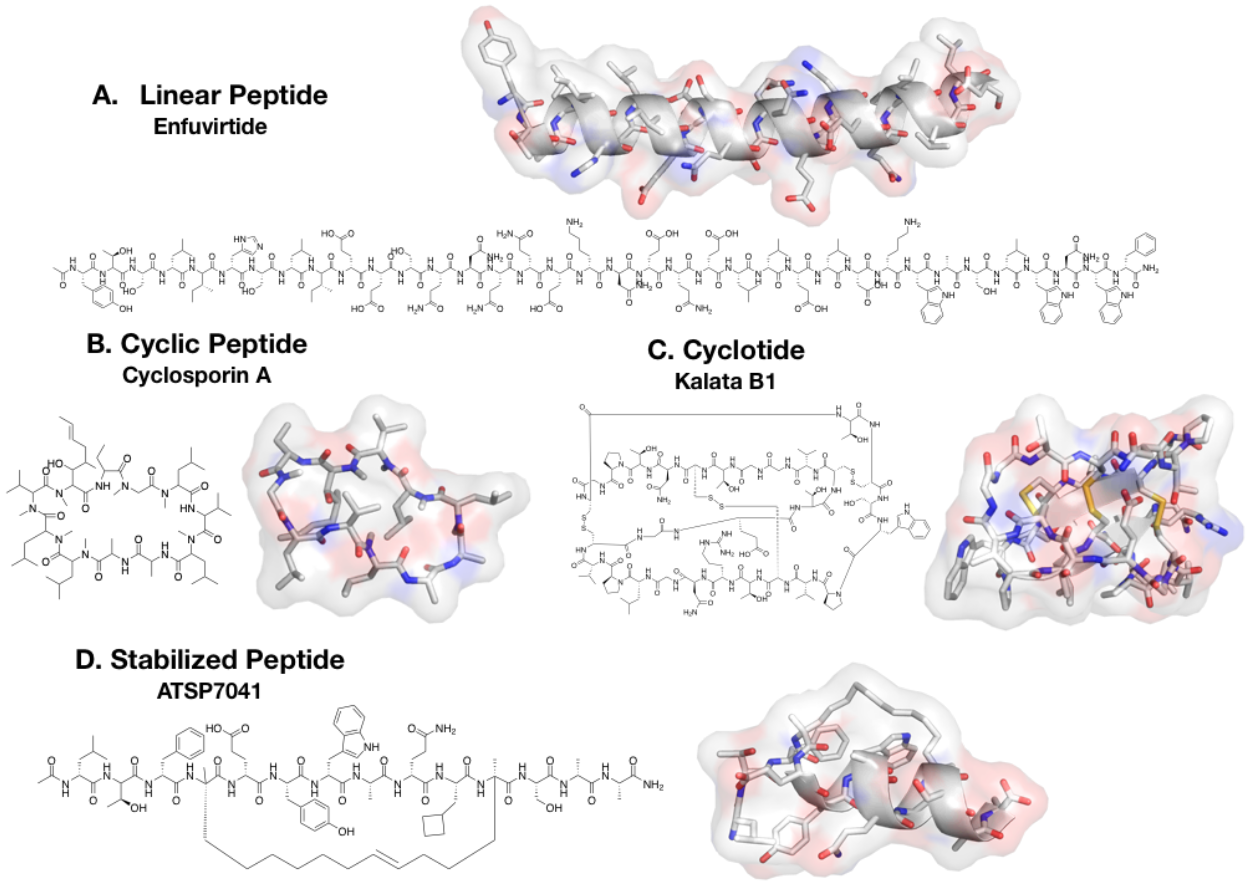

Figure 1.3 Constrained Peptide Types. (A) Linear peptides are those containing no backbone cyclization (neither between termini or residues). Enfuvirtide is a 36 amino acid linear peptide for HIV treatment. (B) Cyclosporine is a cyclic peptide with a completely cyclic backbone, therefore containing no terminus. Cyclosporine A is an immunosuppressant natural product cyclic peptide with several N-methylations in its backbone. (C) Cyclotides are cyclic peptides with intramolecular disulfide bonds, termed cysteine knots. Kalata B1 is a natural product cyclotide commonly used as a scaffold for its physical and chemical stability. (D) Stabilized peptides encompass peptides having residues chemically cross-linked by any one of various methods such as those outlined in Figure 1.1. ATSP-7041 is a clinical-lead stapled peptide by Aileron Therapeutics for inhibiting MDM2 in relevant cancer types.

Although physicochemical properties beyond molecular weight are not reported for these peptides, important structural differences and their presumed effect on efficacy are outlined. Firstly, SAH-p53-8 and ATSP-7041 both contain three key hydrophobic residues (Phe^{19}, Trp^{23}, Leu^{26}) required for binding MDM2/MDMX. However, several phage display studies have

revealed the importance of another key residue, Tyr^{22} [64]. This replaced the residue Leu^{22} in SAH-p53-8, which was preserved from native p53[63]. Furthermore, SAH-p53-8 has additional residues 14-16, all of which are polar, and residues Gln^{17} and Arg^{24} are replaced with Leu and Ala, respectively, in ATSP-7041. Chang and colleagues explain that this enlarges the already existing "hydrophobic patch", leaving only a total of 4 polar residues[63]. This essentially reduces the polar surface area of the peptide while also reducing its total size. These modifications resulted in a peptide with an aqueous solubility too low for peptide characterization. This sequence was therefore further modified to improve solubility without sacrificing amphiphilicity by replacing His^{21} with the charged Glu residue and adding two c-terminal Ala residues to extend the helix. The resulting sequence is ATSP-7041. Cell viability assays in 10% serum show a more than 50-fold increase in potency between SAH-p53-8 (IC50>30uM) and ATSP-7041 (IC50=600nM).

In vivo studies of ATSP-7041 showed that it is primarily excreted intact by the liver, resulting in 79% collected in the feces and < 3% in the urine. The reported half-life in humans is 5.5 hrs[63]. Imetelstat also has a plasma clearance half-life of around 5 hrs in humans[65] with primarily liver uptake but some kidney/bladder signal as measured by radiolabeling[66]. The relatively long half-lives compared to cationic agents provides some evidence that lipophilicity is a feasible mechanism to improve intracellular delivery for this class of drugs. Clinical plasma clearance is not the only shared trait between these intracellular targeted macromolecules. While the targets and structures are very different, they both contain modifications to achieve high stability, lipophilicity, and binding affinity. Imetelstat has a thio-phosphoramidite backbone to improve stability of the nucleic acid backbone[67] (similar to the function of side-chain crosslinking for ATSP-7041), a conjugated 16 carbon fatty acid to increase lipophilicity and cell

penetration[68] (comparable to the all-hydrocarbon staple for ATSP-7041), and high affinity and specificity for its target (45 pM[67] for imetelstat and 900 pM for ATSP-7041) to bind at low intracellular concentrations.

Significant work remains to determine if stabilized peptide scaffolds can generally be used to target intracellular proteins in the clinic. Major outstanding questions remain around the specific mechanisms of cellular uptake and other aspects of development. For example, how important is the distribution of lipophilic groups on the molecular surface versus net-lipophilicity? What is the role of molecular shape? Many stabilized peptides are often seen in endosomes (which are inaccessible to the cytosol). Is this a necessary step for delivery of lipophilic stabilized peptides or simply a function of faster uptake into endosomes than permeability across these membranes? It is clear that multiple approaches for improving cellular permeability can work in cell culture, and lipophilic-mediated delivery may be a tougher approach. However, given the multiple benefits from a quantitative pharmacology standpoint for clinical translation, this may be the tougher road worth choosing.

1.8 Discussion and Future Directions

Few stabilized peptides thus far have been reported to have *in vivo* efficacy. However much can be learned from the combined knowledge in the field of small molecule drug development, biologics, and the few examples of agents that have entered the clinic as discussed here. It is clear that in the case of stabilized peptides, sequence optimization must take into account effects on binding affinity, solubility, membrane partitioning, clearance rate, and other pharmacokinetic processes. Hydrophobicity (lipophilicity) and the existence and location of polar residues seem to be important in the context of not only membrane permeability but also for protease degradation, plasma protein binding, and subsequent uptake and clearance rates as in the case of

ATSP-7041. Furthermore, even large peptides (> 1 kDa) are not precluded from having *in vivo* efficacy (and non-intravenous routes of administration), but the barriers are high. The examples discussed here point to the possibility that lipophilicity may be a useful property to balance cellular uptake with tissue distribution, organ biodistribution, and systemic clearance. Examples with related scaffolds indicate that it should stay within or close to Lipinski's rules, even when other Ro5 guidelines are broken.

Stabilized peptides stand at the interface between traditional small molecule drugs and larger biologics. Future directions should continue to take advantage of the unique contributions from each of these fields. Directed evolution methods developed for biologics can help in the selection of binders in the much larger 'chemical space' of these macromolecules. Similar to biologics, the plasma concentration of these agents is rarely the concentration at the site of action, and the concepts of multi-scale drug delivery can be employed to understand the various transport hurdles in vivo, going beyond the cellular delivery issue. Borrowing from the field of small molecules, leveraging data on lipophilicity, polar-surface area, charge, etc. to understand membrane permeability and partitioning will aid in our understanding of if and how these molecules access the cytosol and their targets. The hurdles for development are high, but the potential payoff – to be able to specifically hit targets beyond the reach of biologics and small molecules – would open up a vast array of new therapeutics.

1.9 Boxes

Box 1.1 Helicity

Alpha helices are coiled protein secondary structures held together by hydrogen bonding between amino acids that are 4 residues apart (*i*, *i*+4), which are commonly found in proteins and at interfaces [3]. Helicity is a widely measured parameter for stabilized peptides, but the multiple

quantitative impacts of this property on binding have led to substantial debate. Increases in helicity result in a more 'structured' peptide, and a more rigid structure has long been known to enable selection of higher binding affinity molecules, whether this is from disulfide 'constrained' libraries in phage display[69], fixing the termini by displaying peptides as 'loops' in a protein[70], or disulfide bonds that are selected in CDR loops of antibodies[71]. However, this general finding is far from uniform and, at the molecular level, is complicated by the allowable ensemble of molecular conformations in the bound versus free states and the contribution of solvent effects[72]. The net impact on affinity can best be described by the thermodynamics of binding. The dissociation constant is related to the Gibbs free energy of binding, which in turn is comprised of the enthalpy of binding (a measure of the energy associated with charge interactions, van der Waals forces, and hydrogen bond contacts at the binding interface versus in free solution) and entropy (a measure of the loss in available conformations when it is bound to the target versus free in solution).

$$K_d = e^{-\Delta G/RT}$$

$$\Delta G = \Delta H - T\Delta S$$

$K_d = dissociation\ constant$
$\Delta G = Gibbs\ free\ energy\ of\ binding$
$R = universal\ gas\ constant$
$T = temperature$
$\Delta H = enthalpy\ of\ binding$
$\Delta S = entropy\ of\ binding$

By 'locking' a peptide in one conformation (or more accurately, increasing the probability that the peptide in free solution is found in this conformation), the 'entropic penalty' for binding can be decreased significantly. This is demonstrated in a study by Sia et al. as a uniform decrease in the –TΔS term with increased helicity; the difference in entropy between bound and free goes

down, increasing affinity[73]. However, unless the molecular conformation of the helix is perfectly aligned with the conformation maximizing all molecular contacts, a more rigid structure can lower the enthalpy of binding (e.g. slightly mis-aligning a hydrogen bond), resulting in an eventual decrease in affinity with increasing rigidity.

From a thermodynamic perspective, a more rigid structure, pre-organized in the optimal bound conformation, will always be higher affinity due to the reduced entropic penalty upon binding *ceteris paribus*. However, in practice, all other aspects of binding are not equal. Improvements in affinity by rigidifying the ligand are often less than (and sometimes opposite of) those predicted by the entropy of binding due to the 'enthalpy/entropy compensation' phenomenon. This effect, where changes in the entropy and enthalpy of binding oppose each other when engineering an affinity ligand, have their origins in a variety of molecular mechanisms including perturbations in a system with multiple closely spaced energy levels, higher 'enthalpic' interactions restricting 'entropic' motion, and importantly, the large thermodynamic contribution of structured waters before and after binding[72]. This makes helicity an imperfect measurement for changes in binding affinity. In summary, while increased structure generally has the potential for higher affinity, this is not guaranteed for any individual interaction.

Box 1.2 Routes of Administration

The three routes of administration that span common delivery approaches for both small molecule drugs and biologics are oral (PO), subcutaneous (SC), and intravenous (IV) delivery. Oral delivery is the most challenging for stabilized peptides due to their low permeability and poor stability from stomach acidity and digestive proteolysis. Some agents, like cyclosporine and

other cyclic peptides mentioned in the main text, can overcome these barriers. Others necessitate subcutaneous injection, or if the dose is too large, intravenous administration.

Oral delivery for larger peptides is typically limited to local delivery in the gastrointestinal tract[74]. The improved stability from side-chain crosslinking can enable some absorption, albeit low, following oral gavage as seen with a 36-residue double stapled enfuvirtide agent[29,75]. A more clinical advanced example is the phase III trial of a formulated version of semaglutide[76]. Here, a permeability enhancer in the formulation aids in protection and absorption for this 4.1 kDa molecular weight peptide. Even with these advances, absolute absorption is still relatively low, but semaglutide is an ideal candidate for this approach given its safety at high doses, high potency, and slow clearance (so a relatively large oral dose and small absorbed fraction are tolerable).

Subcutaneous injection is a common delivery route for peptides since it enables self-administration and avoids degradation in the GI tract. The formulation and dose become important considerations given that a typical SC injection volume cannot exceed ~1 mL. Highly concentrated doses, depending on the physicochemical properties, could also cause local reactions. Recently, Zhang et al. demonstrated that peptide backbone stabilization can help increase the fraction of stabilized peptide absorbed after subcutaneous administration in mice[24].

Intravenous administration is a common delivery method for biologics, such as monoclonal antibodies, that have to be given at high (e.g. multiple mg/kg) doses. For example, ALRN-6924 had a maximum tolerated dose of 3.1 mg/kg when given as a weekly intravenous infusion (3 doses every 4 weeks)[9]. One disadvantage for stabilized peptides is that they have faster clearance than antibodies, necessitating more frequent delivery.

Box 1.3. Lipophilicity and LogP

Lipophilicity is a key determinant of the pharmacokinetic behavior of small molecule drugs. A drug must be lipophilic enough to partition into membranes for efficient absorption and distribution and for long circulation time (high plasma protein binding and kidney reabsorption). However, it must not be too lipophilic that it suffers from high first-pass metabolism or insufficient aqueous solubility making it unsuitable for delivery. Lipophilicity is traditionally quantified as LogP, the octanol-water partitioning coefficient, a measure of the extent to which a molecule partitions into octanol (a surrogate for the lipid bilayer) versus the aqueous phase. Molecules with a logP > 0 favor lipids over aqueous dissolution. Lipinski's rule of 5 states that a drug molecule should have a logP < 5 (generally between 0 and 5)[25]. This quantity can be calculated experimentally; however several computational programs exist allowing for high-throughput logP measurements for drug libraries[25]. Though computational programs are often accurate for small molecules, it has previously been shown that calculated logP values for peptides often deviate greatly from the experimentally measured values and that the discrepancy increases as peptide size increases[77,78]. This is attributed to the failure of fragment-based approaches to adequately consider intramolecular interactions such as hydrogen bonding and the effects of cyclization[30]. One method to circumvent inaccuracies of computational peptide logP measurements is to measure HPLC retention times and compare it to the retention times of small molecules with known logPs using the same HPLC method. Bird and colleagues have recently used HPLC retention times to compare lipophilicities of several peptide variants to aid in optimization of stapled Bcl-2 targeting peptides and have correlated this parameter with improved cellular uptake[44]. Valko et al. have also recently developed HPLC retention time methods to assess the lipophilicities of various potential peptide therapeutics[79]. This approach

could be useful for giving more accurate predictions of lipid partitioning given the challenges of predicting intramolecular hydrogen bonding.

Chapter 2 Identifying Determinants of Cellular Uptake of Stabilized Peptides

2.1 Abstract

Intracellular delivery has long been considered a major shortcoming of peptide stabilized peptide therapeutics due to their large molecular weight. In this Chapter, we study two physicochemical properties that have the potential to enhance uptake—lipophilicity and positive charge. We take an incremental and quantitative approach to explicitly measuring the effects of these two properties by starting with a peptide sequence containing two negatively charged glutamic acid residues and incrementally replacing them with non-charged glutamine residues. We subsequently stabilize the resulting three sequences with three different cyanine dye-linker conjugates of varying lipophilicity as measured by apparent LogD. The resulting 9 stabilized peptide variants, each with a different combination of charge and lipophilicity, are incubated with cells, imaged, and analyzed for the amount of intracellular uptake. Results showed that less negative charge does increase uptake but lipophilicity had the most significant influence on uptake with a LogD~3-3.1 being the optimum range for maximum uptake in this series of peptides.

2.2 Introduction

As previously mentioned, alpha helices (**Fig 2.1a**) are the most common secondary structures among proteins and are often involved in protein-protein binding interactions. Identifying these interactions and designing peptides from helices engaged in the binding pocket as well as chemically stabilizing them to promote protease stability and increase binding affinity is the approach that several have taken. One widely studied protein/protein interaction that is a common drug target for cancer therapy is the p53/MDM2 interaction. P53 is a transcription factor that regulates cell growth and apoptosis as a response to DNA damage and cellular stress. Its activity is regulated by MDM2, an E3 ubiquitin ligase that marks p53 for degradation when its functions are not necessary. Loss of p53 activity is the most common deficiency in human cancer, whether due to mutation of the gene or due to overregulation of MDM2[16]. Several groups have developed p53-based MDM2 inhibiting peptides, as discussed in Chapter 1. The most common stapling technique among these peptides is the all-hydrocarbon staple, which is the technique that was used for ATSP-7041 that led to the clinical lead compound, ALRN 6924, developed by Chang et al. of Aileron Therapeutics[9]. This stapling method, however, reduces the design space with regard to the linker. Iterative optimization of the peptide is completely sequence dependent. Lau and colleagues, who also designed a p53-based peptide for therapeutic modulation of the p53-MDM2 interaction, introduced a more simple method of creating different peptide variants. This

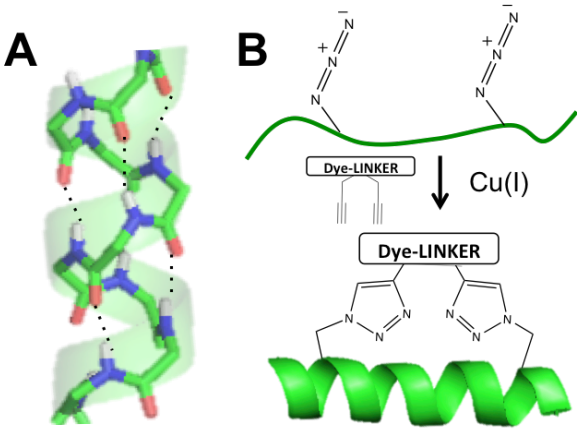

Figure 2.1 Alpha Helix and Double-Click Stabilization. (A) Alpha helix with dotted lines representing hydrogen bonds. (B) Double-click stabilization via copper-catalyzed azide-alkyne cycloaddition of linear peptide with bis-alkyne dye-linker.

method was first demonstrated by Torres and colleagues. Instead of cross reacting two complementary residues, they placed two azido-functionalized residues in *i, i*+7 locations and stapled the peptide with a di-alkyne linker by copper-catalyzed azide-alkyne cycloaddition (Fig 2.1b) —a well characterized click chemistry reaction[21,22]. Lau employed this strategy and termed this technique "double-click" stabilization[23]. After optimizing non-natural amino acid placement, they altered stabilized peptide properties via iterative optimization of the linker instead of the sequence. That is, they altered linker properties such as charge and lipophilicity, and stapled their di-azido peptide with several of these linker variants. They performed many of the same experiments to assess the efficacy of the peptide including binding affinity for MDM2, proteolytic stability in mouse serum, and *in vitro* incubation with a cancer cell line to determine permeability and the effect on native p53 activity. They found that the peptide with the most positively charged linker proved to have the most therapeutic effect. This result is expected as positively charged molecules would have an affinity toward cell membranes, which are negatively charged. However, this therapeutic effect was observed at 100μM peptide concentrations[6]. Typical therapeutic drug doses yield plasma concentrations between .01-10μg/μL[80]. This is over one order of magnitude lower than the *in vitro* concentrations used by Lau. Therefore, drug toxicity to healthy cells is a concern for *in vivo* applications, especially for positively charged molecules such as theirs that readily interact with negatively charged membranes. Although this peptide has poor efficacy, we will use this peptide as a model for measuring cellular uptake.

There is still much to be learned about the mechanisms by which peptides enter cells, however, Verdine and colleagues have determined that staple type and peptide charge are the two most important factors that determine cellular entry, with positively charged peptides more readily permeating cell membranes[39]. It is therefore not surprising that many of the "successful" MDM2

inhibiting peptides reported in literature with regard to stabilized peptide permeability and efficacy have been with positively charged peptide sequences and linkers. In many cases, however, these successes have been reported with no definitive proof that the peptides are having on-target efficacy. Cationic molecules at high concentrations can disrupt cell membranes, thereby causing cellular stress and toxicity. Seeing as though p53 is a transcription factor activated by cellular stress signals, upregulation of p53 and induction of apoptosis may not be due to target binding of the peptide, but by membrane disruption. Furthermore, as mentioned previously, cellular activity of stabilized alpha helices is typically achieved at high concentrations (20-100μM)[11]. This further supports the likelihood that these cationic stabilized peptides are having membrane toxicity, which has now been shown to be true for many published stabilized peptides[11,44]. Given the risk of lytic activity with cationic peptides, in this chapter, we will maintain charges of no more than +1, and in future chapters where we test for efficacy of drug candidates, we will directly assess lytic activity.

Various literature studying many types of peptide therapeutics (cyclic peptides, cyclotides, etc.) and 'Beyond Rule of 5' drug molecules has shown that lipophilicity (logD) and size are important determinants of membrane permeability, which is in line with the principles in Lipinski's Rule of Five[55]. For 'beyond Rule of Five' molecules however, permeability decreases more rapidly with an increase in molecular weight. Furthermore, the larger the molecule, the smaller the window in which permeability and aqueous solubility co-exist[81,82]. As discussed in Chapter 1, FDA-approved drug molecules with added lipophilic moieties have emerged over the past few years, also signaling the importance of lipophilicity. We will therefore do a more controlled analysis of the effects of lipophilicity and charge on cellular uptake of stabilized peptides.

2.3 Results & Discussion

In order to analyze the effects of charge and lipophilicity on cellular uptake of stabilized peptides, we chose a model peptide that would allow us to make incremental changes to its charge and LogD with minimal residue modifications. The peptide, which we call Plp (p53-like peptide) (**Fig 2.2**), was developed by Lau et al. and was based upon residues 17-29 of native p53

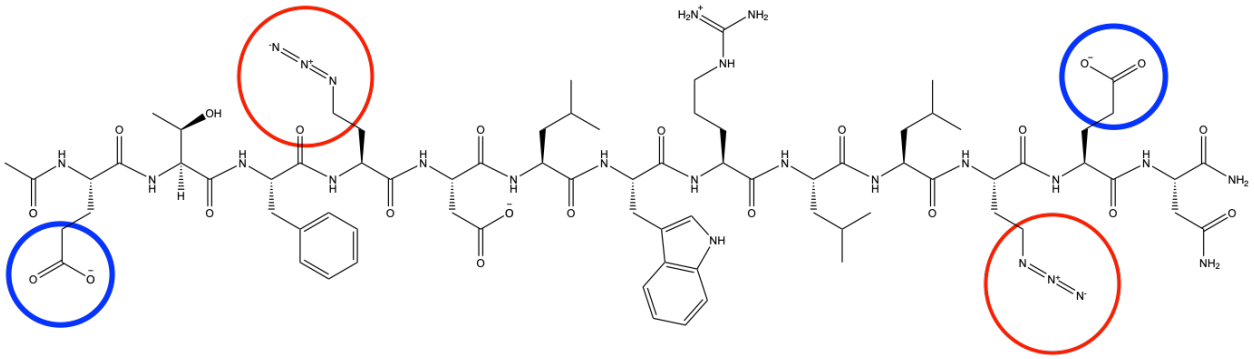

Figure 2.2 Chemical Structure of Plp. Circled for emphasis: the two glutamic acid residues (blue circles) that are modified to alter charge as well as the two azidohomoalanine side chains (red circles) for double-click stabilization with various linkers.

with residue modifications made to increase helicity and binding affinity[83]. The sequence (ETFXDLWRLLXEN, where X=Azidohomoalanine) features three carboxylic acid residues and an arginine residue, yielding a net charge of -2. It also features two azidohomoalanine residues in *i, i*+7 positions for double-click stabilization. Substituting the two glutamic acid residues for their carboxamide analogues (glutamine) and stabilizing the peptide with linkers of varying lipophilicities will allow us to generate a series of peptides with different charges and lipophilicities. We opted to use fluorophore-conjugated linkers to track and quantify uptake. The three fluorophores chosen are cyanine dyes Cy5.5, Cy7.5 and Sulfo-Cy7 with charges of +1, +1, and -1, respectively (**Fig 2.3**). The resulting series of peptides is listed in Table 2.1. We

stabilized three sequences, ranging in charge from -2 to 0, which yielded a total of 9 stabilized peptides.

2.3.1 Lipophilicity (LogD) and Charge

As discussed in Chapter 1, the octanol/water partitioning coefficient is widely used as a measure

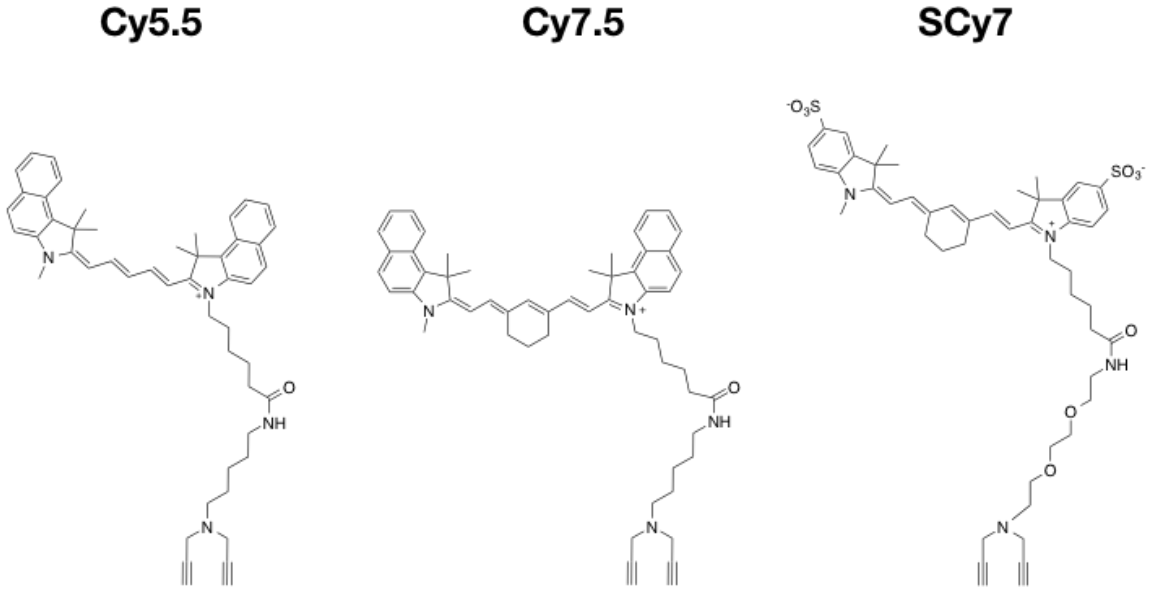

Figure 2.3 Dye-Linkers. Cyanine dyes, developed for their excellent far-red to near-infrared fluorescent properties, are typically hydrophobic from the conjugated ring structure (e.g. Cy5.5, left). The longer methine bridge of Cy7.5 increases the wavelength of fluorescence and the lipophilicity (center). Many cyanine dyes have sulfate groups added to improve hydrophilicity and solubility (e.g. SCy7, right).

of lipophilicity, and these values are typically estimated computationally. These computational methods do not consider intramolecular interactions such as hydrogen bonding within peptides. Therefore, we opted to measure lipophilicities by HPLC retention times and estimated apparent LogD values (Table 2.1) based on standards with known LogD.

Table 2.1 Stabilized Peptide Variants

Peptide [charge]	sequence	Dye	Charge	Apparent LogD (pH 7.4)
—		cy5.5	+1	3.07
—		cy7.5	+1	3.75
—		scy7	-1	***
PLP[-2]	ETFXDLWRLLXEN	none	-2	2.43
		cy5.5	-1	3.05
		cy7.5	-1	3.60
		scy7	-3	2.37
PLP[-1]	QTFXDLWRLLXEN	none	-1	2.55
		cy5.5	0	3.08
		cy7.5	0	3.63
		scy7	-2	2.38
PLP[0]	QTFXDLWRLLXQN	none	0	2.66
		cy5.5	+1	3.09
		cy7.5	+1	3.66
		scy7	-1	2.39

*** not measured

Cy7.5 is the most lipophilic of the fluorophores with a logD of 3.75, followed by Cy5.5 and finally Sulfo-Cy7 which is a hydrophilic sulfonated dye. As expected, the Cy7.5 conjugated variants were the most lipophilic while the Sulfo-Cy7 conjugated variants were the least lipophilic. It is also important to note that the non-stabilized peptides themselves are more lipophilic than Sulfo-Cy7 dye and that stabilization with Sulfo-Cy7 linkers made the peptides

less lipophilic. Given that Sulfo-Cy7 is a sulfonated, negatively charged dye, this is not surprising. Conversely, Cy7.5 and Cy5.5 are positively charged non-sulfonated cyanine dyes and are therefore much more lipophilic than the non-stabilized peptides. Cy7.5 features an additional ring structure within the cyanine group, thereby increasing its lipophilicity over Cy5.5. We expect that the Cy7.5 and Cy5.5 conjugated peptides will more readily partition into the cell's lipid membrane than the Sulfo-Cy7 variants. However, we will use the difference in lipophilicities between the two to determine whether there is an optimum lipophilicity. That is, if the peptide is approaching the limit of aqueous solubility, it may readily partition into the cell membrane but be slow to diffuse through. This may be the case for Cy5.5 as well, but if so, we expect this to be exacerbated with the Cy7.5 variants. For variants with the same linker but different sequences, the more negatively charged variants were less lipophilic than the more positively charged variants. This is due to the lack of solvent hydrogen bonding offered by the original glutamic acid residues upon substitution with glutamine. We will determine the effect that these incremental differences in charge has on cellular uptake, with the expectation that more positive charge will cause higher uptake.

2.3.2 Imaging

The first step to assessing uptake was imaging of cells incubated with peptide over various time points. To do this, we utilized HT1080 cells and incubated them with each stabilized peptide at 100nM concentration for up to 24 hours. Though not quantitative with respect to uptake, images show that for all variants, the peptide is localized in punctate spots within the cells, signaling

uptake by endocytosis (Fig 2.4). Though diffuse cytosolic signal is not visible, we may not be

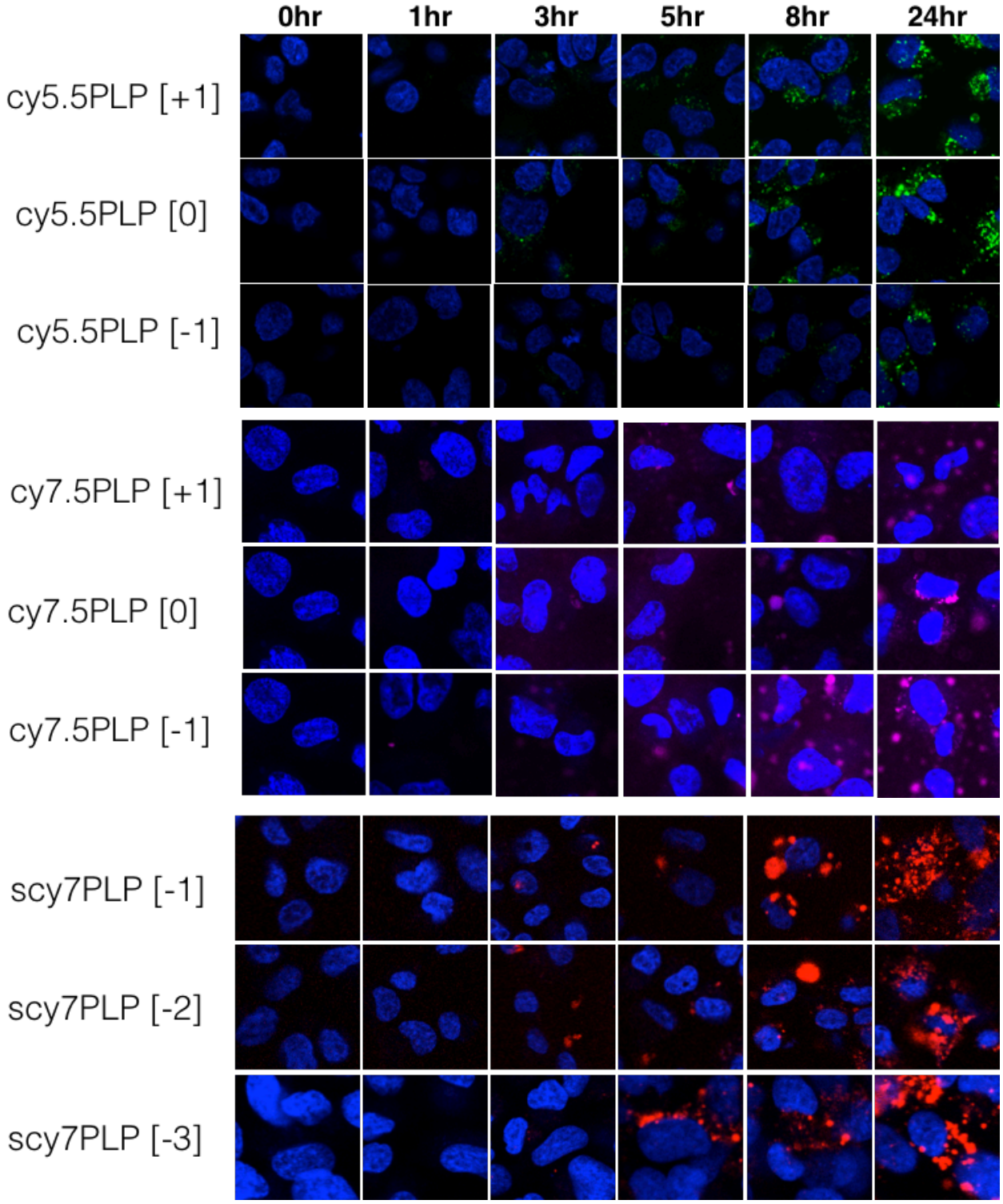

Figure 2.4 Cell Uptake Images. Dye-conjugated peptides were incubated with cells for up to 24 hours and imaged. Images with the same fluorophore were window-leveled the same but window-leveling is different for different fluorophores to best visualize peptide localization.

able to qualitatively observe this if it was present, especially given the brightness of the punctate spots. Therefore, it is impossible to conclude from these results which peptide variants, if any, are able to diffuse through the membrane to reach the cytosol, whether directly from the bulk media, or through escaping endosomes. Another aspect that cannot be verified from this imaging alone is whether the peptides were partitioned into the membrane before being endocytosed or whether they were primarily pinocytosed. We expect that the more negatively charged and hydrophilic the peptides, the more likely it remains in the aqueous bulk and gets pinocytosed while the more lipophilic and positively charged variants partition into the membrane and enter the cell through endocytosis (as well pinocytosis). Quantitative uptake data will offer more insight into what uptake phenomena are occurring.

The images demonstrate that charge does seem to have an effect on uptake rate. In the case of Cy5.5 and Cy7.5-conjugated peptides, the negatively charged variants show slower uptake over time compared to the neutral and positively charged variants. In the case of Sulfo-Cy7 variants where all are negatively charged, it is more difficult to discern differences in uptake rate, however the most negatively charged variant (-3 charge) only begins to show uptake at 5 hours while the others show uptake (qualitatively) starting at 3 hours. The actual amount of uptake over time will be quantified via bulk uptake measurements.

2.3.3 Bulk Cell Uptake

Uptake of stabilized peptides into HT1080 cells over 24 hours was quantified using bulk cell measurements in 96-well plates. The number of peptides per cell over time are plotted and the final 24 hour values are listed (Fig 2.5). As expected, across all dyes, the least negatively charged variants had the fastest uptake. That is, the stabilized plp[0] variants had the highest

uptake compared to plp[-1] and plp[-2] stabilized with the same dye-linker. Furthermore, Sulfo-Cy7 variants had the lowest uptake with 10^5 peptides per cell at 24 hours. Given that these variants are the least lipophilic (and most negatively charged), pinocytosis is likely a major

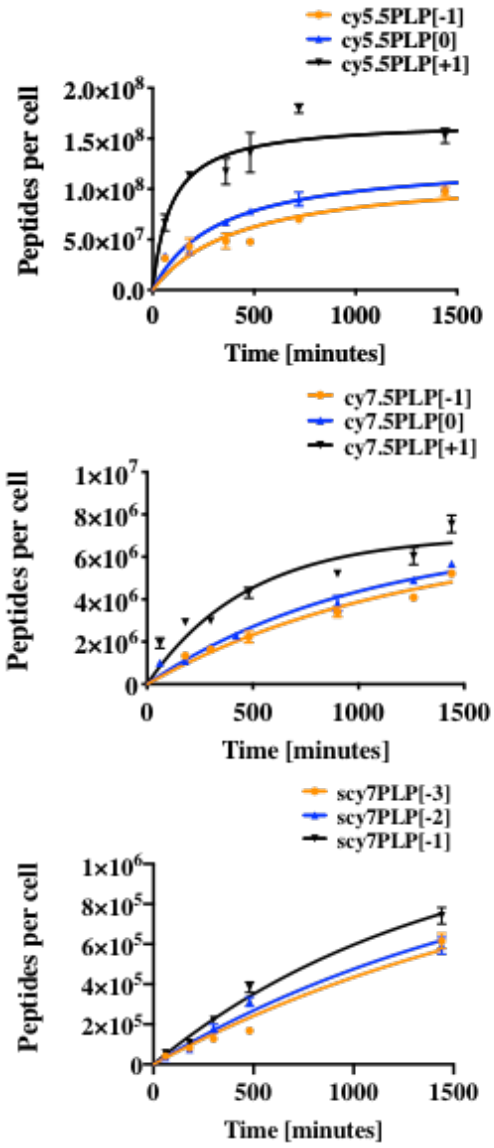

Peptide	Peptides per cell (24hr)
cy5.5PLP[+1]	1.5E+08
cy5.5PLP[0]	1.0E+08
cy5.5PLP[-1]	9.8E+07
cy7.5PLP[+1]	7.6E+06
cy7.5PLP[0]	5.7E+06
cy7.5PLP[-1]	5.2E+06
scy7PLP[-1]	7.4E+05
scy7PLP[-2]	5.9E+05
scy7PLP[-3]	6.2E+05

Figure 2.5 Bulk Cell Uptake Measurements. Uptake curves (left) and maximum uptake amounts at 24 hours (right) are shown for all stabilized variants. Cy5.5 stabilized variants had maximum uptake amounts of ~10^8, followed by Cy7.5 stabilized variants which had uptake amounts of ~10^6 and lastly SCy7 variants which had uptake amounts of ~10^5.

contributor to uptake of these variants which would lead to slower uptake overall. This is supported by the uptake curves which are much more linear than the Cy5.5 and Cy7.5 uptake

curves, suggesting at least partial 0 order kinetics which is consistent with pinocytosis. In contrast, the Cy5.5-stabilized variants had the fastest uptake with 10^8 peptides per cell at 24 hours. Uptake curves follow 1st order kinetics, suggesting non-specific, linear uptake (either directly across membranes or via endosomal uptake). As previously discussed, one of the goals of this project was to determine the optimal lipophilicity for efficient uptake and determine what is too lipophilic. The Cy7.5 variants with just 10^6 peptides per cell at 24 hours seem to be beyond the ideal lipophilicity range for uptake. Their uptake is more efficient than the more hydrophilic Sulfo-Cy7 variants, suggesting that the uptake mechanism is likely driven by more than pinocytosis. Given the high lipophilicity, the peptides are likely partitioning into the membrane and endocytosed; however, passive diffusion through the membrane after partitioning is slower with such a hydrophobic peptide. Increased serum binding may be another cause for slower internalization of the Cy7.5 variants compared to Cy5.5 variants. The Cy5.5 peptide variants are lipophilic enough to partition into the membrane, but may avoid extremely high protein binding of Cy7.5 peptides. Since the Cy5.5 and Cy7.5 uptake curves both seem to indicate first order kinetics, we conclude that the uptake rates are likely governed by both mechanisms and that the Cy5.5 variants are more efficiently able to be taken up by cells.

2.4 Conclusions

The goal of the work in this chapter was to elucidate the roles of charge and lipophilicity on cellular uptake. Literature has shown that both are important, but not in the controlled manner that we have presented here. Using the same peptide sequence with slight side chain modifications to incrementally change charge and various stabilizing linkers to alter LogDs, we showed that both impact uptake efficiency. Although we limited positively charged variants to a single +1 charge, those variants had significantly higher uptake (~50% more for Cy5.5plp[+1])

than the neutral charged variant with the same linker. This result is promising for peptide design when trying to avoid membrane toxicity. Furthermore, even going from a negative charge to neutral charge provides improvements in uptake. The glutamic acid to glutamine substitution provided a minimalistic way to achieve the required charge modifications, however, there is a possibility that an increase in uptake yielded by an increase in charge could sacrifice other desirable properties, such as binding affinity, stability, and helicity. These effects will be explored in Chapter 2.

Lipophilicity proved to be the most significant driver of uptake. Although the charge differences within dye groups caused changes in uptake, the difference in uptake between variants of different linkers was much more distinct. Cy5.5 variants had 24-hour uptake values of 10^8—almost two orders greater than the Cy7.5 variants and 3 orders greater than the Sulfo-Cy7 variants. Furthermore, although Cy7.5 variants are the most lipophilic with LogDs of 3.6-3.7, this proved to be too lipophilic for efficient uptake. We hypothesize that those variants may partition quickly into the membrane but are slow to diffuse through the membrane. Serum binding and aggregation may also be major factors precluding these variants from entering the cell more efficiently. We therefore conclude that the Cy5.5 variants are in the best lipophilicity range for this series of peptides (logD 3-3.1) and that Cy5.5plp[+1] has the most efficient uptake with a logD of 3.1 and a +1 charge. These results will help inform peptide design and characterization in Chapters 2 and 3.

2.5 Experimental Methods

2.5.1 Peptide Conjugate Synthesis

Peptides used in this chapter (plp[-2], plp[-1], and plp[0])were purchased in linear form from InnoPep, Inc.

Dye-conjugated bis-alkyne linkers were synthesized as described by Zhang[84]. Briefly, to make the lipophilic and hydrophilic bis-alkyne linkers for conjugation to NHS ester fluorophores, N-boc-cadaverine or N-boc- 2,2'-(ethylenedioxy)diethylamine was dissolved in acetonitrile and mixed with DIPEA (3 equiv) and propargyl bromide (3 equiv). After stirring overnight, the reaction mixtures were subjected to flash chromatography (80:7:1 chloroform:methanol:ammonium hydroxide). The desired linker fractions were collected, deprotected in 50% TFA in DCM, purified using reverse-phase HPLC, and characterized by electrospray ionization mass spectrometry (ESI-MS). All reagents were purchased from Sigma Aldrich.

Linkers were conjugated to NHS ester fluorophores (Cy5.5, Cy7.5 and Sulfo-Cy7, purchased from Lumiprobe) in water buffered with 7.5% sodium bicarbonate. Reactions were stirred for 20 minutes before purification with reverse-phase HPLC in water and acetonitrile buffered with 0.1% TFA. Products were characterized via MALDI-TOF mass spectrometry.

Peptides were double-click stabilized via copper catalyzed azide alkyne cycloaddition in 1:1 tert-butanol:water with the bisalkyne dye-conjugated linkers (1 equiv). The peptides and linkers were mixed with copper (II) sulfate (10 equiv), tris-hydroxypropyltriazolylmethyl)amine (10 equiv) and sodium ascorbate (50 equiv) at room temperature overnight before HPLC purification in water and acetonitrile buffered with 0.1% TFA. Products were characterized via MALDI-TOF mass spectrometry.

2.5.2 HPLC Retention Time

Peptides and standards were run on a reverse-phase HPLC column in mobile phase containing 50mM ammonium acetate at pH 7.4 in water and acetonitrile with a gradient of 10-95% over 50 minutes. Standards were chosen based on a previously published method for estimating logD from HPLC retention time [85]. All standards used here have a logD(pH 7.4) greater than 0 as measured by ChemAxon MarvinSketch software and are acidic (with the exception of Cyclosporin A which is a neutral cyclic peptide) to best reflect the peptides analyzed, all of which are acidic and mostly water insoluble. A standard curve was generated and apparent logD's were calculated from the standard curve equation (Appendix A).

2.5.3 Imaging

HT1080 fibrosarcoma cells cultured in DMEM supplemented with 10% fetal bovine serum and 1% penicillin/streptomycin were plated in 8-well chamber slides at $1x10^5$ cells/well and incubated at 37C overnight. The following day, peptides were dissolved in media to a final concentration of 100nM. Media was removed from the cell wells and replaced with media containing peptide. Cells were incubated with peptide for 0, 1, 3, 5, 8, and 24 hours before removing the peptide, washing with PBS, and imaging using an Olympus FV1200 confocal microscope with a 60x water immersion objective and the appropriate lasers for each fluorophore. Images in the same sample set were window-leveled with the same settings using ImageJ software.

2.5.4 Bulk Cell Uptake

HT1080 cells were plated in a 96 well plate at $1x10^5$ cells/well and incubated at 37C overnight. In addition to the negative control and experimental wells, a set of wells was reserved for a final cell count at the end of the experiment to allow quantification of peptides per cell. The day after

plating, media was removed from the wells and replaced with media containing peptide at 100nM. After peptide incubation, media was removed, cells were washed, cells reserved for the cell count were harvested and counted, and the experimental cell wells were treated with RIPA buffer with 0.5% BSA. Plates were covered with foil to protect from light and stored at 4C overnight. The following day, lysed cell samples were transferred to another plate and imaged using an OdysseyClx Imaging Systerm from LI-COR. Fluorescence intensity was converted to peptide conjugate concentration using standards curves generated with peptide dissolved in the lysis buffer (RIPA buffer with 0.5% BSA). Using the cell count, the volume of sample, and Avogadro's number, peptide concentration was converted to the number of peptides per cell.

Chapter 3 Choosing Novel Early Stage Stabilized Peptide Drug Candidates

3.1 Abstract

In this Chapter, we analyze a series of novel stabilized peptides to determine which peptides have the best therapeutic potential based on binding affinity and *in vitro* efficacy and toxicity. The peptides presented here were discovered via Stabilized Peptide Engineering with E. Coli Display (SPEED)—a high throughput bacterial surface display and stabilization technique to screen peptide libraries against targets of interest. Select high affinity MDM2 binders identified through this method were synthesized via solid phase peptide synthesis and tested for in solution binding affinity, helicity, cell-killing efficacy, and off-target membrane toxicity. We found that although helicity increased upon stabilization, helicity itself was not an indicator of high binding affinity or efficacy when comparing between peptides. The most promising of the peptides in the series is pepC—a disulfide containing peptide with a K_d of 1.7nM stabilized. When compared to a highly potent all-hydrocarbon stapled peptide with a 0.91nM K_d, ATSP-7041, stabilized pepC has similar *in vitro* efficacy in two cell lines as well as negligible membrane toxicity. Surprisingly, another novel peptide discovered via SPEED with a k_d of 5.1nM stabilized, pepG, showed no efficacy despite its high binding affinity. We conclude that on-target efficacy in cells is not directly proportional to binding affinity for these agents.

3.2 Introduction

There are several methods that have been developed to discover novel peptides to block PPIs. Once a PPI has been identified, one must design a peptide sequence with more favorable binding

to the protein of interest than the native binding partner. The most high-throughput of these peptide discovery methods are display techniques (e.g. phage display, mRNA display, etc.)[86,87] that exploit cellular machinery to create vast libraries of unique peptides that can be screened against targets, sorted, and identified via genetic sequencing. One such technique, developed by my colleague, is Stabilized Peptide Engineering with E. Coli Display (SPEED)[88]. This is a bacterial surface display technique yielding libraries of up to 10^9 peptides that are double-click stabilized directly on the bacterial surface prior to screening with the target protein. Using this method, we identified a series of high affinity stabilized peptide binders to MDM2. Although peptides may show good target binding on the bacterial surface, this does not necessarily translate to efficient in-solution binding as well as other properties. The objective of this chapter is to identify possible drug candidates for further study of physicochemical properties based on in-solution binding affinity and *in vitro* efficacy.

The starting peptide used as a template in Chapter 2, plp[-2], was used as a point of comparison in the bacterial surface screening of MDM2-binding peptides with SPEED. As discussed in Chapter 2, plp[-2] has shown *in vitro* efficacy at only high concentrations. In this chapter, we probe the binding affinity and efficacy of this peptide and the other charged variants, plp[-1] and plp[0], alongside the novel sequences discovered with SPEED. These results provide insight into ultimately identifying the most important parameters that determine efficacy in addition to the determinants of cellular penetration which were explored in Chapter 2.

3.3 Results and Discussion

3.3.1 Binding affinity

The peptides in this study were discovered via SPEED with propargyl ether as the chosen linker. Since MDM2-inhibiting peptides are lipophilic given the hydrophobic binding pocket, this linker provides some added aqueous stability. For the in-solution studies (in contrast to the initial cell surface characterization), we opted to use this same linker as the results of the bacterial surface selection process. Recent work has demonstrated that the peptide properties are linker-dependent and target binding affinities could be drastically altered with the use of a different linker. The binding affinities of the propargyl ether stabilized peptides in solution, measured by biolayer interferometry, are listed in Table 3.1. Plp[-2] has a binding affinity of 15nM, a 7.5-fold improvement over its non-stabilized form. In Chapter 2, we saw that incrementally increasing the charge of plp[-2] yielded improvements in cellular penetration; however, those results did not provide information on how those changes would affect target engagement. Here, we see that those changes negatively impacted the binding affinity of the peptide, with plp[-1] and plp[0] having 17nM and 74nM K_d's, respectively. This result exposes a potential issue when engineering peptides without the help of high-throughput directed evolution techniques. Even small changes to one sequence in hopes of creating more favorable biophysical characteristics can alter the binding interaction with the target. We therefore shift our focus to the novel sequences discovered.

Table 3.1 Peptide Molecular Weights and Binding Affinities

Name	Sequence	Molecular Weight		Binding Affinity (nM)		
	X= Azidohomoalanine	Stabilized	Non-stabilized	Stabilized	Non-stabilized	△
plp-2	ETFXDLWRLLXEN	1823.0	1728.9	15 ± 5.3	113 ± 16	7.5
plp-1	QTFXDLWRLLXEN	1822.0	1727.9	17 ± 3.4	157 ± 29	9.2
plp0	QTFXDLWRLLXQN	1821.0	1726.9	74 ± 28	454 ± 106	6.1
pepG	GGTFXGYWADLXAF	1690.8	1596.7	5.1 ± 4.7	21 ± 3.7	4.1
pepV	VLSFXDYWNLLXGS	1800.9	1706.8	14 ± 4.3	131 ± 40	9.4
pepC	VCDFXCYWNDLXGY	1881.0	1787.7	1.7 ± 0.16	6.8 ± 2.8	4
plp-2 F19A	ETAXDLWRLLXEN	1746.9	1652.8	604 ± 177	>10,000	-
pepC F19A	VCDAXCYWNDLXGY	1805.7	1712.8	2781 ± 1202	3888 ± 2007	1.4

The novel peptides displayed here were the variants with the lowest K_d's. PepG, the lowest molecular weight peptide in the series, has a 5.1nM binding affinity—a 3-fold improvement over plp[-2] and a modest 4-fold improvement over the non-stabilized pepG. PepV has a binding affinity of 14nM, similar to plp[-2], but with a 9.4-fold improvement over its non-stabilized form—the largest fold improvement in binding affinity from non-stabilized to stabilized out of all peptides in this series. PepC, which features i, i+4 cysteine residues that form a disulfide (Fig. 3.1), has the best binding affinity with a Kd of 1.7nM. Even in non-stabilized form, its 6.8nM K_d is lower than the K_d of all other stabilized variants except pepG. The final two peptides in Table 3.1 are the non-binding F19A mutants of plp[-2] and pep[C],

both of which serve as negative controls for the binding affinity assay. In the next section, we examined the helicity of each variant in the context of the binding affinities.

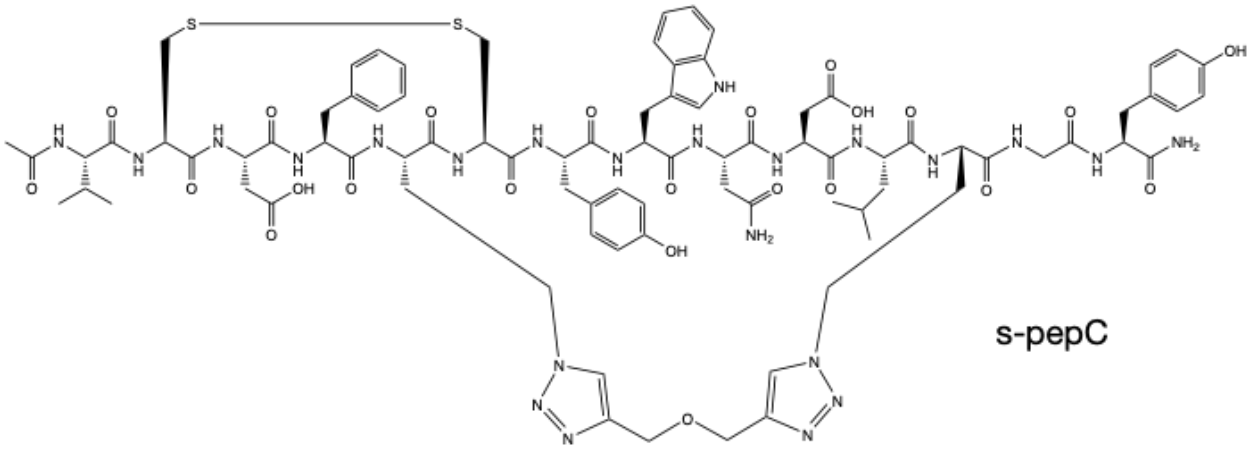

Figure 3.1 Chemical Structure of PepC

3.3.2 Helicity

As discussed in Chapter 1, increased helicity, achieved by chemically stabilizing peptides, often promotes increased binding affinity as well as proteolytic stability. The affinity measurements showed that for all peptides, stabilization increased binding affinity. Here, we measure the percent helicity of each peptide in non-stabilized and stabilized form to determine 1) whether stabilization did in fact increase the helicity and 2) if more helical peptides are generally tighter

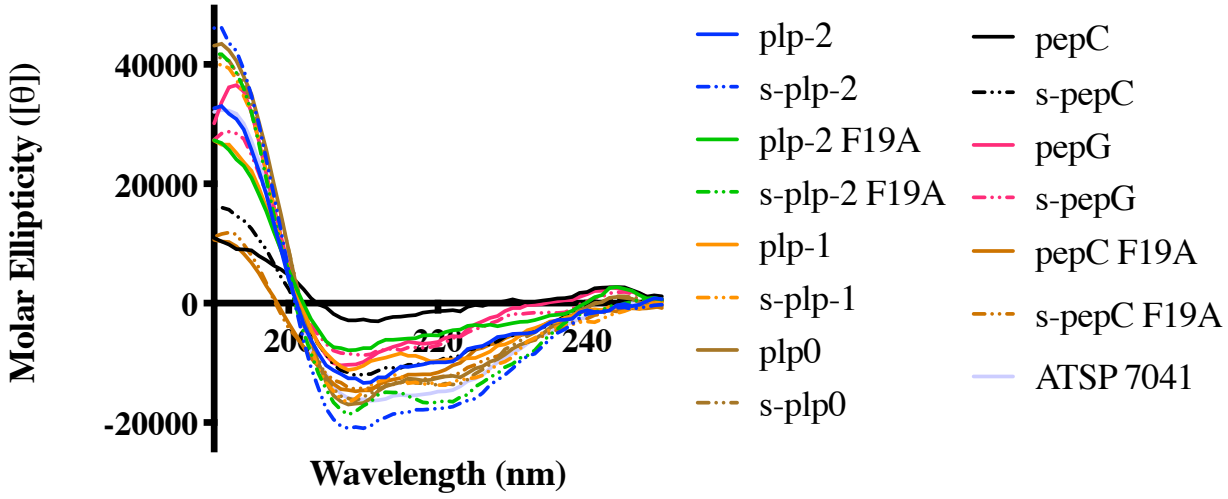

Figure 3.2 Graph of Molar Ellipticities

binders. Helicities were calculated from molar ellipticities measured by circular dichroism (Figure 3.2). Table 3.2 shows the percent helicities for each peptide. Firstly, the data shows that all peptides are more helical in stabilized form than in non-stabilized form, however the fold-change in helicity varies widely. Plp[-2] is by far the most helical peptide with 53% helicity in stabilized form, a 1.8-fold increase over non-stabilized. Interestingly, plp[-2] has the lowest binding affinity despite having the highest helicity, suggesting that binding affinity is more

Table 3.2 Peptide Helicities

Name	Helicity (%)		
	Stabilized	Non-stabilized	△
plp-2	53	30	1.8
plp-1	40	29	1.4
plp0	41	37	1.1
pepG	18	17	1.1
pepV	NM	NM	-
pepC	28	4	7
plp-2 F19A	50	14	3.7
pepC F19A	37	31	1.2

sequence dependent than helicity dependent, as others have also shown[83,89]. PepG has the lowest percent helicity despite having the second-best binding affinity. Furthermore, stabilization had a minimal effect on helicity with a modest increase of 1% upon stabilization. The lack of helicity in this peptide is not surprising as it contains 3 glycine residues which are considered to be "helix-breakers"[90] similar to the effects of proline, n-methylated amino acids and D-amino acids. Though still a strong binder despite low percent helicity, pepG may be susceptible to more rapid

degradation than the more helical peptides in the series, which could ultimately hinder efficacy. PepC experienced the largest increase in helicity upon stabilization with a 7-fold increase from just 4% to 28% helicity. The lack of helicity is likely due in part to the disulfide bond, as the reduced form of the peptide is more helical than the oxidized, as we have previously reported[88]. Again, given that the binding affinity of the non-stabilized pepC is stronger than most stabilized variants in this series, the sequence dependence is more significant than the percent helicity. Lastly, pepV, the variant with the biggest improvement in binding affinity upon stabilization, does not have a reported percent helicity due to the peptide being too hydrophobic to perform the measurement. Since helicity measurements were taken in 1:1 water: acetonitrile, the lack of solubility in this partly organic solvent could be a significant liability in the aqueous extracellular and intracellular environments.

3.3.3 In vitro efficacy

Based on the binding affinities, we chose a subset of peptides in this series to assess efficacy—pepC, pepG, plp[-2] and the non-binding control, pepC F19A. PepC and pepG have the best binding affinities and therefore show promise as possible early stage lead compounds. Though previously reported data for plp[-2] shows low efficacy at high concentrations (Chapter 2), we measured the efficacy with a propargyl ether linker, which has not been reported. We did not include the other charged variants, plp[-1] and plp[0] due to their low binding affinities compared to plp[-2]. We also did not include pepV due to its low aqueous solubility, making it difficult to handle in *in vitro* assays. As a point of comparison for efficacy, we included the all-hydrocarbon stapled MDM2-inhibiting peptide, ATSP-7041, that has a reported binding affinity of 0.91nM and is the precursor to a clinical lead compound currently undergoing clinical trials[9,63].

Cell viability in the presence of stabilized peptides (denoted with s-) after a 5-day incubation was measured in two p53-sensitive cell lines, SJSA-1 and LnCAP (Figure 3.3), and two p53-insensitive cell lines, Saos2 and DU145 (negative controls) (Figure 3.4). Results show that ATSP-7041 is the most potent in both SJSA-1 and LnCAP cell lines with IC50's of 579nM and 168nM, respectively. PepC follows closely in efficacy with 665nM and 182nM IC50's, respectively. Surprisingly, pepG shows little to no efficacy in these cell lines, despite having only 3-fold lower binding affinity than pepC. Not surprisingly, however, plp[-2] also shows little to no efficacy in these p53-sensitive cell lines.

Cell viability in the p53-insenstive cell lines Saos2 and DU145 was measured to assess off-target toxicity, as these cell lines do not express a functional p53 gene and are therefore insensitive to MDM2 inhibition. In Saos2, all peptides showed little toxicity in the measured concentration range. In DU145 however, pepG showed some toxicity (IC50=1629nM), suggesting some off-target toxicity. In order to further study the off-target effects of these peptides, we directly assessed membrane toxicity, a major concern for peptides with intracellular targets.

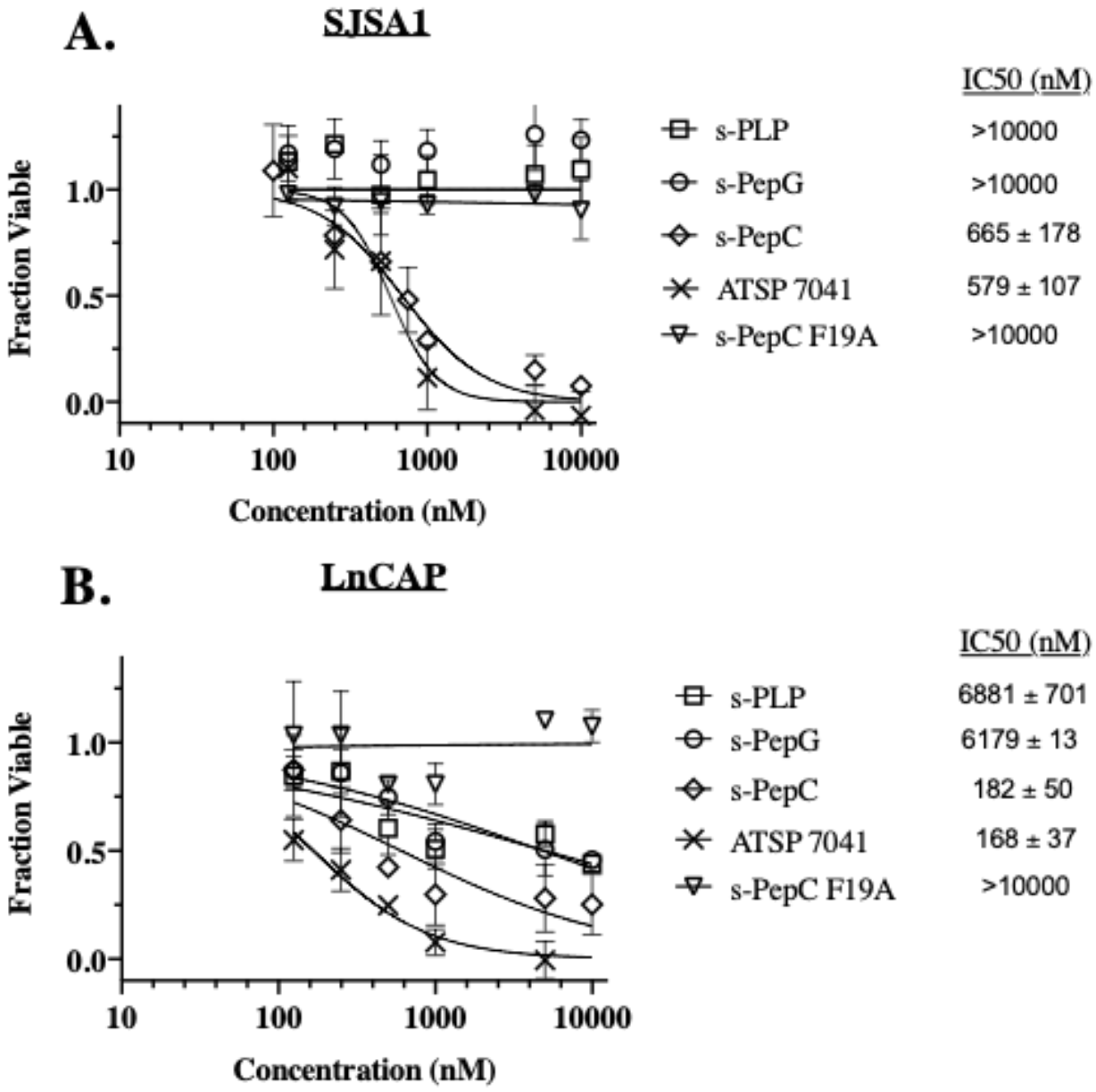

Figure 3.3 Cell Viability in p53-sensitive Cell Lines

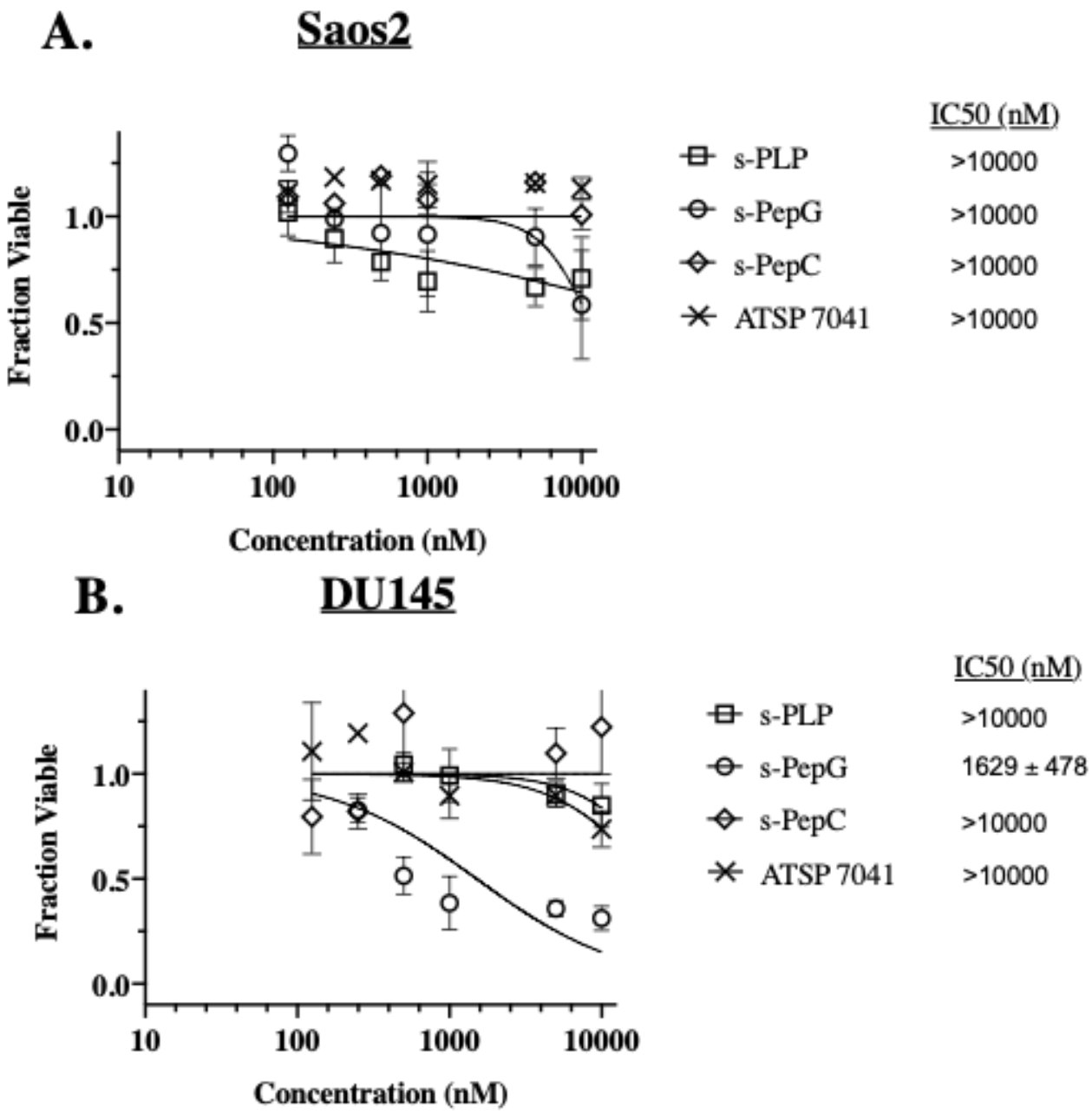

Figure 3.4 Cell Viability in p53-null Cell Lines

3.3.4 Membrane Toxicity

Lipophilic and amphiphilic peptides, particularly those that are positively charged, can induce non-specific cell death by directly interacting with and permeabilizing cell membranes [11]. To detect if any of these peptides were permeabilizing cells, we used lactate dehydrogenase leakage

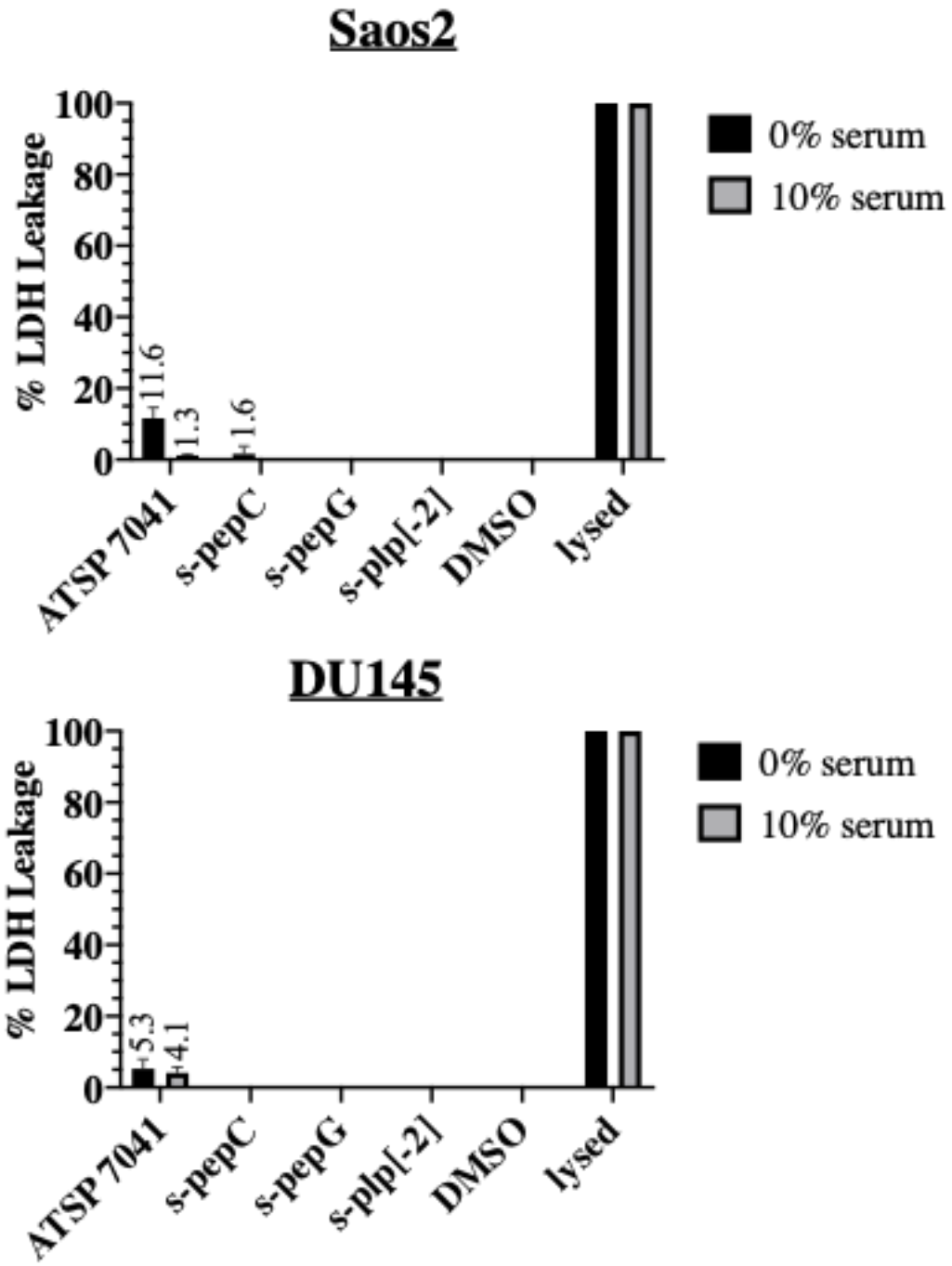

Figure 3.5 LDH Leakage

(LDH) as a measure of membrane toxicity. Using the same p53-null cell lines, Saos2 and DU145, cells and peptide were incubated with and without serum for 24 hours (to minimize the

effects of cell doubling on assay sensitivity). Results, shown in Figure 3.5, show that only ATSP-7041 and pepC show minimal LDH leakage in Saos2 which is exacerbated by the removal of serum. Furthermore, only ATSP-7041 shows minimal LDH leakage in DU145. Given that the LDH leakage assay was done over 24 hours while the cell viability assay was done over the course of 5 days, there is a possibility that damage might occur over 5 days that is not captured in just 24 hours. However, given the lack of any LDH leakage by pepG and the slight LDH leakage of ATSP-7041 which did not show considerable cell-killing in the 5-day viability assay in the insensitive cell lines, it is likely that the mechanism of pepG's cell-killing in DU145 is caused by something other than membrane damage. Furthermore, these data, as well as the cell killing results above, support the notion that the efficacious peptides are largely cell penetrant in a manner that leaves cell membranes intact.

3.4 Conclusions

In this chapter we explored a series of peptides engineered through a bacterial surface display and stabilization method developed in our lab. We took the sequences that yielded the best binding affinities on the bacterial surface, synthesized and stabilized the peptides in solution, and measured their in-solution binding affinities, helicities, and *in vitro* efficacy. Binding affinity results showed that incrementally increasing the charge of plp[-2] by substituting the glutamic acid residues with glutamine caused a decrease in binding affinity, especially for plp[0] which had a drastic 5-fold increase in K_d over plp[-2]. This supports the need for a high-throughput screening technique like SPEED so that various high affinity peptides can be engineered and later tested for favorable *in vitro* properties without needing to make potentially detrimental alterations to an existing sequence. Furthermore, binding affinity results showed that there are

two novel high affinity peptides, pepC and pepG, with 9 and 3-fold lower K_d's than plp[-2]. Both peptides proved to be far less helical than plp[-2], showing that binding affinity is more sequence dependent than helicity dependent when comparing across various peptides. Although we might have expected both pepC and pepG to have better *in vitro* efficacy than plp[-2], data showed that only pepC has efficacy, signaling that binding affinity may be only a partial factor in the efficacy (or lack thereof) of pepG and peptides in general. Finally, pepC is remarkably close in potency to ATSP-7041, making it a promising lead peptide for further therapeutic development.

The goal of this chapter's work was to identify early stage lead peptides for further study of physicochemical properties that promote efficacy. We have identified one peptide, pepC, with high *in vitro* potency, comparable to the published ATSP-7041. Many outstanding questions remain, including why pepC and ATSP-7041 have efficacy while the other peptides (plp[-2] and pepG) do not. ATSP-7041 and pepC have the best binding affinities, but peptides with only slightly higher Kd values, such as pepG, have no detectable on-target cell killing. Clearly, other factors impact the quantitative efficacy of these agents, but the magnitude of these factors remains unknown. The rate of cellular penetration, which is determined by a number of factors including lipophilicity, amphiphilicity, and charge, is widely acknowledged to be important. One must also consider proteolytic stability which affects how much peptide is available to engage with the target once inside the cell. In Chapter 4, we quantify the physicochemical properties we believe are the biggest determinants of efficacy in order to answer the question of why some peptides in our series showed efficacy while others did not.

3.5 Experimental Methods

3.5.1 Peptide Synthesis

Peptides were synthesized via solid phase peptide synthesis in dimethylformamide (DMF) on a CEM Liberty Blue Microwave Peptide Synthesizer using Fmoc amino acids, HBTU activator, diisopropylethylamine (DIPEA), hydroxybenzotriazole (HOBt) and Rink amide resin. Post-synthesis, peptides were rinsed with dichloromethane (DCM) and cleaved with a cocktail of 95% (v/v) trifluoroacetic acid (TFA), 5% (v/v) H_2O, 5% (w/v) phenol, and 2% (v/v) triisopropylsilane (TIPS) under nitrogen bubbling for 2-4 hours. After cleavage, TFA was evaporated under nitrogen and the remaining peptide solution was ether precipitated in tert-butyl methyl ether and stored at -20C overnight before lyophilizing to powder. Fmoc amino acids, HBTU and resin were purchased from ChemPep, Inc. All other reagents were purchased from Sigma Aldrich.

Peptides were stabilized with propargyl ether via copper catalyzed azide-alkyne cycloaddition as described in section 2.4.1. Peptides were characterized with electrospray ionization mass spectrometry and HPLC (Table 3.3).

ATSP-7041 was provided by the University of Michigan Peptide Synthesis Core.

3.5.2 Biolayer Interferometry

Binding affinity of peptides to MDM2 truncate (residues 10-118) was performed with biolayer interferometry (BLI) using an Octet Red96 system (ForteBio). MDM2 truncate was biotinylated with NHS-PEG4-Biotin (Thermo Fisher) and diluted to 500nM in assay buffer (0.3% (w/v) BSA in phosphate buffered saline (PBS)) before being immobilized onto Super Streptavidin Biosensors. Peptides were diluted in assay buffer at 10 concentrations—each plated in a 96-well plate for binding affinity measurements according to the manufacturer's protocol. Resulting

binding kinetics curves were fit in GraphPad Prism. Binding curves are documented in Navaratna 2020[88].

Table 3.3 Peptide Characterization

Name	Sequence	Stabilized		% Purity	Non-stabilized		% Purity
		Predicted Mass	Observed Mass	HPLC 214nm	Predicted Mass	Observed Mass	HPLC 214nm
plp-2	ET**FX**DL**W**RL**LX**EN	1823.0	1823.0	97.7%	1728.9	1728.9	>98%
plp-1	**Q**T**FX**DL**W**RL**LX**EN	1822.0	1822.0	95.8%	1727.9	1727.9	95.4%
plp0	**Q**T**FX**DL**W**RL**LX****Q**N	1821.0	1821.0	95.1%	1726.9	1726.9	97.7%
pepG	GGT**FX**GY**W**AD**LX**AF	1690.3	1690.8	96.2%	1596.7	1596.7	>98%
pepV	VLS**FX**DY**W**NLL**X**GS	1800.9	1800.9	>98%	1705.8	1705.8	>98%
pepC	VCD**FX**CY**W**ND**LX**GY	1881.7	1881.0	>98%	1787.7	1787.7	97.5%
plp-2 F19A	ET**A****X**DL**W**RL**LX**EN	1746.9	1746.9	>95%	1652.8	1652.8	>95%
pepC F19A	VCD**A****X**CY**W**ND**LX**GY	1805.7	1805.6	>98%	1712.8	1712.7	>98%

3.5.3 Circular Dichroism

Percent helicity was measured by circular dichroism using a JASCO J-815 spectropolarimeter. Peptides were diluted in assay buffer (1:1 water:acetonitrile) to 10uM and transferred to a 1mm path length quartz cuvette. All measurements were taken in three accumulations from 25nm to 190nm and percent helicities were computed based on molar ellipticities at 222nm.

3.5.4 Cell Viability Assay

Cell viabilities in the presence of stabilized and non-stabilized peptides were assessed in four human cancer cell lines. The p53-sensitive cells lines used here are SJSA-1 (osteosarcoma) and LnCAP (prostate adenocarcinoma) with Saos2 (osteosarcoma) and DU145 (prostate adenocarcinoma) serving as p53-null and mutant p53-expressing negative control cell lines, respectively. Each cell line was passaged with 10% Fetal Bovine Serum (FBS), 1% penicillin/streptomycin, and respective culture media: SJSA-1, LnCAP, and DU145 in RPMI 1640; Saos2 in DMEM. Upon confluency, cells were plated in triplicate in 96-well plates at the following cell densities: DU145 and SJSA-1 at 500 cells/well, Saos2 at 2,000 cells/well, and LnCAP at 4,000 cells/well, and incubated at 37°C for 24 hours. Each cell line was treated with each of the four peptides: pepG, pepC, plp[-2] and ATSP-7041. PepG, pepC and plp[-2] were tested in non-stabilized and propargyl ether stabilized forms while ATSP-7041 was tested as is and in its hydrocarbon stapled form. Peptides were added to cells in concentrations ranging from 0 (vehicle only control) to 10μM in media with 10% FBS and plates were incubated for five days at 37ºC. Assays were ended with PrestoBlue cell viability reagent according to manufacturer's protocol (ThermoFisher). Excitation and emission were measured at 560 nm and 590 nm, respectively, using a Biotek plate reader. Data from peptide treated wells were normalized to the vehicle-treated peptide-free control and corrected for background fluorescence. The resulting data were curve-fit and IC50s were calculated with GraphPad Prism v.8 software using a log(inhibitor) vs. response variable slope model.

3.5.5 Lactose Dehydrogenase Leakage Assay

Plasma membrane damage, as indicated by lactate dehydrogenase (LDH) leakage, in the presence of stabilized peptides was assessed in two p53-null human cancer cell lines, Saos2 (osteosarcoma)

and DU145 (prostate adenocarcinoma). Each cell line was passaged with 10% Fetal Bovine Serum (FBS), 1% penicillin/streptomycin, and respective culture media: DU145 in RPMI 1640 and Saos2 in DMEM. Upon confluency, cells were plated in triplicate in 96-well plates at the following cell densities: DU145 at 5,000 cells/well and Saos2 at 20,000 cells/well, and incubated at 37°C for 24 hours. Media was then aspirated from all wells and cells were washed with their respective assay media (with or without serum) before being treated. Each experiment included side-by-side sets of triplicate wells where one set was tested with serum and the other without. Within each of these sets was one experimental condition-- cells treated with peptide at 10uM in media--and two controls. Vehicle-only treated cells served as a negative LDH control and vehicle-only treated cells with lysis buffer (0.8% Triton X-100) added at the end of the experiment served as a positive LDH control. Each set also contained cell-free wells mimicking the experimental and control wells to normalize for background fluorescence in each condition. Plates were incubated at 37°C for 24 hours and lysis buffer was added to positive control wells 45 minutes prior to the assay endpoint. LDH leakage was quantified with the CyQuant LDH Cytotoxicity Assay Kit (Invitrogen C20301) per manufacturer's protocol. Fluorescence measurements were taken with a Biotek plate reader. Percent LDH leakage was calculated with the following equation:

$$\%\ LDH\ Leakage = \frac{(peptide - peptide\ background) - (vehicle - vehicle\ background)}{(lysed - lysed\ background) - (vehicle - vehicle\ background)}\ x\ 100$$

Chapter 4 Profiling Physicochemical Properties of Peptide Candidates and Analyzing Correlation to Efficacy

4.1 Publication Information

L. Atangcho, T. Navaratna, M. Mahajan, M. Case, K. Deprey, H. Levy, R. Gopinath, G. Gueorgiev, J. Kritzer, G. Thurber. Protease stability correlates with efficacy for high-affinity, cell-penetrant MDM2-binding stapled peptides. *In prep*.

4.2 Abstract

Nearly two-thirds of all disease-associated proteins are 'undruggable' by modern therapeutics, meaning they are inside cells, out of the reach of biologics, but lack small molecule binding pockets. Stabilized peptides have the potential to hit these targets. However, the design criteria for developing agents that can reach and disrupt their target are poorly understood. This work focuses on the physicochemical properties of three newly-developed high affinity double-click stabilized MDM2/p53 inhibiting peptides that have favorable *in vitro* characteristics including protease stability, cytosolic access, and target-specific cell killing. These properties are distinct from ATSP-7041, the only p53-based peptide that has led to a clinical lead compound. We highlight a promising peptide variant with an added disulfide-bond backbone modification that demonstrates sub-micromolar cell-killing in the presence of serum, comparable to the published *in vitro* potency of ATSP-7041. Overall, these peptides help better define the landscape needed for effective intracellular biologics.

4.3 Introduction

Drug development for intracellular targets is dominated by small molecules that can readily cross cell membranes and can often be administered orally. The screening and discovery of lead compounds was significantly advanced when the capabilities of high-throughput screening were paired with heuristics, such as Lipinski's Rule of Five[25], that identified compounds with appropriate 'drug-like' properties like solubility and membrane permeability. These advances led to a dramatic reduction in clinical attrition rates due to pharmacokinetics and bioavailability[91], with contemporary drugs able to rapidly enter cells and bind their targets in minutes[26]. Nonetheless, small molecules are unable to target the majority of disease-associated protein-protein interactions (PPIs)[2,3] because PPIs involve large binding interfaces often 2000 to 4000 $Å^2$ or more of buried surface area[92]. Furthermore, these targets reside inside the cell, out of the reach of traditional biologics (i.e. antibodies) with extracellular targets. This spurred new research into novel classes of agents that had the potential to reach these 'undruggable' targets.

To target intracellular PPI's, a significant effort has focused on molecules at the interface of traditional small molecule drugs and macromolecular therapeutics. These so-called 'Beyond Rule of Five' molecules, often cited as 500-5,000 Da in size, in theory possess the ability to cross membranes but bind larger, more hydrophilic interfaces such as PPI's. Many of these compounds are inspired by natural products, such as cyclosporin and cyclotides/knottin peptides[49,93–95] and several have demonstrated clinical efficacy and FDA approval[65,77,96,97]. However, the diverse pharmacokinetics, cytosolic delivery mechanisms, and overall design criteria for this broad class of agents is not well-defined, and continued advances are needed[98].

Stabilized peptide therapeutics are one class of agents in the Beyond Rule of Five space being explored as a solution to this shortcoming. Given that many PPIs have alpha-helical binding

interfaces[3], helical peptides in particular are being developed to inhibit these interactions with high specificity[99]. Furthermore, structural stabilization via covalent chemical modification generally yields enhanced target binding affinity as well as increased proteolytic stability and cell penetration[20,88,100–102]. All-hydrocarbon linkers (stapled peptide therapeutics) were pioneered by Walensky and colleagues (Verdine and Korsmeyer groups) against a variety of targets including BCL-2 and MDM2 domains[5,14,17,41,44,103]. Lau and colleagues (Spring group) developed peptides for the same target but employed the use of the double-click stabilization technique for an added degree of freedom in chemical modification[6,21,83]. In 2013, Chang and colleagues published a stapled p53/MDM2 inhibiting peptide, ATSP-7041, that went on to be the basis for the first and only stabilized peptide therapeutic in clinical trials thus far, ALRN-6924[9,96,104]. The demonstrated clinical effects of this peptide are a big step for the field; however there is still much progress to be made for an overall mechanistic understanding of the physicochemical properties required for these agents to be clinically effective drugs. Recent literature in stapled peptide design has shown advancements in sequence optimization strategies for cell penetration and protease stability in addition to high affinity [41,44,89]. These kinetic processes are the major rates controlling cell efficacy: cytosolic delivery versus clearance determine intracellular concentration while affinity establishes the target fraction bound (Fig 4.1). However, the quantitative trade-offs between properties are

incompletely understood, making it challenging to define criteria for successful agent design. Here, we quantify the cytosolic penetration rate, membrane interaction, target binding, and protease stability of a series of high affinity MDM-2 binding agents to identify the combination of properties needed for cell efficacy.

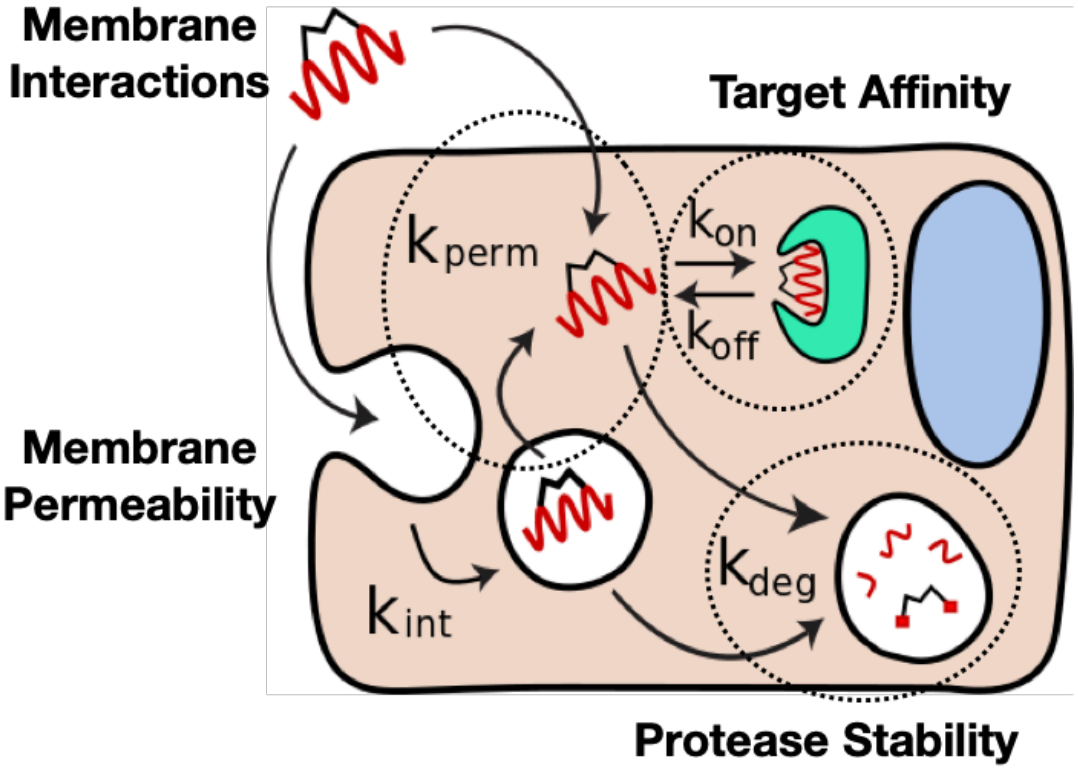

Figure 4.1 Overview of Relevant Rates

We previously developed a series of MDM2-binding stapled peptides with high affinity via Stabilized Peptide Evolution by E. Coli Display (SPEED)[88]. (Here, 'stapled peptide' refers broadly to side-chain cross-linked peptides, not exclusively hydrocarbon metathesis chemistry.) With propargyl ether as the stabilizing linker, the resulting clones were screened against MDM2. Those with the highest binding affinity were sequenced and synthesized via solid phase peptide synthesis (SPPS), stapled with the propargyl ether linker, and re-tested in solution. In this work, we measured the quantitative cellular pharmacology of these agents to access and inhibit MDM2.

Continuing on from Chapter 3, here we begin with measuring cellular penetration followed by biophysical membrane interactions and ending with proteolytic stability.

4.4 Results

4.4.1 Cytosolic Penetration

The chloroalkane penetration assay (CAPA), developed by Peraro and colleagues, is a HaloTag-based pulse-chase assay that provides a quantitative measure of cytosolic penetration[105]. Briefly, chloroalkane-tagged peptides are incubated with HeLa cells expressing HaloTag that is localized to the outer membrane of mitochondria, positioned in the cytosol. Upon entry into the cytosol, the chloroalkane-tagged peptide binds irreversibly to HaloTag, thereby blocking those HaloTag active sites. After washing away unbound peptide, cells are incubated with a chloroalkane-dye which quickly penetrates the cells and reacts with the remaining HaloTag sites. After washing away unbound chloroalkane-dye, the resulting fluorescence signal is quantified via flow cytometry. The signal is inversely proportional to the amount of chloroalkane-tagged peptide that penetrated the cell.

All peptides were N-terminally tagged with a chloroalkane group and incubated with the HaloTag-expressing cells for 4 hours or 24 hours at various concentrations (Figs 4.2a, 4.2b). CP_{50} values, derived from a simple IC_{50} curve fit, indicate the concentration at which 50% of HaloTag sites are saturated with ct-peptide after a given incubation time [106]. At 4 hours, we observe very little penetration of ATSP-7041 into the cytosol while the double-click stapled peptides penetrate

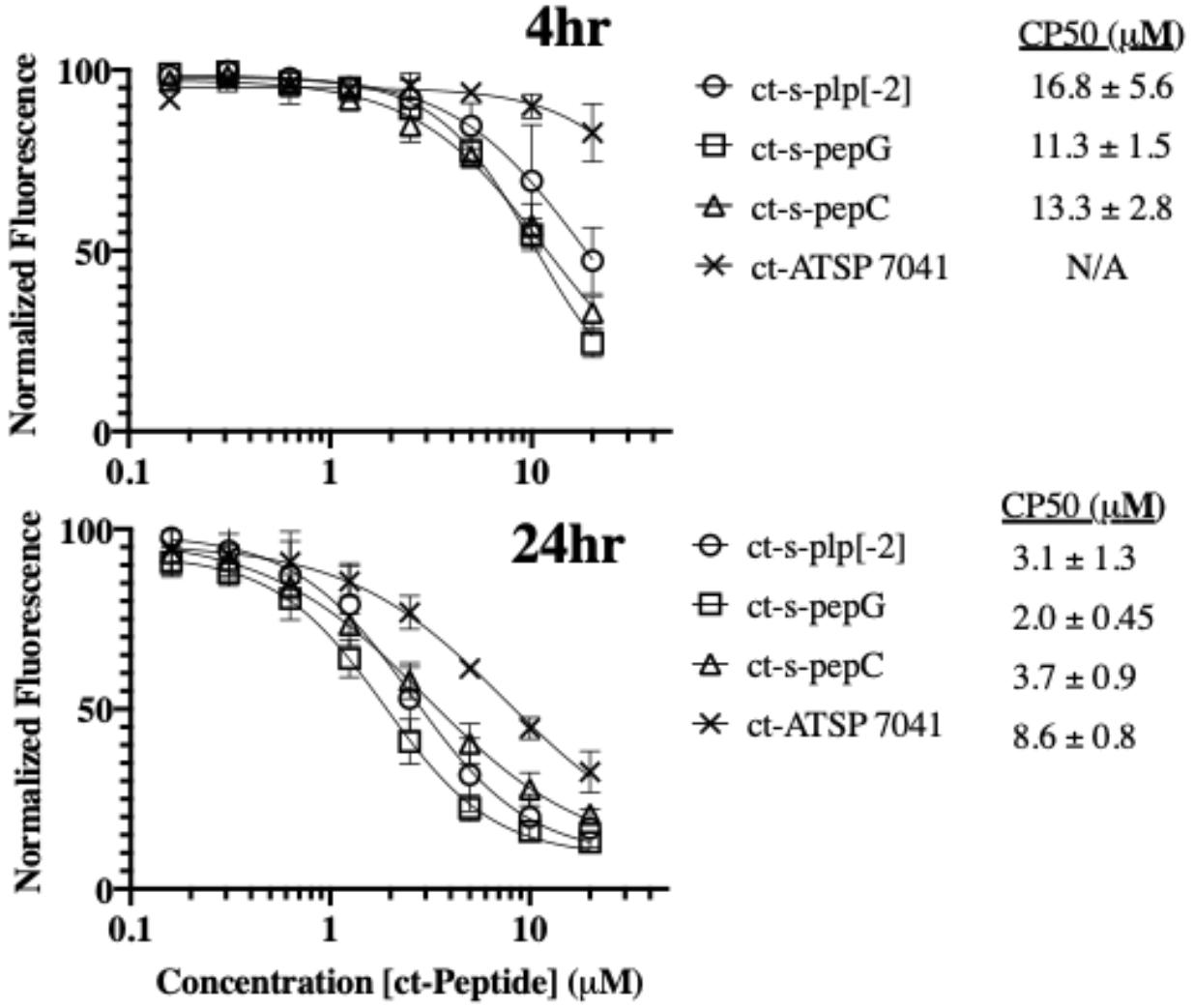

Figure 4.2 CAPA Results

the cytosol at concentrations 10 μM and above (Fig 4.2a). At 24 hours, all peptides had lower CP_{50} values, with the double-click stapled peptides roughly 2- to 4-fold more penetrant than ATSP-7041. Surprisingly, given its high target affinity but lack of cellular efficacy, pepG exhibits the

highest penetration with a CP_{50} of 2 μM at 24 hours (Fig 4.2b). These and other peptides largely follow a 1st-order penetration rate in time and concentration (S Fig 4.1). Using a simple 1st order model, the rate of cytosolic penetration (and associated equilibrium half-life) for pepG is 1.9 hours (Table 4.1) (Note that this does not mean it takes this long to saturate the target; rather it is the time to theoretically equilibrate with the extracellular concentration.)

Table 4.1 Cellular Penetration Rates

Peptide	Uptake Rate Constant (1/hr)	Equilibrium Half-Life (hr)
ct-s-plp[-2]	0.213	3.2
ct-s-pepG	0.365	1.9
ct-s-pepC	0.267	2.6
ct-ATSP-7041	0.084	8.3

The fast cytosolic penetration of pepG was unexpected considering it has reasonable target affinity (5 nM) but showed no efficacy in SJSA-1 and LnCAP, even at 10 μM over 5 days. It was also unexpected that ATSP-7041 had the lowest penetration rate with a CP_{50} of 8.6 μM at 24 hours and half-life of 8.3 hours—4 fold higher than pepG. Together, these data indicate the peptide with the lowest *in vitro* efficacy paradoxically has the fastest cytosolic penetration while the most efficacious peptide had the slowest cytosolic penetration of the series. pepC and plp[-2] both have moderate penetration rates with half-lives of 2.6 and 3.3 hours, respectively. The ability to traverse the lipid bilayer is often tied to the lipophilicity of a molecule, which is often represented by an octanol/water partitioning coefficient. Therefore, we decided to perform additional biophysical characterization of the peptides to help explain the cytosolic penetration.

4.4.2 Membrane Partitioning

As discussed in Chapter 2, lipophilicity and charge two of the primary determinants of cell membrane permeability for low molecular weight compounds including peptides[89]. As shown in Table 4.2, all of the peptides tested here are negatively charged, having either a -1 or -2 charge.

Table 4.2 Peptide Sequences and Charges

Name	Sequence	Charge
	X=Azidohomoalanine	
plp-2	Ac-ET**FX**DL**W**RL**LX**EN-NH2	-2
pepG	Ac-GGT**FX**GY**W**AD**LX**AF-NH2	-1
pepC	Ac-VCD**FX**CY**W**ND**LX**GY-NH2	-2
ATSP-7041	Ac-LT**F**xEY**W**AQxxSA-NH2 x1=R8, x2=Cba, x3=S5	-1

Given that there were no positively charged variants in this series with high or moderate binding affinity, we could unfortunately not include this in our selection criteria. We therefore focus on lipophilicity. Classically, octanol/water partition coefficients are measured for small molecules, and computational approaches can be used to predict these values. Experimental measurements of octanol/water partitioning coefficients are often limited by sensitivity when dealing with highly lipophilic or hydrophilic molecules, and computational tools often fail to accurately represent peptides by not accounting for intramolecular interactions such as hydrogen bonds [55,107].

Therefore, we used HPLC retention times (e.g. [44,85,108]) to compare the lipophilicity of various peptides and estimate the logD based on a series of standards (S Fig 4.2). We utilized reverse-phase HPLC with ammonium acetate buffered water (pH 7.4) and acetonitrile as the mobile phase. ATSP-7041 has the highest retention time and apparent logD (3.0), likely due to the high abundance of hydrophobic residues and the all-hydrocarbon staple. pepC, pepG and plp[-2] have similar apparent logD values of 2.1, 2.2, and 2.3, respectively (Fig 4.3). To characterize the peptide/membrane interaction, we next measured peptide/liposome interactions spectroscopically.

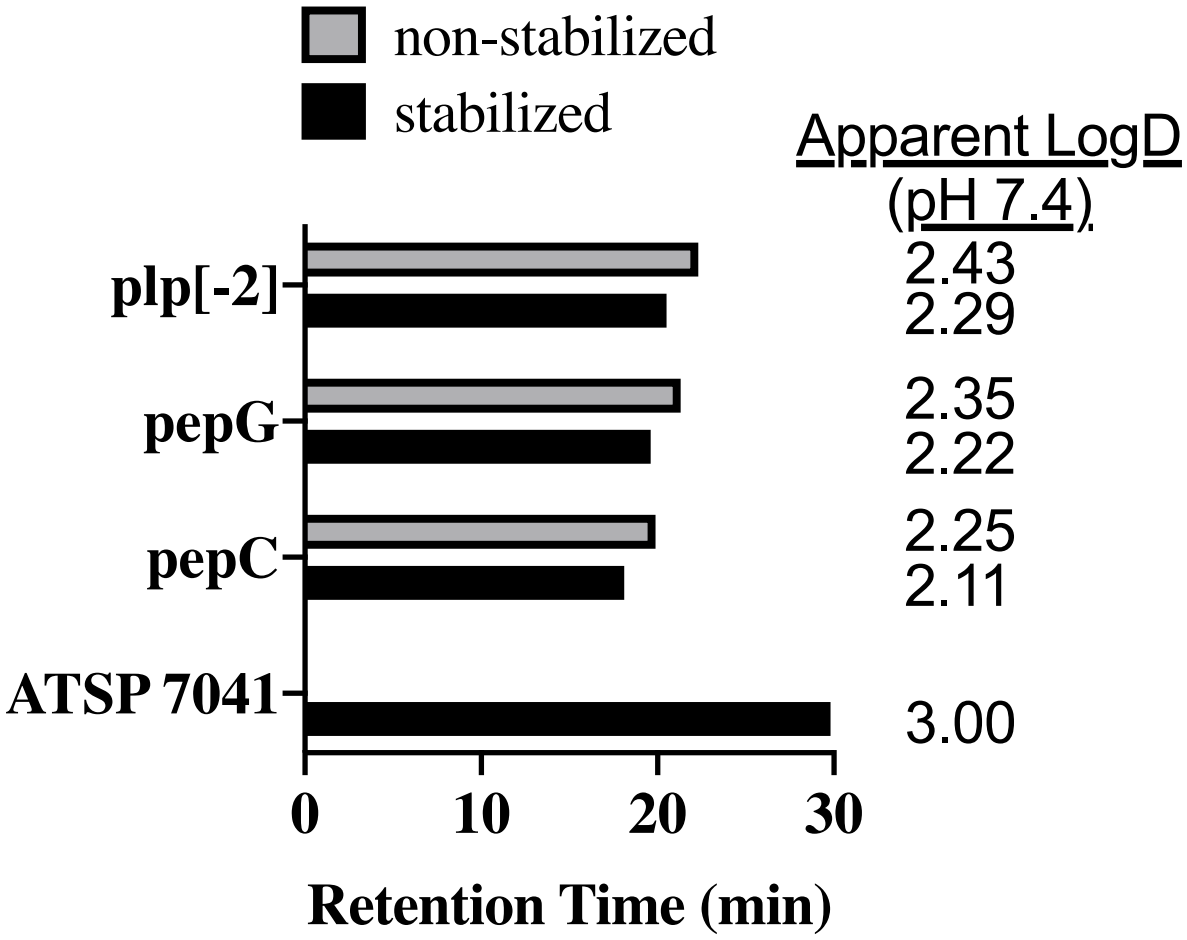

Figure 4.3 HPLC Retention Times and Apparent LogD

The lone tryptophan within the peptide sequences enabled spectroscopic measurements of peptide interactions with lipid bilayers (liposomes)[109]. First, intrinsic tryptophan fluorescence was measured with increasing concentrations of lipids (liposomes). The environmentally sensitive fluorescence peak of tryptophan blue shifts when it moves from a hydrophilic to a hydrophobic environment [110]. Only ATSP-7041 showed a definitive shift in fluorescence, indicating it is buried deep within the lipid bilayer, while pepG showed a slight shift and the other peptides showed no detectable change (S Fig. 4.3). To determine if the other peptides were interacting with the membrane, acrylamide quenching experiments were conducted. The Stern-Volmer constant (K_{sv}), the slope of normalized fluorescence vs. acrylamide concentration[111], was measured in the presence or absence of liposomes (Fig 4.4). Acrylamide, a water-soluble quencher, is unable to

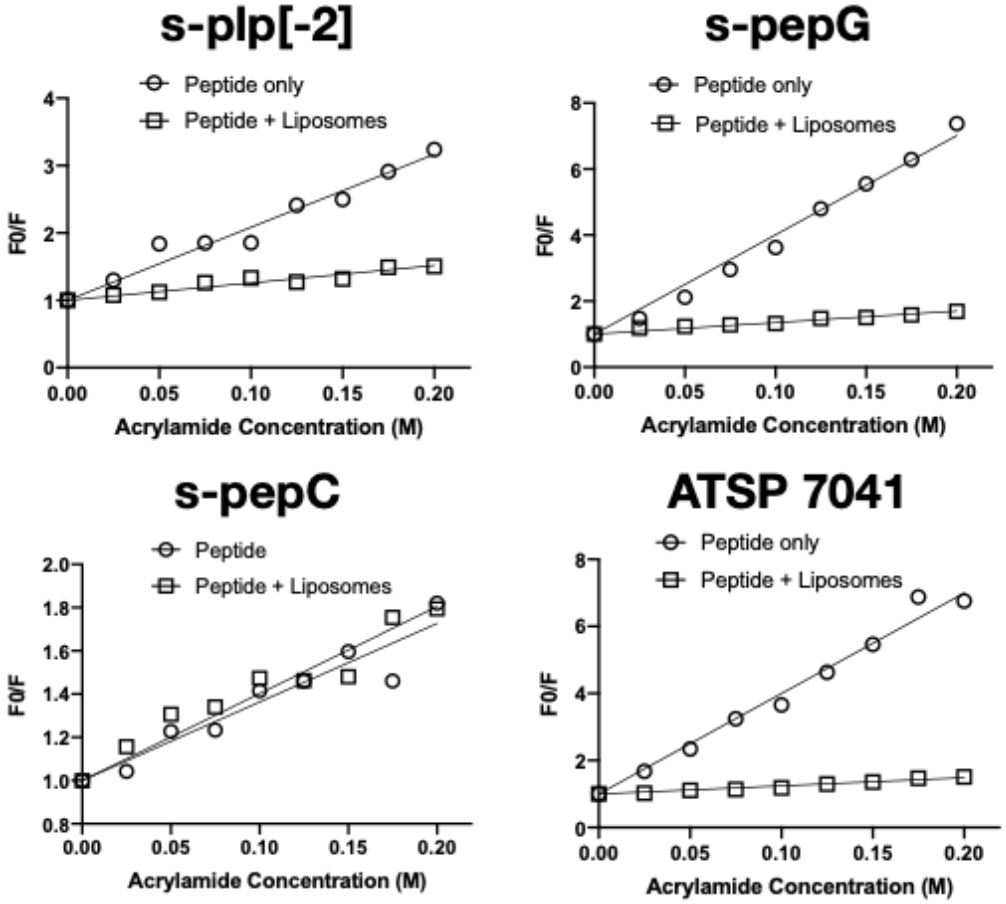

Figure 4.4 Tryptophan Fluorescence Acrylamide Quenching Plots

penetrate hydrophobic environments, so only tryptophan residues not embedded in the membrane can be quenched. ATSP-7041 and pepG had the highest Stern-Volmer constant ratios (12.3 and 8.6, respectively) (Table 4.3), indicating these peptides had the strongest interaction with the membrane, followed by plp[-2] and pepC.

Table 4.3 Stern-Volmer Constants

Stern-Volmer Constants			
	Peptide Only	**Peptide + Liposomes**	**ratio**
s-plp[-2]	10.84	2.59	4.2
s-pepG	30.08	3.50	8.6
s-pepC	3.63	4.02	0.9
ATSP-7041	29.97	2.43	12.3

A helical wheel representation of the sequences shows the distribution of hydrophobic and hydrophilic residues as well as the hydrophobic moment values [112] computed from the published structures of pepC and ATSP-7041 [88,104]. All peptides have a large hydrophobic face including the hydrophobic binding interface of the conserved F, W, and L residues with slight differences in the overall number of hydrophilic residues and their locations. pepC and ATSP-7041, having the least and most tryptophan acrylamide quenching, respectively, are different in that the all-hydrocarbon staple of ATSP-7041 contributes to the lipophilicity of ~3/4 of the residues while the less lipophilic linker of pepC contributes to a more evenly split distribution of hydrophilic and hydrophobic residues (and resulting high hydrophobic moment). This allows for more aqueous solvent interactions and a lower propensity for the tryptophan to partition into the liposomal membrane. The deeply membrane embedded ATSP-7041 could potentially slow the transient rate of

membrane translocation in the CAPA assay by retaining the peptide. However, these results still did not match the rank order of cellular efficacy.

4.4.3 Protease Stability

The lack of efficacy from pepG despite its high affinity and efficient cytosolic penetration could not be explained by affinity and permeability alone. Therefore, we tested protease resistance as a measure of stability inside the cell. Using chymotrypsin as a model protease (2-3 cleavage sites per peptide), plp[-2] and pepG completely degraded within minutes in non-stapled form. Interestingly, non-stapled pepC was significantly more resilient than other non-stapled peptides, likely due to the disulfide loop present within the structure. When stapling with propargyl ether, plp[-2] was substantially more resistant, with a half-life of over 70 min, while pepG only modestly improved (11.2 min). The bicyclic pepC had a ~440 min half-life under these conditions. For comparison, ATSP-7041 did not have detectable degradation at this enzyme concentration before autolysis of the enzyme reduced activity. When using a 10-fold higher enzyme concentration, ATSP-7041 degraded with a 2 hour half-life, followed by 20 min for pepC and 8 min for plp[-2] (Figure 4.5). PepG degraded too quickly to measure under these conditions. The lack of stability, despite the high cytosolic penetration and binding affinity of pepG, is consistent with low intracellular concentrations and lack of target engagement for this stapled peptide.

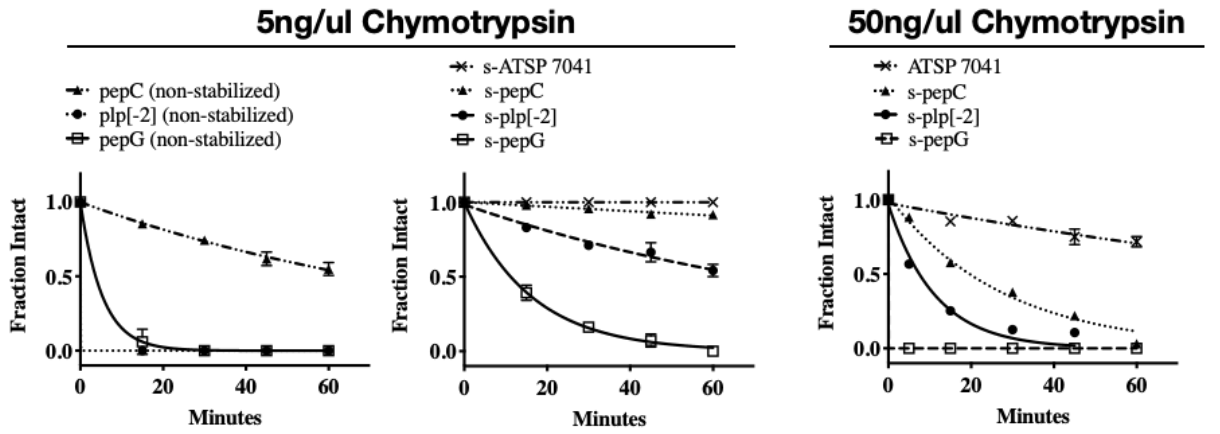

Name	5ng/uL Chymotrypsin		50ng/uL Chymotrypsin
	Half-Life (Non-stabilized)	Half-Life (Stabilized)	Half-Life (Stabilized)
Plp-2	Unstable	70.7 ± 5.6	7.8 ± 1.3
pepG	3.7 ± .05	11.2 ± .4	Unstable
pepC	68.0 ± 2.0	438.7 ± 51.0	19 ± 1.7
ATSP 7041	-	Not Detectable*	128.5 ± 21.9

*** autolysis**

Figure 4.5 Chymotrypsin Degradation Half-Lives

4.5 Discussion

In this work, we profiled the *in vitro* efficacy, cytosolic penetration, lipophilicity/hydrophobicity, and protease stability of a series of high affinity MDM2-binding stabilized peptides developed through SPEED along with the well-studied clinical lead compound, ATSP-7041. Based on affinity alone, we hypothesized that the double-click stabilized peptides tested would have *in vitro* activity. However, only one, pepC, showed efficacy, and this was similar to the potency of ATSP-7041 in the cell lines tested. As previously discussed, affinity is only one relevant parameter in the overall efficacy of a peptide. Our aim was to use subsequent experiments to characterize why the other peptides showed no efficacy and to gain general knowledge about the range of

physicochemical properties and cellular kinetics for this series of peptides that enable cell entry and efficacy.

The affinity of intracellular targeting agents clearly plays a role in efficacy. Given the relatively poor cytosolic penetration of stapled peptides, high affinity is likely required given anticipated low intracellular concentrations, and we tested several stapled peptides with moderate to high affinity . The increased structure of stapled helices can increase target affinity by lowering the entropic penalty of binding, and affinity screens often select for more rigid structures, such as those containing disulfide bonds [70,113]. Helix stabilization increased affinity for the current series of peptides, although this is not always true when comparing different sequences [114,115]. This can be due to complex factors like solvent interactions and entropy/enthalpy compensation [72], where a more rigid structure may improve the entropy of binding but reduce the flexibility needed for optimal enthalpic interactions (e.g. hydrogen bond angles) and vice versa. ATSP-7041 with its sub-nanomolar binding affinity appeared to be the best binder in this series of peptides, as well as one of the most helical (44%, data not shown) falling just behind the helicity of plp[-2]. Given that the latter has the lowest binding affinity despite being the most helical, it is clear that helicity itself does not result in strong binding affinity. Furthermore, the fact that pepG has the lowest helicity but 3-fold better binding affinity than plp[-2] may be due to the abundance of glycine residues which are often considered 'helix breakers' [90]. The sequence and linker-dependence play a more pronounced role in determining affinity, as others have also shown [6]. While both ATSP-7041 and pepC had the highest affinity and potency, affinity could not explain the complete lack of efficacy for pepG. Therefore, the cytosolic penetration rate was determined for each peptide since penetration into the cytosol is a major hurdle for stabilized peptides, and the target, MDM2, resides in the cytosol.

The CAPA assay provided a quantitative measure of peptide accumulation in the cytosol over 4 and 24 hour periods. Because affinity did not explain all the efficacy results, we hypothesized that efficacy would track with cytosolic penetration, the major hurdle in delivery for intracellular biologics. However, this was surprisingly not the case. All of the double-click stabilized peptides had faster apparent cytosolic penetration than the more lipophilic clinical lead compound, ATSP-7041. Due to its lipophilicity as exhibited by a high HPLC retention time and apparent logD, we expected ATSP-7041 to rapidly partition into the lipid bilayer. However, if a molecule inserts too deep in the membrane, it can slow translocation across the lipid bilayer and transit into the aqueous cytosolic environment[116]. In contrast, molecules with moderate lipophilicity may have lower membrane partitioning, but this may enable quicker diffusion into the aqueous (cytosolic) phase (e.g. from an endosomal compartment). We suspected this was why the double-click stabilized peptides had roughly 3 to 4-fold faster penetration rates than ATSP-7041. To probe this hypothesis and determine the mechanistic behavior of peptides interacting with lipid bilayers, we utilized liposomes as a proxy for cell membranes. Taking advantage of the fact that all these peptides have a conserved W23 residue, we measured tryptophan fluorescence quenching in the presence of POPC liposomes and acrylamide. ATSP-7041 rapidly partitioned into the liposomal bilayer as evidenced by the dramatic leftward shift in fluorescence in the presence of liposomes, a phenomenon not exhibited by the other peptides. Furthermore, the Stern-Volmer constants resulting from acrylamide quenching studies show that the tryptophan residue in ATSP-7041 is heavily shielded by the liposomal bilayer. This result supports our hypothesis regarding rapid membrane partitioning and explains the trends seen in the CAPA assay: the highly lipophilic sequence and all-hydrocarbon staple enable deeper penetration of the tryptophan into the lipid bilayer core as seen in the helical wheel diagram. However, as others have found, this

partitioning can sequester the peptide within the membrane, slowing transport across the bilayer [116]. In contrast, the more hydrophilic double-click stabilized peptides did not reside as deep within the lipid bilayer. Notably, pepG has an acrylamide quenching Stern-Volmer constant ratio that is the second highest after ATSP-7041. Interestingly, this peptide has the fastest cytosolic penetration rate while ATSP-7041 has the slowest. We hypothesize that in this series of peptides, pepG may have the most balanced lipophilicity to achieve efficient cell entry—lipophilic enough to partition rapidly into the membrane but not too lipophilic that it gets trapped. However, the fast cytosolic penetration of this high affinity peptide runs counter to the observed lack of efficacy. Therefore, we had to look for mechanisms beyond the ability to reach the site of action and bind the target with high affinity to explain cellular potency.

Up until this point, we had not explicitly measured degradation as a possible contributor to efficacy among the stapled peptides. Degradation rates are relevant *in vitro*, with the presence of lysosomal and cytosolic proteases, and even more-so *in vivo*, where proteases in serum and digestive fluids could degrade a peptide therapeutic before even reaching the target cells. We therefore conducted a protease digest assay, directly comparing degradation of each peptide by chymotrypsin, chosen for its promiscuity in this series of peptides. These results showed that ATSP-7041 is extremely stable in comparison to the other peptides with a 128.8 min half-life at a high chymotrypsin concentration, followed by pepC (19 min), plp[-2] (7.8 min) and pepG which degraded near-immediately. Anecdotally, ATSP-7041 also showed less day-to-day variability in cellular assays, likely due to this extremely high stability.

In contrast to cytosolic penetration rates, the degradation rates seen here correlate well with the efficacy results. plp[-2] has the greatest increase in helicity upon stapling, but it is significantly less stable than ATSP-7041 and pepC. Even with efficient cytosolic penetration, modest stability

inside the cell and moderate affinity of plp[-2] are not enough for cellular efficacy. pepG has high affinity and the highest apparent cytosolic penetration rate, but it is the least stable, likely leading to rapid degradation in lysosomes and/or the cytosol, low intracellular concentrations, and little target engagement. Rapid degradation could result in released chloroalkane tag entering the cytosol (rather than intact peptide), increasing the apparent cell penetration rate as measured by CAPA[106]. However, the rate and magnitude of proteolysis did not match the CAPA results (e.g. pepG has less than two-fold faster cell penetration but degrades almost 40 times faster), indicating this artifact wasn't the main source of CAPA signal, and may not have contributed to the apparent rates of cell penetration. Regardless of the membrane uptake rate, the peptide must remain intact prior to entering the cytosol for efficacy. In comparison with pepC, ATSP-7041 has slower cytosolic penetration, but its extremely high stability and ~2-fold lower K_d enable high intracellular accumulation and target binding. The high helicity, alpha carbon methyl groups, and non-natural amino acids likely all contribute to this stability. pepC, though much less helical (28% versus 44%), has an intrahelix disulfide bond, likely contributing to its protease resistance in oxidizing environments. It is unclear how quickly the disulfide is reduced in the cytosol, but surface display measurements indicate only a 2-fold drop in affinity without the disulfide bond[88]. Together, its high affinity, efficient cytosolic penetration, and good protease stability enable on-target efficacy.

4.6 Conclusions

These results, summarized in Figure 4.6, highlight the rate of protease degradation as a key design parameter in stabilized peptide design. While affinity and cytosolic penetration are critical features and often the focus of stabilized peptide development, intracellular stability (beyond just stapled versus linear peptides) can play an equally important role. In the compounds examined here, high

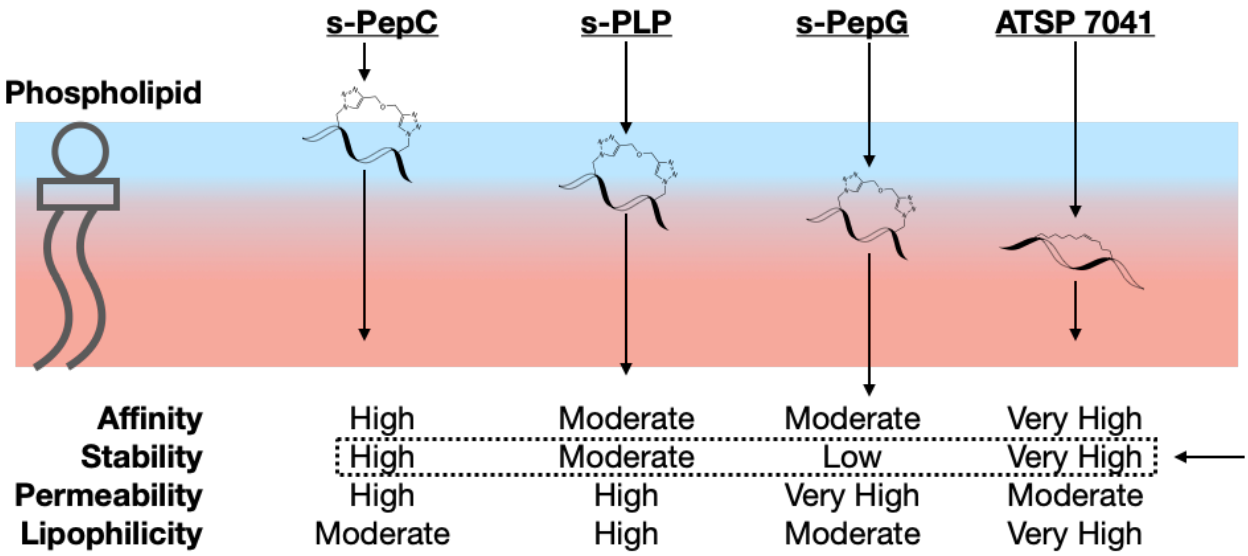

Figure 4.6 Summary of Physicochemical Properties

affinity was pre-selected, so affinity did not play a distinguishing role. The cytosolic delivery rate was also fairly high for this series of stapled peptides. The binding interface of the MDM2 binding peptides is lipophilic, with hydrophilic side chains on the opposite face likely contributing to aqueous solubility. The resulting amphiphilicity likely contributed to the efficient cytosolic penetration, consistent with reports by others [42,89]. With similar apparent cytosolic penetration rates and target affinity, protease stability had the greatest correlation with cellular efficacy in this peptide series. These rates are all interdependent – penetration vs. degradation determine intracellular concentration while affinity determines target engagement. Based on this data, it is possible for agents with lower affinity or slower cell penetration to be more effective *in vitro*. Therefore, all these rates need to be considered together to identify the most effective compound for cellular efficacy.

4.7 Experimental Methods

4.7.1 Synthesis, Purification and Stabilization

Solid phase peptide synthesis and double-click stabilization of *i,i+7* diazido peptides were carried out as previously described [88]. Solid phase synthesis was done using a CEM Liberty Blue Microwave Peptide Synthesizer. Rink amide resin and Fmoc amino acids were purchased from ChemPep Inc. All other reagents were purchased from Sigma Aldrich. After cleavage from resin, purification and lyophilizing, peptides were stabilized in 1:1 water:*tert*-butanol via copper catalyzed azide alkyne cycloaddition with propargyl ether.

Characterization via electrospray ionization mass spectrometry (ESI-MS) and HPLC purities are reported in Table 3.3.

ATSP-7041 was provided by the University of Michigan Proteomics and Peptide Synthesis Core.

4.7.2 Chloroalkane Penetration Assay (CAPA)

Cell culture and maintenance

The cells used in CAPA were grown in DMEM media with 10% fetal bovine serum (FBS), 1% penicillin/streptomycin, and 1 μg/mL of puromycin in tissue culture treated T75 flasks. Cells were passaged at confluency, every 2-3 days.

Ct-Peptide Synthesis

Peptides were synthesized via solid phase peptide synthesis as described but without an n-terminal acetyl cap. Post-synthesis, peptides were mixed on resin with chloroalkane tag (2.5 equiv), PyBOP (2.5 equiv) and DIPEA (7 equiv) for 1 hour with nitrogen bubbling. Peptides were then washed with DCM and cleaved as previously described.

Ct-ATSP-7041 was synthesized and provided by the University of Michigan Proteomics and Peptide Synthesis Core.

CAPA Assay

The chloroalkane penetration assay was performed as described previously [105]. Briefly, HeLa cells that stably express a cytosolically oriented HaloTag-GFP fusion protein were seeded in a 96-well plate to obtain 60-80% confluency at the start of the experiment. The growth media was aspirated from the adhered cells and replaced with 100 µL of optiMEM culture media supplemented with 10% FBS. Serial dilutions of chloroalkane-labelled peptides were performed in optiMEM supplemented with 10% FBS in a separate 96-well plate. Solutions were made at 5x concentration, as 25 µL of these peptide solutions were subsequently added to the cells and incubated for 24 hr at 37 ºC. After incubation, the media was aspirated and cells were washed with 80 µL fresh optiMEM for 15 min at RT. OptiMEM was removed and replaced with 50 µL of 5 µM chloroalkane-labelled tetramethylrhodamine (ct-TMR) in optiMEM. Cells were incubated with ct-TMR for 15 min at RT and then washed with fresh optiMEM for 30 min at RT. Media was replaced with 40 µL 0.05% clear trypsin, diluted from 0.5% in PBS, and incubated for 5 min at 37 ºC. Cells were resuspended in 180 µL PBS and analyzed by flow cytometry, measuring the red fluorescence of 5,000 cells per sample. Raw values were normalized to background fluorescence of the cells (minimum) and the red fluorescence of cells that were treated only with ct-TMR (maximum). Data was curve-fit to give CP50 values in KaleidaGraph using a log(inhibitor) vs. response variable slope model.

Internalization Rate Modeling

CAPA data was fit to following ordinary differential equations:

$$\frac{dc_{in}}{dt} = k_{in}c_{out} - k_{in}c_{in} - k_{deg}c_{in}$$

$$\frac{dc_{halotag}}{dt} = -k_{rxn}c_{in}c_{halotag} + k_{deg}c_{halotag-peptide}$$

$$\frac{dc_{halotag-peptide}}{dt} = k_{rxn}c_{halotag}c_{in} - k_{deg}c_{halotag-peptide}$$

Where the variables stand for: c_{in}, concentration of peptide inside the cell; c_{out}, concentration of peptide outside the cell; $c_{halotag}$, the concentration of HaloTag inside the cytosol; $c_{halotag-peptide}$, the concentration of HaloTag -peptide reacted inside the cell; k_{in}, the rate of peptide entering the cell (1/sec); k_{rxn}, the rate of HaloTag -chloroalkane peptide reaction (1/μM/sec); k_{deg}, the rate of HaloTag turnover inside the cell (1/sec). The following conditions are applied to the system: c_{out} is constant, since the amount of peptide entering cells does not deplete the peptide added to the wells; the kinetics of the reaction between HaloTag and chloroalkane are dependent on the concentration of each in a second order fashion; the amount of HaloTag inside the cell at any point is constant – for each mol of HaloTag or HaloTag -peptide degraded, there is a mol of HaloTag synthesized. Data from Peraro et al. (2018)[117] were fit to these equations using Matlab's fminsearch function for validation. Data fitting curves for the peptides discussed in this work are shown in Figure 4.5. Half-lives for the peptides are calculated from the uptake rate:

$$t_{1/2} = \ln(2)\,/k_{in}$$

4.7.3 Chymotrypsin Digest

To measure resistance to protease degradation, stabilized and non-stabilized peptides were incubated with chymotrypsin at 5ng/uL and 50ng/uL in PBS. Peptides were first diluted to 100μM in PBS before adding the enzyme and incubating at 37ºC. After each time point, samples were flash-frozen in liquid nitrogen to stop digestion and stored at -80ºC until analysis. Samples were analyzed by reverse-phase HPLC at 214nm and 280nm wavelengths. The fraction of intact peptide remaining at each time point was quantified by the area under the curve of the intact peptide peak on the chromatograph. Exponential decay curves were fit in GraphPad Prism v.8.

4.7.4 HPLC Retention Time

Peptides and standards were run on a reverse-phase HPLC column in mobile phase containing 50mM ammonium acetate at pH 7.4 in water and acetonitrile with a gradient of 10-95% over 50 minutes. Standards were chosen based on a previously published method for estimating logD from HPLC retention time [85] (S Fig. 4.2). All standards used here have a logD(pH 7.4) greater than 0 as measured by ChemAxon MarvinSketch software and are acidic (with the exception of Cyclosporin A which is a neutral cyclic peptide) to best reflect the peptides analyzed, all of which are acidic and mostly water insoluble. A standard curve was generated and apparent logD's were calculated from the standard curve equation.

4.7.5 Liposomal Experiments

<u>Preparation of Liposomes</u>

About 2mg of dried POPC (1-palmitoyl-2-oleoyl-glycero-3-phosphocholine) powder was dissolved in chloroform:methanol (3:1) in a round bottom flask. The solvent was then evaporated under a stream of nitrogen gas. This resulted in the formation of a thin film on the sides of the flask which was then lyophilized overnight to completely remove any trace of the solvents. The dried

lipid film was then dissolved in PBS buffer (pH 7.4). The mixture was sonicated in a water bath for 10 minutes. Multilamellar vesicles formed from sonication were extruded through 50 nm membranes and the size of the liposomes was confirmed by dynamic light scattering (DLS). Prepared liposomes were stored at 4°C until use.

Fluorescence studies

All of the fluorescence studies were carried out in a Cary Eclipse fluorescence spectrophotometer (Varian, Inc.) in phosphate buffered saline, PBS (pH 7.4).

Intrinsic tryptophan fluorescence and acrylamide quenching

The localization of stapled peptides in a lipid environment was probed by using tryptophan fluorescence. 5 μM of peptide was dissolved in 200 μl of PBS buffer and the emission spectrum from tryptophan fluorescence was acquired (from 300 to 400 nm) in the free state with excitation at 295 nm. Each peptide sample was titrated with increasing concentrations of POPC lipids, and the fluorescence emission was recorded from 300 to 400 nm. Fluorescence quenching of the tryptophan residue was carried out by adding increasing concentrations of acrylamide from a 2M stock solution to a solution containing only peptide and also to a peptide+liposome solution. The Stern-Volmer constant (K_{sv}) values were then calculated using $F_0/F = 1 + K_{sv}[Q]$, where F_0 and F are the fluorescence intensities before and after the addition of quencher and [Q] is the quencher concentration.

4.8 Supplemental Figures

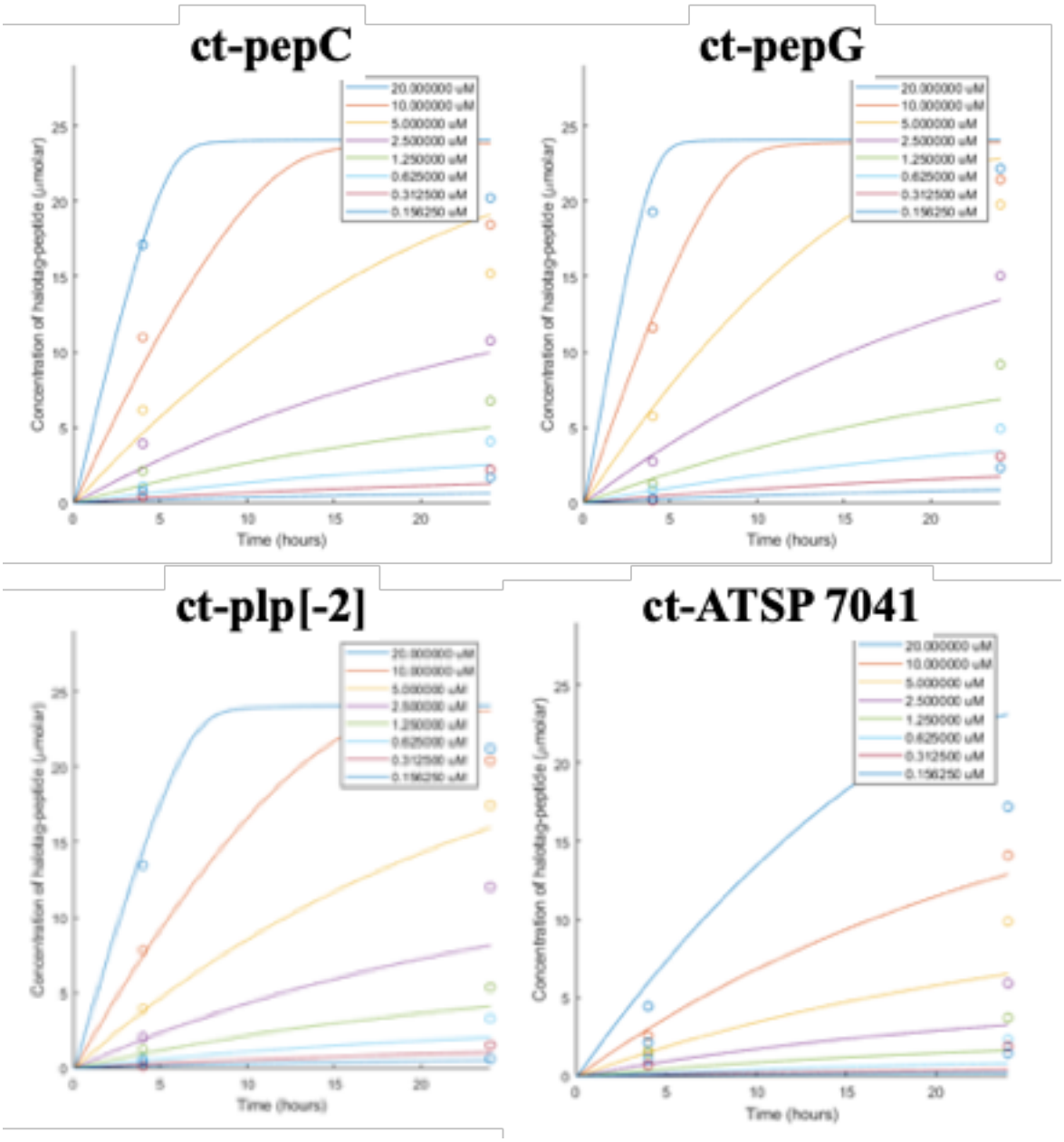

S Figure 4.1 CAPA Uptake Rate Data Fits

A.

Standard Compound	Retention Time	logD (pH 7.4)
4-methoxyphenol	12.333	1.51
phenol	12.752	1.67
2,4,6-trichlorophenol	21.03	2.1
4-phenyl phenol	25.036	3.32
Cyclosporin A	37.668	3.35

B.

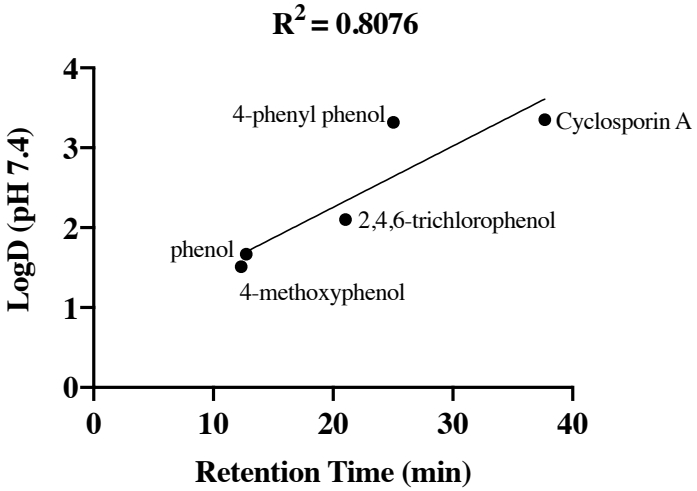

C.

Peptide		Retention Time	Apparent LogD (pH 7.4)
plp[-2]	linear	22.301	2.43
	stapled	20.478	2.29
pepG	linear	21.256	2.35
	stapled	19.584	2.22
pepC	linear	19.91	2.25
	stapled	18.085	2.11
ATSP-7041	hydrocarbon stapled	29.756	3.00

S Figure 4.2 HPLC Retention Time LogD Standards and Peptide Retention Times

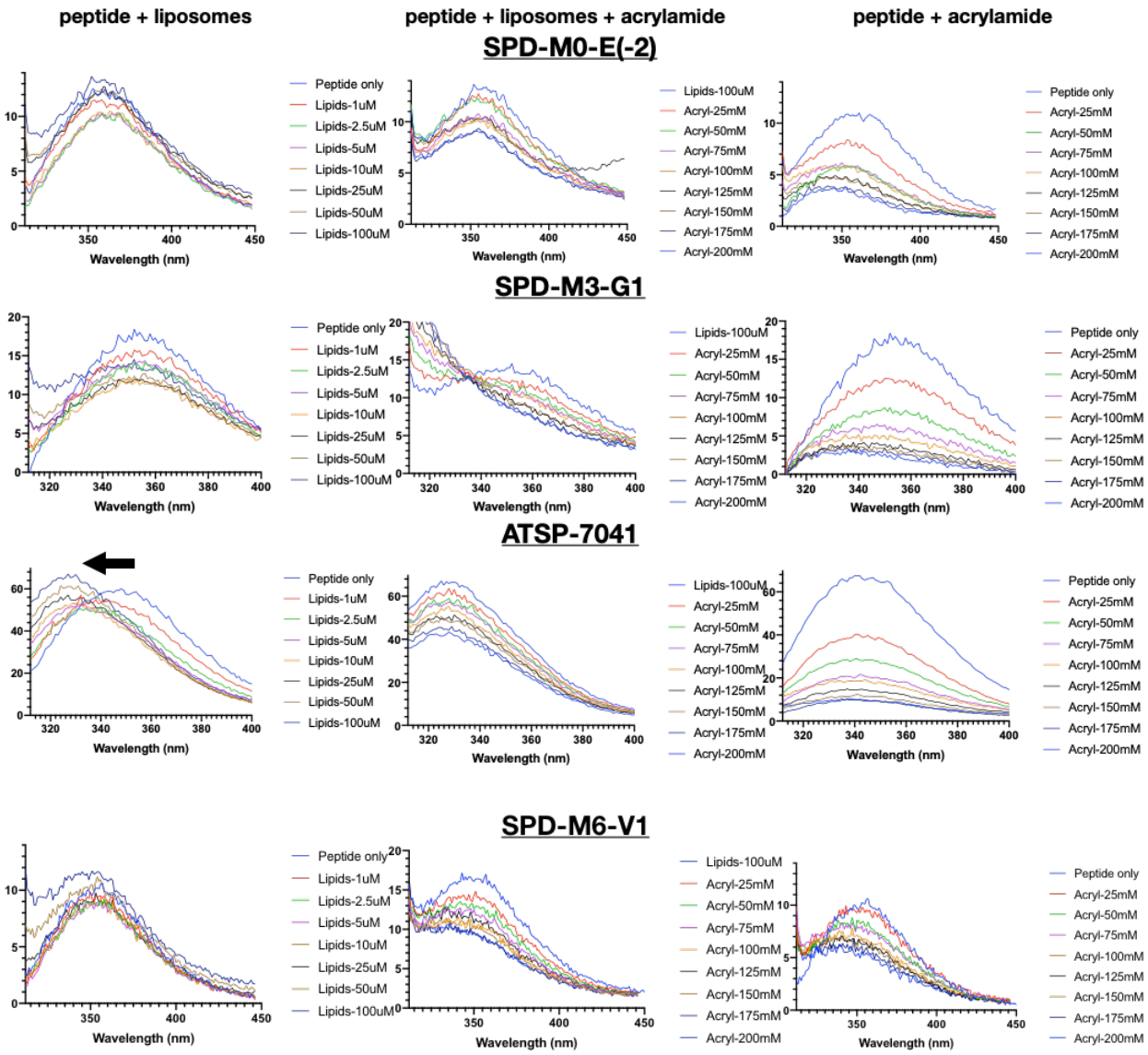

S Figure 4.3 Tryptophan Fluorescence Quenching Curves

Chapter 5 Conclusions and Future Directions

5.1 Summary of Work and Concluding Remarks

This dissertation explored the key properties that determine the efficacy of stabilized peptides for intracellular drug targets. Chapter 1 explored the world of peptide-based therapeutics for intracellular targets with a focus on stapled peptides and the work that has been previously done to make these molecules more cell-penetrant and stable in physiological conditions. This literature review exposed both a common theme in peptide-based drug development—the importance of membrane permeability and the physicochemical properties that promote it—and the lack of successful intracellular stapled peptide drug candidates that have yet emerged in the clinic. The goal of this work was therefore to contribute to this field by elucidating the main contributors to cellular uptake and ultimately, efficacy of stapled peptides. We began by studying two important properties that are widely considered to be key in membrane permeability of molecules—lipophilicity and charge (Chapter 2). We then chose a series of MDM2-inhibiting stabilized peptides discovered through bacterial-surface display and measured their in-solution binding affinities and *in vitro* efficacies to identify early stage lead compounds for further study and identification of favorable physicochemical properties (Chapter 3). Lastly, in Chapter 4, we took the highest affinity and most efficacious peptides in the series and measured their cellular penetration rates, membrane interactions, and proteolytic stabilities. The results of this study showed that in the series of peptides tested, protease stability was the differentiator for efficacy.

Until this point, many have engineered stabilized peptides with various features (linker chemistries, non-natural amino acids, etc.)[6,14,41,63,89,118] and by various methods (phage display, bacterial surface display, computational simulations, etc.)[88,113,119,120] but without an explicit focus on simultaneously quantifying the most important design parameters for efficacy. Nonetheless, previous literature has revealed a great deal about what those important parameters are. A general consensus in the field of stabilized peptides is that intracellular delivery is a limiting factor in achieving efficacy[121]. Furthermore, studies on small molecules and beyond rule-of-five molecules have shown that cellular penetration is enhanced with increased lipophilicity (Chapter 1). Stabilized peptide literature has also shown that positive charge helps enhance cell entry and many have used this as a means of increasing efficacy (Chapter 1). These observations motivated Chapter 2 in which we specifically sought to study the impact of lipophilicity and charge on cellular entry in a controlled manner, using one peptide sequence (plp[-2]) and making minimal residue modifications between experimental conditions. Leveraging the double-click stabilization technique allowed us to alter lipophilicity via the stabilizing linker while substituting glutamic acid residues with glutamine provided a means of increasing charge without drastic sequence modifications. As a result, we created a series of 9 fluorescently labeled stabilized peptides with distinct lipophilicity and charge combinations. Results showed that even incremental increases in charge caused a significant increase in uptake, with neutral and single positive charge being more favorable than a single negative charge. Furthermore, while increased lipophilicity is a useful tool to achieving cellular uptake, results showed that molecules that are too lipophilic can be less cell penetrant (and this was also observed later on in Chapter 4, although uptake mechanisms may be different in these two instances). Although these findings showed us the effects that charge and lipophilicity can have on uptake, they didn't directly relate

to efficacy, as the peptide sequence used is not efficacious and was used only as a proof of concept. We therefore proceeded in Chapter 3 to select peptides that already have efficacy such that we could analyze their physicochemical properties and determine what differentiates peptides with and without efficacy.

The peptides analyzed in Chapter 3 were discovered via SPEED, a bacterial surface stabilized peptide display technique developed by my colleague, Tejas Navaratna. We identified two peptides with single digit nanomolar binding affinities (K_d), pepG and pepC, which we tested for efficacy alongside plp[-2] and ATSP-7041—an all-hydrocarbon stapled peptide with picomolar binding affinity that is the precursor to another peptide currently in clinical trials. A cell viability assay showed that pepC has similar efficacy to ATSP-7041 while pepG, like plp[-2], has no efficacy. Given the lack of efficacy with pepG, despite its high binding affinity, we quantified additional properties that could impact efficacy. This was the focus in Chapter 4. In this chapter, we measured the apparent logD, cytosolic penetration rate, membrane interaction, and protease degradation rate of pepC, pepG, plp[-2] and ATSP-7041. We ultimately found that despite having the fastest cytosolic uptake rate, pepG was the least protease stable. We therefore concluded that in this series of peptides, binding affinity and degradation rate, not cellular uptake rate, played a dominant role in efficacy. Although ATSP-7041 was the slowest to penetrate the cytosol, it was by far the most stable peptide. Its stability in conjunction with its high binding affinity compensated for the slower uptake relative to the other peptides. Likewise, pepC, being the second most stable and having the second best binding affinity, was the second most efficacious. A visual summary of the contributions of each measured physicochemical property is shown in Fig 4.6.

The greatest takeaway from the sum of this research is the fact that the design of stabilized peptide therapeutics, specifically those with intracellular targets, must comprehensively and quantitatively take into account membrane permeability, binding affinity and intracellular stability. There is much room for advancements in the field, including a general design approach that takes into consideration the relevant rates that determine efficacy, not just *in vitro* but also *in vivo*, addressing the challenges that will be met from the molecular level to the systemic level (Fig 5.1). This work is the first step in applying a more wholistic methodology in assessing what leads to an efficacious peptide. Most of the focus in stabilized peptide discovery is iterative optimization to increase binding affinity. Although binding affinity is an important feature, it is necessary to consider it in context with other parameters, as was the case with pepG. Given that this work was only the first step in addressing this, there is much future work that can be done.

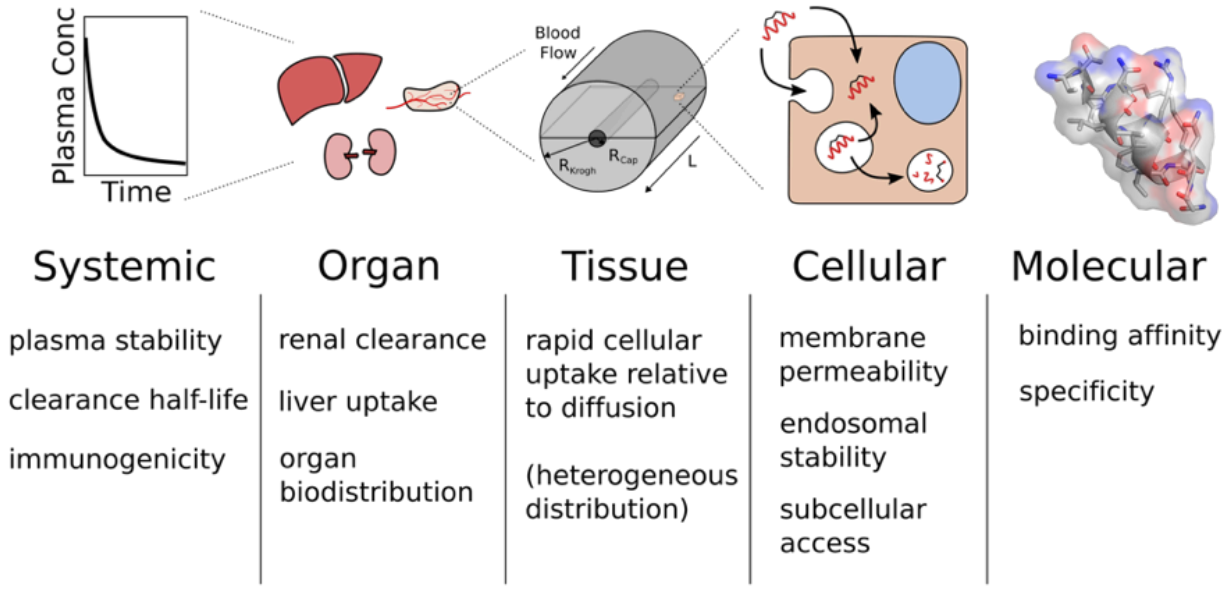

Figure 5.1 Multiscale Pharmacokinetic Challenges of Therapeutic Peptides

5.2 Future Work

5.2.1 Profiling Other Peptide Types and Model Development

The focus of this work has been on stabilized peptide inhibitors of MDM2; however, there are other emerging classes of peptides engineered to target intracellular PPIs. These include knottins which are plant-derived peptides containing three disulfide bonds, forming a "knotted" structure. Cyclotides are a subclass of knottins, featuring a head-to-tail cyclized backbone. They have been shown to be highly stable and cell-penetrant despite their large size and molecular weights (~30-40 residues)[122,123]. Researchers from the Camarero group have engineered an MDM2 inhibiting cyclotide, MCo-PMI (based off of the natural cyclotide MCo-TI-I), with efficacy *in vivo* and strong tumor growth inhibition *in vivo*[49]. This cyclotide features a helical portion with the key MDM2-binding residues found in stabilized peptide MDM2-inhibitors, however this helical motif lies within a larger cyclotide backbone, thereby maintaining the stability and cell permeability benefits provided by the original cyclotide. They have also shown that cyclotides can be used as a peptide drug development scaffold for generating bacterial libraries that can be screened against protein targets[124]. Given the uniqueness of cyclotides as large peptides with measurable membrane permeability and protease stability as well as the potential they have as drug development scaffolds, cyclotides are well-suited candidates for profiling the most important properties for efficacy. Furthermore, it would be useful to have a model that takes into account the rates associated with these properties (i.e. binding affinity, cell penetration, and degradation rate) and predicts efficacy. Currently, measurements of binding affinities and cellular penetration rates are achievable as shown in Chapters 3 and 4. Some knottins are also FDA-approved and can be purchased[123,125], therefore they can be tested in the CAPA assay to get penetration rates. The only parameter lacking is a degradation rate measurement method that is

reflective of intracellular degradation. Controlled single protease assays like what was done with chymotrypsin in Chapter 4 are useful for pushing the limits of degradation by exposing the peptides to high concentrations of a protease with several cleavage sites on the peptide. Additionally, others have shown that specifically chymotrypsin stability correlates with serum stability[126]. Furthermore, although chymotrypsin has specific cleavage sites that may be different than those of proteases inside the cell, resistance to protease degradation is both residue and conformation dependent. The overall structure of a peptide, especially when influenced by backbone modifications such as alpha-carbon methylation[127] as in ATSP 7041 or a disulfide bond[128] as in pepC, can have more global effects on protease resistance, meaning that these effects may correlate to other proteases more generally. Nonetheless, the absolute peptide degradation rate in the presence of chymotrypsin at an arbitrary concentration is not directly translatable to a model that aims to predict efficacy (IC50) since it is the intracellular degradation rate that affects the intracellular concentration of peptide. Therefore, the absolute rate in the context of proteases and concentrations inside the cell are the most relevant. A cellular method, such as an assay in which cells are treated with peptide, lysed, and intact peptide is detected via LC-MS[89], could provide this absolute rate. Since LC-MS requires a substantial amount of material, equipment, and optimization, another option is an HPLC-based detection method in which the peptides of interest are fluorescently labeled. One of my colleagues, Haolong Huang, has already succeeded in synthesizing and conjugating pepC variants with a C-terminal lysine to two different fluorophores (via SPPS and NHS ester amine chemistry). Furthermore, another colleague, Marshall Case, has already succeeded in building a model that outputs cellular penetration rates based on the CAPA results. That model was used to estimate penetration rates

in Chapter 4. Therefore, some preliminary work is already underway that could lead to the development of a model that would predict efficacy based on those three rates.

While acknowledging the shortcomings of a model that predicts cellular efficacy using single protease degradation data, preliminary results in conjunction with our measured binding affinities and cytosolic penetration rates provide insight into the potential of such a model. In a simplified cellular compartmental model, the cytosolic penetration rate and degradation rate determine intracellular concentration of the peptide while the binding affinity determines target occupancy. In order to calculate the target occupancy at IC50, we used the reported IC50s and binding affinities of Nutlin3a[129] (a small molecule MDM2-inhibitor), as well as the assumption that intracellular delivery is not limiting for this small molecule, to calculate a target occupancy (fraction bound) of 95% at the IC50 using the equation below. We then used that occupancy to calculate the effective concentration of peptide inside the cytosol for each peptide using its binding affinity and the equation below.

$$f = \frac{C_{intracellular}}{C_{intracellular} + K_d}$$

$$f = fraction\ bound$$

$$C_{intracellular} = intracellular\ (cytosolic)\ concentration$$

$$K_d = binding\ affinity$$

In order to relate the chymotrypsin degradation rate to an intracellular degradation rate, we solved the following mass balance equation for stabilized pepC in SJSA1 cells using our experimental IC50, k_{in}, and previously calculated intracellular concentration and then calculated degradation rates for all other peptides by normalizing to the calculated pepC degradation rate. Therefore, we used pepC as our reference point for the absolute intracellular degradation rate and

scaled the other peptide's rates based on relative chymotrypsin stability. The results of this simple model are shown in Figure 5.2.

$$k_{in}(IC50) = k_{deg}(C_{intracellular})$$

$$k_{in} = internalization\ rate\ constant$$

$$k_{deg} = degradation\ rate\ constant$$

$$C_{intracellular} = intracellular\ concetration\ of\ drug$$

Even with the simplifications and assumptions made, the computational IC50s measured from this model are very close to the experimental values with deviations of less than 50% across all peptides in both cell lines. Note that concentrations in the experimental assay went up to only 10μM, as denoted with the dotted line. Therefore, IC50s higher than that were not captured experimentally. Nonetheless, this is an encouraging result that signals the possibility of developing a true robust model using cellularly relevant degradation rates.

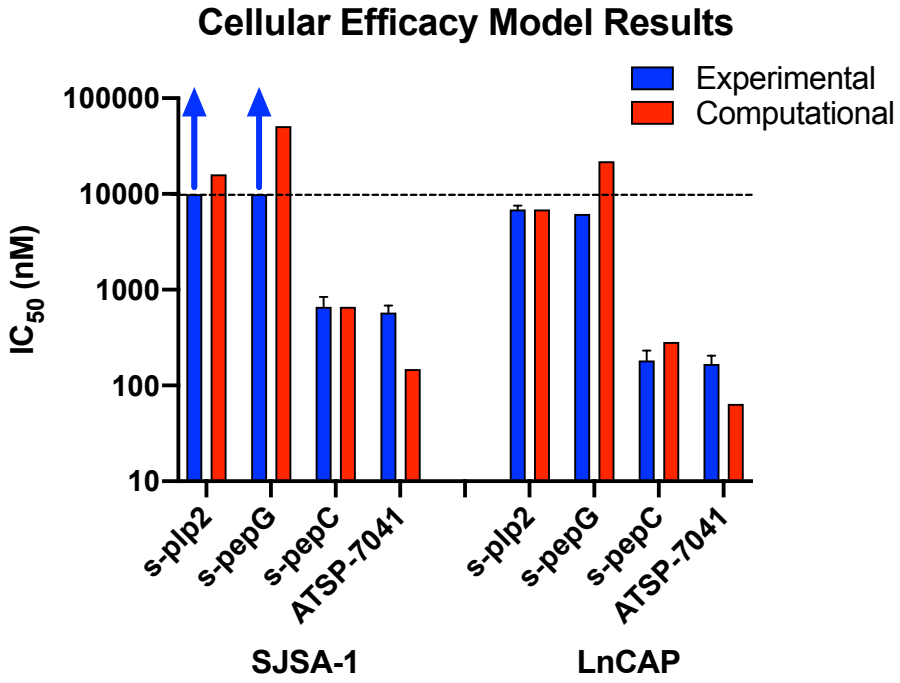

Figure 5.2 Preliminary Cellular Efficacy Model

5.2.2 Chemical Modification of pepC

Another opportunity for future work is further engineering pepC to increase its stability and binding affinity, making it a better candidate for *in vivo* efficacy studies. Although the disulfide bond is a unique feature that undoubtedly provides more stability and may be the primary reason why pepC is the most stable of the SPEED-derived peptides, disulfide bonds are reduced in cellular conditions (*in vitro*) and are at even greater risk of reduction *in vivo*. This could be remedied by replacing the disulfide bond with a more stable linkage, such as a thioether linkage. Preliminary attempts have been made to achieve this through substituting one of the cysteine residues with the non-natural amino acid vinyl glycine and performing the thioether chemistry on-resin, however we have not yet had success incorporating vinyl glycine during synthesis. However, there are other potential chemical linkages that can be used and other chemistries that can be explored.

Another enhancement that could be made to pepC is alpha-methylation of the alpha-carbons on the non-natural amino acids. This is a feature that is included in the non-natural stapling amino acids of ATSP-7041 and has helix inducing properties which could enhance both binding affinity and proteolytic stability[89]. Furthermore, D-amino acid substitution, which is typically considered to be helix-breaking and to disrupt binding for key amino acids, has been shown in the case of Trp7 in an MDM2-binding ATSP-7041 derivative to maintain binding. D-amino acid substitution can be useful in increasing proteolytic stability as well since proteases do not recognize those amino acids. These modifications work only on a case by case basis, so care will need to be taken to ensure that they are not made at the expense of strong MDM2 binding affinity even if proteolytic stability is improved. If both are improved with any of these

modifications, the resulting variant should be fully profiled as was done in Chapter 4 in order to get a wholistic assessment of the peptide's properties after chemical alteration.

5.2.3 In vivo studies

My final recommendation for future work is to perform *in vivo* studies with pepC and the chemically modified pepC. *In vitro* cell viability is only the first step in assessing the efficacy of a drug, and as depicted in Figure 5.1, there are many challenges faced *in vivo* before the peptide can even reach the target. PepC in its current state may be rapidly cleared and degraded *in vivo* given its moderate lipophilicity (compared to ATSP-7041) and the lack of non-natural amino acids and backbone modifications that could help it evade proteolysis. However, these rates should be quantified to determine the current pharmacokinetic liabilities. To do this, pepC can be conjugated to a dye and injected into mice to monitor clearance, the amount intact after clearance, and distribution. Dye conjugation will affect the distribution of the peptide, therefore clearance rate and fraction of intact non-labeled peptide can be quantified with LC-MS. However, using a dye-conjugated peptide will provide a means to measure localization of the peptide within tissue, cellular, and subcellular length scales. As previously mentioned, one of my colleagues has already created dye-conjugated pepC variants that can be used to perform these experiments. They should, however, be done in parallel with ATSP-7041 as a point of reference, therefore a corresponding dye-conjugated version will need to be synthesized and tested. If any of the pepC chemical modifications discussed in the previous section are successful in increasing binding affinity and protease stability, that variant should also be tested *in vivo*.

Bibliography

1. Lau, J. L. & Dunn, M. K. Therapeutic peptides: Historical perspectives, current development trends, and future directions. *Bioorganic Med. Chem.* (2017). doi:10.1016/j.bmc.2017.06.052
2. Hopkins, A. L. & Groom, C. R. The druggable genome. *Nat. Rev. Drug Discov.* **1**, 727–730 (2002).
3. Bullock, B. N., Jochim, A. L. & Arora, P. S. Assessing helical protein interfaces for inhibitor design. *J. Am. Chem. Soc.* **133**, 14220–14223 (2011).
4. Lipinski, C. A. Rule of five in 2015 and beyond: Target and ligand structural limitations, ligand chemistry structure and drug discovery project decisions. *Adv. Drug Deliv. Rev.* **101**, 34–41 (2016).
5. Walensky, L. D. *et al.* Activation of apoptosis in vivo by a hydrocarbon-stapled BH3 helix. *Science* **305**, 1466–70 (2004).
6. Lau, Y. H. *et al.* Functionalised staple linkages for modulating the cellular activity of stapled peptides. *Chem. Sci.* **5**, 1804 (2014).
7. Smith, G. P. & Petrenko, V. A. Phage Display. *Chem. Rev.* **97**, 391–410 (1997).
8. Liu, R., Barrick, J. E., Szostak, J. W. & Roberts, R. W. [19] Optimized synthesis of RNA-protein fusions for in vitro protein selection. in 268–293 (2000). doi:10.1016/S0076-6879(00)18058-9
9. Carvajal, L. A. *et al.* Dual Inhibition of Mdmx and Mdm2 Using an Alpha-Helical P53 Stapled Peptide (ALRN-6924) As a Novel Therapeutic Strategy in Acute Myeloid Leukemia. *Sci. Transl. Med.* **10**, 1–12 (2018).
10. Sawyer, T. K. *et al.* Macrocyclic α helical peptide therapeutic modality: A perspective of learnings and challenges. *Bioorg. Med. Chem.* **26**, 2807–2815 (2018).
11. Li, Y. C. *et al.* A Versatile Platform to Analyze Low-Affinity and Transient Protein-Protein Interactions in Living Cells in Real Time. *Cell Rep.* **9**, 1946–1959 (2014).
12. Thean, D. *et al.* Enhancing specific disruption of intracellular protein complexes by hydrocarbon stapled peptides using lipid based delivery. *Sci. Rep.* **7**, 1–11 (2017).
13. Robertson, N. S. Using Peptidomimetics and Constrained Peptides as Valuable Tools for Inhibiting Protein – Protein Interactions. **3**, (2018).
14. Walensky, L. D. & Bird, G. H. Hydrocarbon-stapled peptides: Principles, practice, and progress. *J. Med. Chem.* **57**, 6275–6288 (2014).
15. Schafmeister, C. E., Po, J. & Verdine, G. L. An All-Hydrocarbon Cross-Linking System for Enhancing the Helicity and Metabolic Stability of Peptides. *J. Am. Chem. Soc.* **122**, 12364–12365 (2000).
16. Moll, U. M., Petrenko, O., Moll, U. M. & Petrenko, O. The MDM2-p53 Interaction The MDM2-p53 Interaction. 1001–1008
17. Bernal, F. *et al.* Reactivation of the p53 Tumor Suppressor Pathway by a Stapled p53 Peptide. *J. Am. Chem. Soc.* 2456–2457 (2007).
18. Ng, S., Jafari, M. R., Matochko, W. L. & Derda, R. Quantitative synthesis of genetically encoded glycopeptide libraries displayed on M13 phage. *ACS Chem. Biol.* **7**, 1482–1487 (2012).
19. Heinis, C., Rutherford, T., Freund, S. & Winter, G. Phage-encoded combinatorial chemical libraries based on bicyclic peptides. *Nat. Chem. Biol.* **5**, 502–507 (2009).
20. Peraro, L. *et al.* Diversity-Oriented Stapling Yields Intrinsically Cell-Penetrant Inducers

of Autophagy. *J. Am. Chem. Soc.* **139**, 7792–7802 (2017).
21. Torres, O., Y??ksel, D., Bernardina, M., Kumar, K. & Bong, D. Peptide tertiary structure nucleation by side-chain crosslinking with metal complexation and double 'Click' cycloaddition. *ChemBioChem* **9**, 1701–1705 (2008).
22. Tornøe, C. W., Christensen, C. & Meldal, M. Peptidotriazoles on Solid Phase : [1 , 2 , 3] -Triazoles by Regiospecific Copper (I) -Catalyzed 1 , 3-Dipolar Cycloadditions of Terminal Alkynes to Azides. *J. Org. Chem.* **67**, 3057–3064 (2002).
23. Lau, Y. H. *et al.* Investigating peptide sequence variations for 'double-click' stapled p53 peptides. *Org. Biomol. Chem.* **12**, 4074–7 (2014).
24. Zhang, L., Navaratna, T. & Thurber, G. M. A Helix-Stabilizing Linker Improves Subcutaneous Bioavailability of a Helical Peptide Independent of Linker Lipophilicity. *Bioconjug. Chem.* **27**, 1663–1672 (2016).
25. Lipinski, C. A., Lombardo, F., Dominy, B. W. & Feeney, P. J. Experimental and computational approaches to estimate solubility and permeability in drug discovery and development settings. *Adv. Drug Deliv. Rev.* **64**, 4–17 (1997).
26. Thurber, G. M. *et al.* Single-cell and subcellular pharmacokinetic imaging allows insight into drug action in vivo. *Nat. Commun.* **4**, 1504–1510 (2013).
27. Thurber, G. M., Reiner, T., Yang, K. S., Kohler, R. H. & Weissleder, R. Effect of Small-Molecule Modification on Single-Cell Pharmacokinetics of PARP Inhibitors. *Mol. Cancer Ther.* **13**, 986–995 (2014).
28. Craik, D. J., Fairlie, D. P., Liras, S. & Price, D. The Future of Peptide-based Drugs. *Chem. Biol. Drug Des.* **81**, 136–147 (2013).
29. Nielsen, D. S. *et al.* Orally Absorbed Cyclic Peptides. *Chem. Rev.* **117**, 8094–8128 (2017).
30. Veber, D. F. *et al.* Molecular properties that influence the oral bioavailability of drug candidates. *J. Med. Chem.* **45**, 2615–2623 (2002).
31. Tian, S., Li, Y., Wang, J., Zhang, J. & Hou, T. ADME evaluation in drug discovery. 9. Prediction of oral bioavailability in humans based on molecular properties and structural fingerprints. *Mol. Pharm.* **8**, 841–851 (2011).
32. Ahlbach, C. L. *et al.* Beyond cyclosporine A: conformation-dependent passive membrane permeabilities of cyclic peptide natural products. *Future Med. Chem.* **7**, 2121–2130 (2015).
33. Qian, Z., Dougherty, P. G. & Pei, D. Targeting intracellular protein – protein interactions with cell-permeable cyclic peptides. *Curr. Opin. Chem. Biol.* **38**, 80–86 (2017).
34. Matsson, P., Doak, B. C., Over, B. & Kihlberg, J. Cell permeability beyond the rule of 5. *Adv. Drug Deliv. Rev.* **101**, 42–61 (2016).
35. Over, B. *et al.* Structural and conformational determinants of macrocycle cell permeability. *Nat. Chem. Biol.* **12**, 1065–1074 (2016).
36. Villar, E. A. *et al.* How proteins bind macrocycles. *Nat. Chem. Biol.* **10**, 723–731 (2014).
37. Moellering, R. E. *et al.* Direct inhibition of the NOTCH transcription factor complex. *Nature* **462**, 182–188 (2009).
38. Walensky, L. D. *et al.* A Stapled BID BH3 Helix Directly Binds and Activates BAX. *Mol. Cell* **24**, 199–210 (2006).
39. Chu, Q. *et al.* Towards understanding cell penetration by stapled peptides. *Medchemcomm* **6**, 111–119 (2014).
40. Huang, Y., Feng, Q., Yan, Q., Hao, X. & Chen, Y. Alpha-helical cationic anticancer peptides: a promising candidate for novel anticancer drugs. *Mini Rev. Med. Chem.* **15**, 73–

81 (2015).
41. Araghi, R. R. *et al.* Iterative optimization yields Mcl-1–targeting stapled peptides with selective cytotoxicity to Mcl-1–dependent cancer cells. *Proc. Natl. Acad. Sci.* 201712952 (2018). doi:10.1073/pnas.1712952115
42. Wachter, F. *et al.* Mechanistic validation of a clinical lead stapled peptide that reactivates p53 by dual HDM2 and HDMX targeting. *Oncogene* **36**, 2184–2190 (2017).
43. Ward, B. P. *et al.* Peptide lipidation stabilizes structure to enhance biological function. *Mol. Metab.* **2**, 468–479 (2013).
44. Bird, G. H. *et al.* Biophysical determinants for cellular uptake of hydrocarbon-stapled peptide helices. *Nat. Chem. Biol.* **12**, 845–852 (2016).
45. Jain, T. *et al.* Biophysical properties of the clinical-stage antibody landscape. *Proc. Natl. Acad. Sci.* **114**, 944–949 (2017).
46. Giordanetto, F. & Kihlberg, J. Macrocyclic drugs and clinical candidates: What can medicinal chemists learn from their properties? *J. Med. Chem.* **57**, 278–295 (2014).
47. Santos, G. B., Ganesan, A. & Emery, F. S. Oral Administration of Peptide-Based Drugs: Beyond Lipinski's Rule. *ChemMedChem* **11**, 2245–2251 (2016).
48. Chen, B. *et al.* Isolation and characterization of novel cyclotides from Viola hederaceae: Solution structure and anti-HIV activity of vhl-1, a leaf-specific expressed cyclotide. *J. Biol. Chem.* **280**, 22395–22405 (2005).
49. Ji, Y. *et al.* In vivo activation of the p53 tumor suppressor pathway by an engineered cyclotide. *J. Am. Chem. Soc.* **135**, 11623–11633 (2013).
50. Christensen, E. I., Birn, H., Storm, T., Weyer, K. & Nielsen, R. Endocytic Receptors in the Renal Proximal Tubule. *Physiology* **27**, 223–236 (2012).
51. Butterworth, J., Lin, Y. A., Prielipp, R., Bennett, J. & James, R. The pharmacokinetics and cardiovascular effects of a single intravenous dose of protamine in normal volunteers. *Anesth. Analg.* **94**, 514–522 (2002).
52. Sarko, D. *et al.* The pharmacokinetics of cell-penetrating peptides. *Mol. Pharm.* **7**, 2224–2231 (2010).
53. Huang, C.-W., Li, Z. & Conti, P. S. In Vivo Near-Infrared Fluorescence Imaging of Integrin 2 1 in Prostate Cancer with Cell-Penetrating-Peptide-Conjugated DGEA Probe. *J. Nucl. Med.* **52**, 1979–1986 (2011).
54. Collado Camps, E. & Brock, R. An opportunistic route to success: Towards a change of paradigm to fully exploit the potential of cell-penetrating peptides. *Bioorg. Med. Chem.* **26**, 2780–2787 (2018).
55. Naylor, M. R., Bockus, A. T., Blanco, M. J. & Lokey, R. S. Cyclic peptide natural products chart the frontier of oral bioavailability in the pursuit of undruggable targets. *Curr. Opin. Chem. Biol.* **38**, 141–147 (2017).
56. Bhatnagar, S., Deschenes, E., Liao, J., Cilliers, C. & Thurber, G. M. Multichannel Imaging to Quantify Four Classes of Pharmacokinetic Distribution in Tumors. *J. Pharm. Sci.* **103**, 3276–3286 (2014).
57. Hicks, K. O. *et al.* Pharmacokinetic/pharmacodynamic modeling identifies SN30000 and SN29751 as tirapazamine analogues with improved tissue penetration and hypoxic cell killing in tumors. *Clin. Cancer Res.* **16**, 4946–4957 (2010).
58. Thurber, G. M., Schmidt, M. M. & Wittrup, K. D. Antibody tumor penetration: Transport opposed by systemic and antigen-mediated clearance. *Adv. Drug Deliv. Rev.* **60**, 1421–1434 (2008).

59. Thurber, G. M., Figueiredo, J. L. & Weissleder, R. Multicolor Fluorescent Intravital Live Microscopy (FILM) for Surgical Tumor Resection in a Mouse Xenograft Model. *PLoS One* **4**, e8053 (2009).
60. Cilliers, C., Guo, H., Liao, J., Christodolu, N. & Thurber, G. M. Multiscale Modeling of Antibody-Drug Conjugates: Connecting Tissue and Cellular Distribution to Whole Animal Pharmacokinetics and Potential Implications for Efficacy. *AAPS J.* **18**, 1117–1130 (2016).
61. Baish, J. W. *et al.* Role of Tumor Vascular Architecture in Nutrient and Drug Delivery: An Invasino Percolation-Based Network Model. *Microvasc. Res.* **51**, 327–346 (1996).
62. Phan, J. *et al.* Structure-based design of high affinity peptides inhibiting the interaction of p53 with MDM2 and MDMX. *J. Biol. Chem.* **285**, 2174–2183 (2010).
63. Chang, Y. S. *et al.* Stapled α-helical peptide drug development: a potent dual inhibitor of MDM2 and MDMX for p53-dependent cancer therapy. *Proc. Natl. Acad. Sci. U. S. A.* **110**, E3445-54 (2013).
64. Pazgier, M. *et al.* Structural basis for high-affinity peptide inhibition of p53 interactions with MDM2 and MDMX. *Proc. Natl. Acad. Sci.* **106**, 4665–4670 (2009).
65. Thompson, P. A. *et al.* A phase I trial of imetelstat in children with refractory or recurrent solid tumors: a Children's Oncology Group Phase I Consortium Study (ADVL1112). *Clin. Cancer Res.* **19**, 6578–84 (2013).
66. Dikmen, Z. G. *et al.* In vivo inhibition of lung cancer by GRN163L: A novel human telomerase inhibitor. *Cancer Res.* **65**, 7866–7873 (2005).
67. Asai, A. *et al.* A novel telomerase template antagonist (GRN163) as a potential anticancer agent. *Cancer Res.* **63**, 3931–3939 (2003).
68. Herbert, B. S. *et al.* Lipid modification of GRN163, an N3′→P5′ thio-phosphoramidate oligonucleotide, enhances the potency of telomerase inhibition. *Oncogene* **24**, 5262–5268 (2005).
69. O'Neil, K. T. *et al.* Identification of novel peptide anagonists for GPIIb/IIIa from a conformationally constrained phage peptide library. **14**, 509–515 (1992).
70. Kruziki, M. A., Sarma, V. & Hackel, B. J. Constrained combinatorial libraries of Gp2 proteins enhance discovery of PD-L1 binders. *ACS Comb. Sci.* (2018). doi:10.1021/acscombsci.8b00010
71. Dumoulin, M. *et al.* Single-domain antibody fragments with high conformational stability. *Protein Sci.* **11**, 500–515 (2009).
72. Fox, J. M., Zhao, M., Fink, M. J., Kang, K. & Whitesides, G. M. The Molecular Origin of Enthalpy/Entropy Compensation in Biomolecular Recognition. *Annu. Rev. Biophys.* **47**, 223–250 (2018).
73. Sia, S. K., Carr, P. a, Cochran, A. G., Malashkevich, V. N. & Kim, P. S. Short constrained peptides that inhibit HIV-1 entry. *Proc. Natl. Acad. Sci. U. S. A.* **99**, 14664–14669 (2002).
74. Sinha, V. R. *et al.* Oral Colon-Specific Drug Delivery of Protein and Peptide Drugs. *Crit. Rev. Ther. Drug Carr. Syst.* **24**, 63–92 (2007).
75. Bird, G. H. *et al.* Hydrocarbon double-stapling remedies the proteolytic instability of a lengthy peptide therapeutic. *Proc. Natl. Acad. Sci. U. S. A.* **107**, 14093–8 (2010).
76. Novo Nordisk. Novo Nordisk successfully completes the first phase 3a trial, PIONEER 1, with oral semaglutide. 24–26 (2018).
77. Doak, B. C., Over, B., Giordanetto, F. & Kihlberg, J. Oral druggable space beyond the rule of 5: Insights from drugs and clinical candidates. *Chem. Biol.* **21**, 1115–1142 (2014).

78. Thompson, S. J., Hattotuwagama, C. K., Holliday, J. D. & Flower, D. R. On the hydrophobicity of peptides: Comparing empirical predictions of peptide log P values. *Bioinformation* **1**, 237–41 (2006).
79. Valko, K. L., Ivanova-Berndt, G., Beswick, P., Kindey, M. & Ko, D. Application of biomimetic HPLC to estimate lipophilicity, protein and phospholipid binding of potential peptide therapeutics. *ADMET DMPK* **6**, 162 (2018).
80. Regenthal, R., Krueger, M., Koeppel, C. & Preiss, R. Drug levels: therapeutic and toxic serum/plasma concentrations of common drugs. *J. Clin. Monit. Comput.* **15**, 529–544 (1999).
81. Pye, C. R. *et al.* Nonclassical Size Dependence of Permeation Defines Bounds for Passive Adsorption of Large Drug Molecules. *J. Med. Chem.* **60**, 1665–1672 (2017).
82. Naylor, M. R. *et al.* Lipophilic Permeability Efficiency Reconciles the Opposing Roles of Lipophilicity in Membrane Permeability and Aqueous Solubility. *J. Med. Chem.* **61**, 11169–11182 (2018).
83. Lau, Y. H. *et al.* Investigating peptide sequence variations for 'double-click' stapled p53 peptides. *Org. Biomol. Chem.* **12**, 4074–4077 (2014).
84. Zhang, L., Navaratna, T., Liao, J. & Thurber, G. M. Dual-Purpose Linker for Alpha Helix Stabilization and Imaging Agent Conjugation to Glucagon-Like Peptide-1 Receptor Ligands. *Bioconjug. Chem.* **26**, 329–337 (2015).
85. Berthod, A. & Carda-Broch, S. Determination of liquid-liquid partition coefficients by separation methods. *J. Chromatogr. A* **1037**, 3–14 (2004).
86. Smith, G. Filamentous fusion phage: novel expression vectors that display cloned antigens on the virion surface. *Science (80-.).* **228**, 1315–1317 (1985).
87. Roberts, R. W. & Szostak, J. W. RNA-peptide fusions for the in vitro selection of peptides and proteins. *Proc. Natl. Acad. Sci.* **94**, 12297–12302 (1997).
88. Navaratna, T. *et al.* Directed Evolution Using Stabilized Bacterial Peptide Display. *J. Am. Chem. Soc.* **142**, 1882–1894 (2020).
89. Partridge, A. W. *et al.* Incorporation of putative helix-breaking amino acids in the design of novel stapled peptides: Exploring biophysical and cellular permeability properties. *Molecules* **24**, (2019).
90. Okamoto, Y. & Hansmann, U. H. E. *Thermodynamics of Helix-Coil Transitions Studied by Multicanonical Algorithms*. (1995).
91. Kola, I. & Landis, J. Can the pharmaceutical industry reduce attrition rates? *Nat. Rev. Drug Discov.* **3**, 711–715 (2004).
92. Ran, X. & Gestwicki, J. E. Inhibitors of protein-protein interactions (PPIs): an analysis of scaffold choices and buried surface area. *Curr. Opin. Chem. Biol.* **44**, 75–86 (2018).
93. Troeira Henriques, S. & Craik, D. J. Cyclotide Structure and Function: The Role of Membrane Binding and Permeation. *Biochemistry* **56**, 669–682 (2017).
94. Cox, N., Kintzing, J. R., Smith, M., Grant, G. A. & Cochran, J. R. Integrin-Targeting Knottin Peptide-Drug Conjugates Are Potent Inhibitors of Tumor Cell Proliferation. *Angew. Chemie Int. Ed.* **55**, 9894–9897 (2016).
95. Thell, K. *et al.* Oral activity of a nature-derived cyclic peptide for the treatment of multiple sclerosis. *Proc. Natl. Acad. Sci. U. S. A.* **113**, 3960–3965 (2016).
96. Shustov, A. R. *et al.* Pseudoprogression (PsP) in Patients with Peripheral T-Cell Lymphoma (PTCL) Treated with the Novel Stapled Peptide ALRN-6924, a Dual Inhibitor of MDMX and MDM2. *Blood* **132**, 5348–5348 (2018).

97. Gandhi, L. *et al.* Phase I Study of Navitoclax (ABT-263), a Novel Bcl-2 Family Inhibitor, in Patients With Small-Cell Lung Cancer and Other Solid Tumors. *J. Clin. Oncol.* **29**, 909–916 (2011).
98. Peraro, L. & Kritzer, J. Getting in: emerging methods and design principles for cell-penetrant peptides. *Angew. Chemie* (2018). doi:10.1002/ange.201801361
99. Azzarito, V., Long, K., Murphy, N. S. & Wilson, A. J. Inhibition of α-helix-mediated protein-protein interactions using designed molecules. *Nature Chemistry* **5**, 161–173 (2013).
100. Abdeljabbar, D. M., Piscotta, F. J., Zhang, S. & James Link, a. Protein stapling via azide-alkyne ligation. *Chem. Commun. (Camb).* **50**, 14900–3 (2014).
101. Iegre, J. *et al.* Two-Component Stapling of Biologically Active and Conformationally Constrained Peptides: Past, Present, and Future. *Adv. Ther.* **1**, 1800052 (2018).
102. Garner, J. & Harding, M. M. Design and synthesis of alpha-helical peptides and mimetics. *Org. Biomol. Chem.* **5**, 3577–3585 (2007).
103. Bernal, F. *et al.* A Stapled p53 Helix Overcomes HDMX-Mediated Suppression of p53. *Cancer Cell* **18**, 411–422 (2010).
104. Chang, Y. S. *et al.* Stapled α−helical peptide drug development: A potent dual inhibitor of MDM2 and MDMX for p53-dependent cancer therapy. *Proc. Natl. Acad. Sci.* **110**, E3445–E3454 (2013).
105. Peraro, L. *et al.* Cell Penetration Profiling Using the Chloroalkane Penetration Assay. *J. Am. Chem. Soc.* **140**, 11360–11369 (2018).
106. Deprey, K. & Kritzer, J. A. Quantitative measurement of cytosolic penetration using the chloroalkane penetration assay. *Methods Enzymol.* (2020). doi:10.1016/bs.mie.2020.03.003
107. Atangcho, L., Navaratna, T. & Thurber, G. M. Hitting Undruggable Targets : Viewing Stabilized Peptide Development through the Lens of Quantitative Systems Pharmacology. *Trends Biochem. Sci.* 1–17 (2018). doi:10.1016/j.tibs.2018.11.008
108. Valkó, K. Chromatographic hydrophobicity index by fast-gradient RP-HPLC: A high-throughput alternative to log P/log D. *Anal. Chem.* **69**, 2022–2029 (1997).
109. de Planque, M. R. *et al.* Sensitivity of Single Membrane-Spanning R-Helical Peptides to Hydrophobic Mismatch with a Lipid Bilayer: Effects on Backbone Structure, Orientation, and Extent of Membrane Incorporation †. **40**, 5000–5010 (2001).
110. Vivian, J. T. & Callis, P. R. Mechanisms of tryptophan fluorescence shifts in proteins. *Biophys. J.* **80**, 2093–2109 (2001).
111. Tallmadge, D. H., Huebnert, J. S. & Borkman, R. F. Aceylamide Quenching of Tryptophan Photochemistry and Photophysics. *Photochem. Photobiol.* **49**, 381–386 (1989).
112. Eisenberg, D., Weiss, R. M. & Terwilliger, T. C. The helical hydrophobic moment: A measure of the amphiphilicity of a helix. *Nature* **299**, 371–374 (1982).
113. Bessette, P. H., Rice, J. J. & Daugherty, P. S. Rapid isolation of high-affinity protein binding peptides using bacterial display. *Protein Eng. Des. Sel.* **17**, 731–739 (2004).
114. Okamoto, T. *et al.* Stabilizing the Pro-Apoptotic BimBH3 Helix (BimSAHB) Does Not Necessarily Enhance Affinity or Biological Activity. *ACS Chem. Biol* **8**, (2013).
115. Bird, G. H., Gavathiotis, E., Labelle, J. L., Katz, S. G. & Walensky, L. D. Distinct BimBH3 (BimSAHB) stapled peptides for structural and cellular studies. *ACS Chem. Biol.* **9**, 831–837 (2014).

116. Jobin, M. L. *et al.* The role of tryptophans on the cellular uptake and membrane interaction of arginine-rich cell penetrating peptides. *Biochim. Biophys. Acta - Biomembr.* **1848**, 593–602 (2015).
117. Peraro, L. *et al.* Cell Penetration Profiling Using the Chloroalkane Penetration Assay. *J. Am. Chem. Soc.* **140**, jacs.8b06144 (2018).
118. Verdine, G. L. & Hilinski, G. J. *Stapled peptides for intracellular drug targets*. *Methods in Enzymology* **503**, (Elsevier Inc., 2012).
119. Smith, G. P. & Scott, J. K. [15] Libraries of peptides and proteins displayed on filamentous phage. in *Methods in Enzymology* **217**, 228–257 (1993).
120. Getz, J. a, Schoep, T. D. & Daugherty, P. S. Peptide discovery using bacterial display and flow cytometry. *Methods Enzymol.* **503**, 75–97 (2012).
121. Chu, Q. *et al.* Towards understanding cell penetration by stapled peptides. *Med. Chem. Commun.* **6**, 111–119 (2015).
122. Gould, A. & Camarero, J. A. Cyclotides: Overview and Biotechnological Applications. *ChemBioChem* **18**, 1350–1363 (2017).
123. Yin, H. *et al.* Cellular Uptake and Cytosolic Delivery of a Cyclic Cystine Knot Scaffold. *ACS Chem. Biol.* **15**, 1650–1661 (2020).
124. Camarero, J. A. & Campbell, M. J. The potential of the cyclotide scaffold for drug development. *Biomedicines* **7**, (2019).
125. Postic, G. *et al.* KNOTTIN: the database of inhibitor cystine knot scaffold after 10 years, toward a systematic structure modeling. *Nucleic Acids Res.* **46**, (2018).
126. Howell, S. M. *et al.* Serum stable natural peptides designed by mRNA display. *Sci. Rep.* **4**, 1–5 (2014).
127. Werner, H. M., Cabalteja, C. C. & Horne, W. S. Peptide Backbone Composition and Protease Susceptibility: Impact of Modification Type, Position, and Tandem Substitution. *ChemBioChem* **17**, 712–718 (2016).
128. Kong, X. D. *et al.* De novo development of proteolytically resistant therapeutic peptides for oral administration. *Nat. Biomed. Eng.* **4**, 560–571 (2020).
129. Tovar, C. *et al.* MDM2 antagonists boost antitumor effect of androgen withdrawal: Implications for therapy of prostate cancer. *Mol. Cancer* **10**, 49 (2011).